AD_____

Award Number: DAMD17-99-1-9252

TITLE: Repair Machinery for Radiation-Induced DNA Damage

PRINCIPAL INVESTIGATOR: David Wilson, Ph.D.

CONTRACTING ORGANIZATION: Lawrence Livermore National Laboratory
Livermore, California 94550

REPORT DATE: July 2001

TYPE OF REPORT: Annual

PREPARED FOR: U.S. Army Medical Research and Materiel Command
Fort Detrick, Maryland 21702-5012

DISTRIBUTION STATEMENT: Approved for Public Release;
Distribution Unlimited

REPORT DOCUMENTATION PAGE

Form Approved
OMB No. 074-0188

1. AGENCY USE ONLY (Leave blank)	2. REPORT DATE	3. REPORT TYPE AND DATES COVERED
	July 2001	Annual (1 Jul 00 - 30 Jun 01)

4. TITLE AND SUBTITLE
Repair Machinery for Radiation-Induced DNA Damage

5. FUNDING NUMBERS
DAMD17-99-1-9252

6. AUTHOR(S)
David Wilson, Ph.D.

7. PERFORMING ORGANIZATION NAME(S) AND ADDRESS(ES)

Lawrence Livermore National Laboratory
Livermore, California 94550

E-Mail: wilson61@llnl.gov

8. PERFORMING ORGANIZATION REPORT NUMBER

9. SPONSORING / MONITORING AGENCY NAME(S) AND ADDRESS(ES)

U.S. Army Medical Research and Materiel Command
Fort Detrick, Maryland 21702-5012

10. SPONSORING / MONITORING AGENCY REPORT NUMBER

11. SUPPLEMENTARY NOTES
Report contains color

12a. DISTRIBUTION / AVAILABILITY STATEMENT
Approved for Public Release; Distribution Unlimited

12b. DISTRIBUTION CODE

13. ABSTRACT *(Maximum 200 Words)*
Understanding the repair mechanisms for ionizing radiation (IR)-induced DNA damage and having prior knowledge of a patient's IR-specific repair capacity will help determine which patients will be most responsive to radiation therapy and design more effective treatment regimes. The objective of this work has been to define the contributions of the mammalian protein Ape1, and other candidate nucleases, to the repair of IR-induced genetic damage. We are currently constructing cell lines that lack Ape1 protein and will determine the sensitivity of these mutant cells to various DNA-damaging agents, e.g. IR. In the course of these studies, we generated a mammalian cell line that overexpresses Ape1 ~ 7-fold (AA8-Ape1). In combination with previous findings, our data indicates that Ape1 activity is not a good prognostic indicator for sensitivity to the alkylating agent methyl methanesulfonate or the oxidizing agent hydrogen peroxide, but may in some circumstances be for IR and bleomycin. Moreover, the AA8-Ape1 line displays ~1.7 fold elevated resistance to the replication-blocking nucleoside analog dioxolane cytidine, a slightly increased resistance to azidothymidine, but normal sensitivity to arabinosylcytosine and 2',3'-dideoxy-2',3'-dihydrothymidine. This is the first cell-based study demonstrating a role for Ape1 in influencing cellular resistance to anti-cancer/viral antimetabolites. Additionally, we completed the biochemical characterization of two protein factors, human Sfn and Hem45/Isg20, and have found that these proteins are unlikely involved in repairing IR-induced DNA damage. It thus appears that Ape1 is a predominant repair factor for 3'-damages, although alternative corrective mechanisms exist. Future studies will focus more on obtaining a quantitative determination of the overall contribution of Ape1 to 3'-damage repair and IR protection.

14. SUBJECT TERMS
Breast Cancer

15. NUMBER OF PAGES
82

16. PRICE CODE

17. SECURITY CLASSIFICATION OF REPORT	18. SECURITY CLASSIFICATION OF THIS PAGE	19. SECURITY CLASSIFICATION OF ABSTRACT	20. LIMITATION OF ABSTRACT
Unclassified	Unclassified	Unclassified	Unlimited

Table of Contents

Proposal Title: Repair Machinery for Radiation-Induced DNA Damage

Principal Investigator: David M. Wilson III, Ph.D.

Biology & Biotechnology Research Program, L-441
Lawrence Livermore National Laboratory
Regents of the University of California
7000 East Avenue
Livermore, CA 94551-0808

Office: (925) 423 0695
Fax: (925) 422 2282

INTRODUCTION

Current methods to treat breast cancer and preserve normal tissue involve total mastectomy followed by radiotherapy. The use of postoperative radiotherapy however has produced mixed results. While some randomized studies indicate that there is no major benefit from postmastectomy radiation treatment, there exists a subgroup of patients that benefit from this type of strategy. Thus, it is imperative that we design effective prognostic tools to identify patients that will profit, as well as those that may be harmed, by adjuvant radiotherapy. Ionizing radiation (IR) is cytotoxic to cells largely because it introduces lethal genetic damage. Thus, understanding the repair mechanisms for IR-induced DNA alterations and having prior knowledge of a patient's radiation-specific repair capacity will help design more effective treatment regimes and help determine which patients will be most responsive to radiation exposure. We intend to identify and characterize factors involved in correcting common radiation-induced damages. Such studies will provide the necessary tools (both specific DNA repair genes and biochemical assays) for predicting an individual's repair capacity and thus potential IR sensitivity (genetic predisposition).

BODY

Objectives:

1. **To construct an *APE1* knockout cell line (months 1-24) and examine the role of Ape1 in DNA repair (months 25-36).**

Radiation induces an array of DNA damages, including abasic lesions and strand breaks harboring 3'-blocking termini such as phosphoglycolate and phosphate groups (1,2). The human Ape1 protein has been shown to incise at AP sites and remove a subset of 3'-damages, as well as to stimulate the DNA-binding activity of several oncoproteins (e.g. p53, Fos and Jun) *in vitro* (3,4,5,6). Yet despite the basic understanding of the biochemical properties of Ape1, the *in vivo* function of the protein remains largely unclear, particularly as it relates to IR protection. *APE1* knockout cell lines represent an essential step towards defining the biological contribution of this mammalian protein.

We predict that Ape1-deficient cells will demonstrate a quantitatively significant defect in the repair of certain DNA damages, but of which damages needs to be determined. We have selected Chinese Hamster Ovary (CHO) as the target cell line for knockout generation, since they present the many advantages described in the original proposal. As reported in our prior update, we determined that APE1 is a single copy gene in AA8 by fluorescence *in situ* hybridization using an APE1 bacterial artificial chromosome (BAC) genomic fragment isolated from a CHO BAC library. Sequence information from a previously obtained APE1 CHO genomic clone (graciously provided by Pablo Arenas, UTEP) was simultaneously used to construct the LARA.TK, pLARA and pLARA.TK targeting vectors (Figure 1, see Appendix), designed to delete a portion of the Ape1 C-terminal domain known to be essential for nuclease activity. We discuss below our attempts to isolate a knockout cell line (see Table 1 in Appendix for summary).

In our first screen of 360 colonies for an APE1 knockout, we did not identify a targeted deletion event (Table 1, LARA.TK). This result prompted us to consider the possibility that APE1 null cell lines are inviable. Thus, to prevent future complications of this sort, we stably integrated a tetracycline (Tc)-regulated human APE1 cDNA into the AA8 genome (Schild et al., submitted; see Appendix). Using this line (termed AA8-Ape1), we performed another targeting screen with the original knockout vector, and again were unable to detect a targeted event in >700 independent clones (Table 1, LARA.TK). We subsequently designed a new targeting construct, assuming that the initial construct was problematic, and performed analysis of genomic DNA from >560 newly transfected AA8-Ape1cells (Table 1, pLARA). A third vector and additional large-scale screenings also proved unsuccessful (Table 1, pLARA.TK).

To explain the inability to isolate APE1 genetic knockouts to date, we propose the following possibilities: 1. inefficient detection of a knockout by the PCR methods employed and 2. the AA8 derivative of CHO is unable to undergo efficient targeting at the APE1 locus. Towards addressing "1", we will rescreen the last two large-scale experiments (encompassing 10,000-12,500 clones) utilizing improved PCR primers (which will yield results for both non-targeted and targeted events) to identify a knockout. Towards addressing "2", we have developed a second human Ape1 overexpressing cell line in the AT3-2 derivative (Figure 2, see Appendix). The CHO AT3-2 cell line has been utilized by other laboratories and has demonstrated efficient targeting capabilities (7), and we will begin a new set of targeting screens immediately. As described in the original proposal, once we have obtained an APE1-deleted, human Ape1-Tc-regulated CHO line, we can reduce or shut off (in a controlled manner) Ape1 gene expression by addition of Tc to the medium, and monitor cell growth as well as sensitivity to DNA-damaging agents, specifically IR.

As a fortuitous product of the research performed here, the AA8-Ape1cell line has allowed us to assess the role of Ape1 as a rate-limiting factor in the repair of various DNA damages (Schild et al., submitted). These studies revealed that Ape1 activity is not rate-limiting for the repair of cytotoxic damages induced by the alkylating agent methyl methanesulfonate (MMS), the oxidizing agent hydrogen peroxide (H_2O_2) or IR. In contrast, AA8-Ape1 cells did exhibit increased resistance to bleomycin following a chronic 24 hour or 3 day exposure, but not to more acute challenges (1 hr). In combination with previous findings, these data indicate that Ape1 activity is not a good prognostic indicator for sensitivity to MMS and H_2O_2, but may in some circumstances be for IR or bleomycin. Moreover, the AA8-Ape1 line displayed ~1.7 fold elevated resistance to the replication-blocking nucleoside analog dioxolane cytidine (L-OddC), a slightly increased resistance to azidothymidine (AZT), but normal sensitivity to arabinosylcytosine (AraC) and 2',3'-dideoxy-2',3'-dihydrothymidine (d4T). This is the first cell-based study demonstrating a role for Ape1 in influencing cellular resistance to anti-cancer/viral antimetabolites. While more research is still needed, the results

from the experiments here are an important stepping stone towards building a more strategic platform for approaching anti-cancer treatments.

2. To characterize hYjeR and hXPMC2/Hem45 as 3' to 5' exonucleases and 3'-repair enzymes (months 1-36).

Ape1 has been shown to possess a poor 3'-repair activity on certain 3'-damage-containing DNA substrates (3), indicating the potential existence of alternative 3'-repair mechanisms. Using traditional protein expression and purification methods, we isolated the human YjeR and ISG20/Hem45 proteins and characterized their 3'-nuclease activities. Notably, these proteins contain the structurally-conserved exonuclease motifs of the 3′-5′ exonuclease superfamily (8,9) and thus represented candidate 3'-repair enzymes. However, our analysis has revealed that the human YjeR protein (named Sfn) exhibits nuclease activity on primarily nucleic acid substrates of <5 nucleotides in length (Nguyen et al., 2000; see appendix). Such a substrate specificity indicates that Sfn is *not* likely involved in repairing genetic damage on large chromosomal DNA, yet presumably plays a role in recycling short DNA fragments, such as those generated during repair excision events. Substrate analysis of ISG20/Hem45 found that this human protein degrades both RNA and DNA substrates, with DNA at roughly 50-fold less efficiency (Nguyen et al., 2001; see Appendix). These results suggest that this protein, like Sfn, is unlikely involved in resistance to IR-induced DNA damage. We had suggested characterization of hXPMC2, however, given its high sequence similarity to ISG20/Hem45, we will not pursue detailed biochemical studies with this protein. As Objective 2 of the original proposal has been completed, we will focus our future efforts on constructing the APE1 knockout cells (Objective 1) in the final year, and hopefully begin detailed characterization of this line.

KEY RESEARCH ACCOMPLISHMENTS

- Completed characterization of the human YjeR equivalent, which we have termed Sfn for small fragment nuclease. This data appeared in the *Journal of Biological Chemistry*.
- Completed characterization of the human ISG20/Hem45 protein. This data appeared in the *Biochemistry*.
- Established an Ape1-overexpressing mammalian cell line (AA8-Ape1) that has permitted analysis of the role of this protein in DNA damaging agent resistance, particularly as a rate-limiting factor. This work has been submitted for publication to the journal *Carcinogenesis*. Note: the available Ape1 Tc-regulated cell lines (see above) are being used in the knockout targeting experiments in the event that a null cell is lethal.
- Constructed three targeting constructs for knocking out the APE1 gene in CHO cells. The first construct was abandoned after screening over 1000 colonies for a targeting event without success. Over 500 colonies were screened utilizing the second targeting construct. Rescreening, using improved PCR primers, of over 10,000 colonies is ongoing after transfection of the third targeting construct into the AA8-Ape1cell line.

REPORTABLE OUTCOMES

- Nguyen, L.H., J.P. Erzberger, J. Root and D.M. Wilson III. (2000) The human homolog of *E. coli* Orn degrades small single stranded RNA and DNA oligomers. *J. Biol. Chem.* **275**:25900-25906.

- Nguyen, L.H., L. Espert, N. Mechti and D.M. Wilson III. (2001) The human inteferon and estrogen-regulated *ISG20/HEM45* gene product degrades single stranded RNA and DNA in vitro. *Biochemistry*. **40**:7174-7179.

- Schild, L.J., K.W. Brookman, L.H. Thompson and D.M. Wilson III. (2001) Ape1 as a Rate-Limiting Factor in Cellular Resistance to DNA-damaging and Anti-cancer Agents. Submitted to *Carcinogenesis*.

CONCLUSIONS

Understanding the repair mechanisms for IR-induced DNA damage and having prior knowledge of a patient's radiation-specific repair capacity will help determine which patients will be most responsive to radiation therapy and design more effective treatment regimes. The objective of this work has been to define the contributions of the mammalian protein Ape1, and other candidate nucleases, to the repair of IR-induced genetic damage. We are currently constructing cell lines that lack Ape1 protein and will determine the sensitivity of these mutant cells to various DNA-damaging agents, e.g. IR. In the course of these studies, we generated a mammalian cell line that overexpresses Ape1 roughly 5 to 8-fold. This line, relative to the parental controls, will be used to examine whether Ape1 operates as a rate-limiting factor in the repair of certain exogenously-induced DNA damages (e.g. abasic sites and 3'-phosphate and phosphoglycolate blocking damages). Such studies will address the potential value of modulating Ape1 repair capacity in terms of protecting or sensitizing target cells from the effects of IR anti-cancer treatments. Additionally, we have completed the biochemical characterization of two protein factors, human Sfn and Hem45/Isg20. Results from these studies indicate that neither protein has a substrate specificity that is consistent with a major role in repairing IR-induced DNA damage. It thus appears that Ape1 is the predominant (and perhaps only) repair factor for 3'-damages, although alternative less prominent corrective mechanisms must exist. Future studies will focus more on obtaining accurate quantitative determinations of the overall contribution of Ape1 to 3'-damage repair and IR protection and less on the search for alternative 3'-repair mechanisms.

REFERENCES

1. von Sonntag C (1987) The Chemical Basis of Radiation Biology. Taylor and Francis (London)
2. Ward JF (1988) DNA damage produced by ionizing radiation in mammalian cells: identities, mechanisms of formation, and reparability. *Prog Nucleic Acid Res Mol Biol* 35:95-125
3. Wilson DM 3rd, Takeshita M, Grollman AP, & Demple B (1995) Incision activity of human apurinic endonuclease (Ape) at abasic site analogs in DNA. *J Biol Chem* 270 (27): 16002-16007

4. Suh D, Wilson DM 3rd, & Povirk L (1997) 3'-Phosphodiesterase activity of human apurinic/apyrimidinic endonuclease at DNA double-strand break ends. *Nucleic Acids Res.* 25:2495-2500.
5. Xanthoudakis S, Miao G, Wang F, Pan YC, & Curran T (1992) Redox activation of Fos-Jun DNA binding activity is mediated by a DNA repair enzyme. *EMBO J.* 11:3323-3335.
6. Jayaraman, L., Murthy, K. G., Zhu, C., Curran, T., Xanthoudakis, S., & Prives, C. (1997) Identification of redox/repair protein Ref-1 as a potent activator of p53. *Genes Dev.* 11:558-570.
7. Adair GM, Rolig RL, Moore-Faver D, Zabelshansky M, Wilson JH, Nairn RS. (2000) Role of ERCC1 in removal of long non-homologous tails during targeted homologous recombination. *EMBO J* 19:5552-61
8. Moser MJ, Holley WR, Chatterjee A, Mian IS (1997) The proofreading domain of *Escherichia coli* DNA polymerase I and other DNA and/or RNA exonuclease domains. *Nucleic Acids Res* 25:5110-5118
9. Koonin EV (1997) A conserved ancient domain joins the growing superfamily of 3'-5' exonucleases. *Curr Biol* 7:R604-R606
10. Izumi T, Hazra TK, Bodogh I, Tomkinson AE, Park MS, Ikeda S, & Mitra S (2000) Requirement for human AP endonuclease 1 for repair of 3'-blocking damage at DNA single-strand breaks induced by reactive oxygen species. Carcinogenesis 21:1329-1334.

APPENDICES

Figure 1. Schematic of *chAPE1* locus and gene knockout constructs.

Figure 2. Tc regulation of Ape1 protein expression and activity in CHO AT3-2.

Table 1. Recombinant clones analyzed for *cgAPE*1 targeted events

Nguyen, L.H., J.P. Erzberger, J. Root and D.M. Wilson III. (2000) The human homolog of *E. coli* Orn degrades small single stranded RNA and DNA oligomers. *J. Biol. Chem.* **275**:25900-25906.

Nguyen, L.H., L. Espert, N. Mechti and D.M. Wilson III. (2001) The human inteferon and estrogen-regulated *ISG20/HEM45* gene product degrades single stranded RNA and DNA in vitro. *Biochemistry*. **40**:7174-7179.

Wilson III, D.M. and D. Barsky (2001) The Major Human Abasic Endonuclease Ape1: Formation, Consequences and Repair of Abasic Lesions in DNA. *Mutat. Res.* **484**:283-307.

Schild, L.J., K.W. Brookman, L.H. Thompson and D.M. Wilson III. (2001) Ape1 as a Rate-Limiting Factor in Cellular Resistance to DNA-damaging and Anti-cancer Agents. Submitted to *Carcinogenesis*.

Role on Project	Name	Degree	Scientific Discipline	Institutional Affiliation
PI	David M. Wilson III	Ph.D.	Molecular Biology & Protein Biochemisty	Lawrence Livermore National Laboratory, University of California (LLNL-UC)
Post-doctoral Scientist	Laura Schild	Ph.D.	Molecular & Cellular Biology	LLNL-UC
Consultant	Larry Thompson	Ph.D.	Mammalian Genetics	LLNL-UC

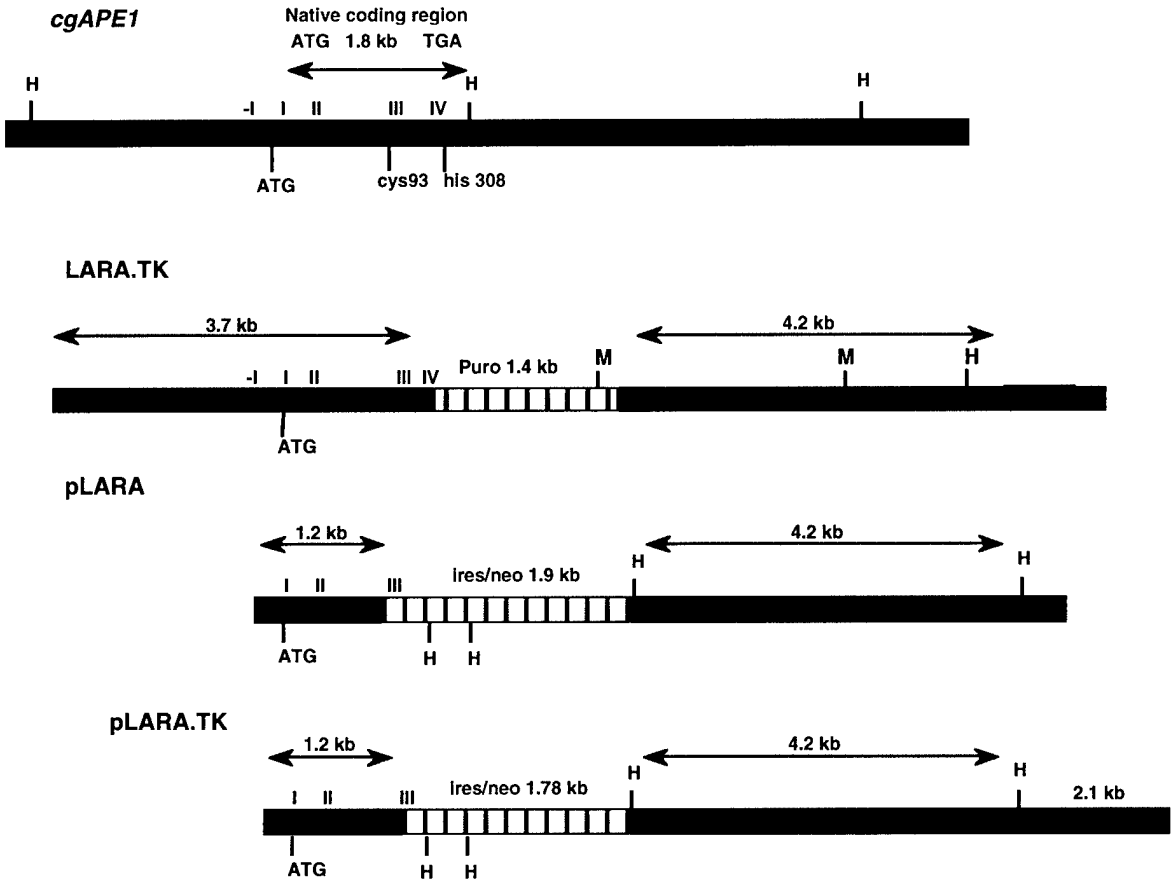

Figure 1. Schematic of *chAPE1* locus and gene knockout constructs. The 1.8 kb coding region of *chAPE1* gene encodes a 318 amino acid protein. The exons (numbered in roman numerals) are indicated in red boxes and the critical residues for redox activity (Cys 93) and nuclease activity (His 309) are noted. *Hin*dIII and *Mfe*1 recognition sites are noted by H and M, respectively. Three targeting vectors were constructed. LARA.TK contains 7.5 kb of homology to *chAPE1*. The left arm interrupts exon IV with the puromycin (puro) gene, thereby eliminating His 309. The 4.2 kb right arm is positioned between puro and the negative selection marker, *hsvTK,* which suppresses nonhomologous integration. A promoterless targeting vector, pLARA, utilizes the endogenous *chAPE1* promoter to drive expression of the neomycin (neo) gene, which interrupts *chAPE1* in exon III. The 1.2 kb left arm terminates *cgAPE1* translation at residue 87, and eliminates Cys 93. pLARA.TK was created by introducing a 2.1 kb *hsvTK* cassette at the 3' *Hin*dIII site of the right arm of the pLARA vector, and allows use of the negative selection marker.

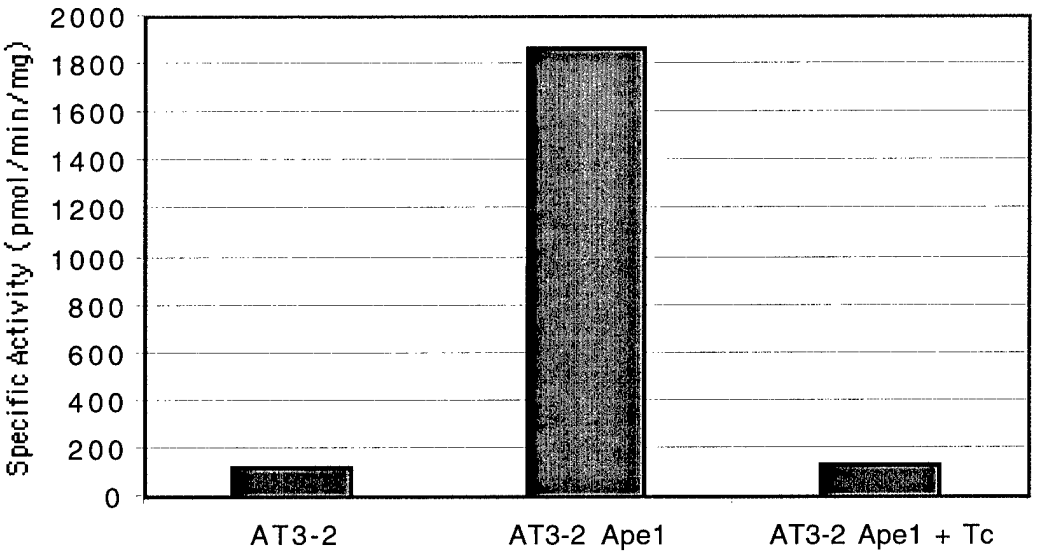

Figure 2. Tc regulation of Ape1 protein expression and activity in CHO AT3-2. CHO AT3-2 and AT3-2 Ape1 cells (expressing the human APE1 cDNA under the control of a Tc-off promoter) were exposed to 0 (-) or 0.3 (+) μg Tc/ml for 96 hr and protein extracts were isolated. One tenth μg cell extract from either AT3-2 or AT3-2 Ape1 ± Tc was assayed for incision activity for 5 min at 37°C with 1 pmol of 18F DNA substrate (see Schild et al., submitted in Appendix). AT3-2 Ape1 demonstrated background parental levels of AP site incision activity after incubation with Tc. In the absence of Tc, AT3-2 Ape1 cells exhibited a ~13 fold increase in AP endonuclease activity.

Table 1. Recombinant clones analyzed for *cgAPE1* targeted events

Vector — Expt[1]	Line	µg linear	DNA Pools[2]	Clones
LARA1 — 1	AA8	14.4	60 pools of 6	360
LARA1 — 2	AA8-Ape1	20.0	139 pools of 5-6	730
pLARA — 3	AA8-Ape1	30.0	Single clones (see below)	562
pLARA.TK[3] — 4	AA8-Ape1	10.0	98 pools of ~10-25	980-2,500
pLARA.TK — 5	AA8-Ape1	40.0	67 pools of ~120	~10,000

[1]Electroporation conditions

LARA1	300 volts,1600 µF; 5 µg DNA, 1-2 x 10^7 cells/vial
pLARA and pLARA.TK	250 volts,1600 µF; 10 µg DNA, 2-3 x 10^7 cells/vial

[2]Recombinant selection conditions

LARA1	10 µg/ml puromycin, 0.1 µM fiau (2'-fluoro-2'-deoxy-5-iodo-1-<beta>-D-arabinofuranosyluracil)
pLARA	G418 at 2 mg/ml (332 clones), 5 mg/ml (157 clones), 10 mg/ml (73 clones)
pLARA.TK	G418 1.7 mg/ml, 0.1 µM fiau

[3]fiau enrichment

LARA1	8 fold (selectable marker puro present with promoter)
pLARA.TK	2-3 fold (selectable marker neo without promoter)

THE JOURNAL OF BIOLOGICAL CHEMISTRY

Vol. 275, No. 34, Issue of August 25, pp. 25900–25906, 2000
Printed in U.S.A.

The Human Homolog of *Escherichia coli* Orn Degrades Small Single-stranded RNA and DNA Oligomers*

Received for publication, March 29, 2000, and in revised form, May 11, 2000
Published, JBC Papers in Press, June 12, 2000, DOI 10.1074/jbc.M002672200

Lam H. Nguyen, Jan P. Erzberger‡, Jeffrey Root, and David M. Wilson III§

From the Molecular and Structural Biology Division, Lawrence Livermore National Laboratory, Livermore, California 94551

We report here the identification of human homologues to the essential *Escherichia coli* Orn protein and the related yeast mitochondrial DNA-escape pathway regulatory factor Ynt20. The human proteins appear to arise from alternatively spliced transcripts, and are thus identical, except the human Ynt20 equivalent contains an NH_2-terminal extension that possesses a predicted mitochondrial protease cleavage signal. *In vitro* analysis revealed that the smaller human protein exhibits a 3′ to 5′ exonuclease activity for small (primarily ≤5 nucleotides in length) single-stranded RNA and DNA oligomers. We have named this human protein Sfn for small fragment nuclease to reflect its broad substrate range, and have termed the longer protein hSfnα. Sfn prefers Mn^{2+} as a metal cofactor and displays a temperature-resistant (to 50 °C) nuclease activity. Kinetic analysis indicates that Sfn exhibits a similar affinity for small RNAs and DNAs (K_m of ~1.5 μM), but degrades small RNAs ~4-fold more efficiently than DNA. Mutation of a conserved aspartate (Asp^{136}) to alanine abolishes both nuclease activities of Sfn. Northern blot analysis revealed that a 1-kilobase transcript corresponding to *SFN* and/or *SFNα* (these mRNAs differ by only two nucleotides) is expressed at varying levels in all fetal and adult human tissues examined. Expressed tag sequence clone analysis found that the two splice variants, *SFN* to *SFNα*, are present at a ratio of roughly 4 to 1, respectively. The results presented within suggest a role for human Sfn in cellular nucleotide recycling.

Nucleases are critical components of DNA and RNA metabolism, carrying out functions in DNA repair, replication and recombination, and RNA processing and degradation. Several candidate nucleases were recently classified as members of the 3′ to 5′ exonuclease superfamily (1). This superfamily includes RNases (such as RNase T and D), the proofreading domains of pol I family DNA polymerases, and DNases that exist as independent proteins (such as *Escherichia coli* ExoI) or as domains within larger polypeptides (such as a region within the Werner's syndrome helicase) (1–3). Homology within the superfamily is centered around three conserved exonuclease motifs (Exo I, II, and III) (2). The crystal structure of the Klenow fragment of *E. coli* DNA polymerase I and complementing site-directed mutagenesis studies indicate that the Exo I, II, and III motifs are clustered around the active site and contain four conserved negatively charged residues that are critical for coordinating the two metal ions involved in phosphodiester bond cleavage (reviewed in Ref. 4).

Based on conservation of the Exo motifs, the protein encoded by the *E. coli* open reading frame *YjeR* was placed into the 3′ to 5′ exonuclease superfamily (5). This protein was subsequently shown *in vitro* to be an exonuclease specific for RNA molecules shorter than about 5 nucleotides (nt)[1] in length (6). Based on this ribonuclease activity, *YjeR* was renamed *Orn* for oligoribonuclease (6). Data base mining revealed a human EST homolog to *YjeR*, indicating an evolutionary conserved role for the encoded protein (5).

Orn is one of eight distinct 3′ to 5′ exoribonucleases present in *E. coli* (7). It is a processive enzyme that initiates attack at a free 3′ hydroxyl group on single-stranded RNA, releasing 5′-mononucleotides in a sequential manner (6). Notably, unlike previously characterized *E. coli* ribonucleases, *ORN* is an essential gene. Experiments using a temperature-sensitive *ORN* construct and pulse-chase experiments with radiolabeled RNA revealed an accumulation of small RNA oligonucleotides at the non-permissive temperature (8). These observations suggested a role for Orn in the final steps of mRNA degradation, since mRNA-degrading enzymes such as RNase II and polynucleotide phosphorylase generate small oligonucleotide fragments that require further processing to mononucleotides (8).

An *ORN* homologue is also present in yeast *Saccharomyces cerevisiae* (5, 9). This *YNT20* gene encodes a larger protein that has been shown to localize to the mitochondria (9). *YNT20* plays a role in a *S. cerevisiae* mitochondrial DNA escape pathway, a process that involves the transfer of genetic material from the mitochondria to the nucleus (9).

It was suggested, based on sequence comparisons, that the *S. cerevisiae* Ynt20 protein is potentially capable of hydrolyzing both DNA and RNA (9). Although it has been reported that the *E. coli* Orn protein exhibits no detectable DNase activity on double stranded T7 chromosomal DNA (10), its ability to degrade short deoxyribonucleotides apparently has not been examined. We set out to examine the substrate specificity of the human Orn equivalent, with a particular interest in its activity for DNA molecules, and demonstrate here that this protein cleaves not only short RNAs but also short DNAs in a 3′ to 5′ direction. Thus, we suggest that the human enzyme be named Sfn for small fragment nuclease. We discuss our results as they may relate to the cellular role of this protein in nucleic acid metabolism.

* This work was supported by the U. S. Department of Energy by Lawrence Livermore National Laboratory under contract number W-7405-ENG-48 and supported by National Institutes of Health Grant CA79056 and U. S. Army Grant BC980514 (to D. M. W.). The costs of publication of this article were defrayed in part by the payment of page charges. This article must therefore be hereby marked "*advertisement*" in accordance with 18 U.S.C. Section 1734 solely to indicate this fact.

‡ Present address: Dept. of Molecular and Cellular Biology, University of California, Berkeley, CA 94720.

§ To whom correspondence should be addressed. Tel.: 925-423-0695; Fax: 925-422-2282; E-mail: wilson61@llnl.gov.

[1] The abbreviations used are: nt, nucleotide(s); EST, expressed sequence tag; PCR, polymerase chain reaction.

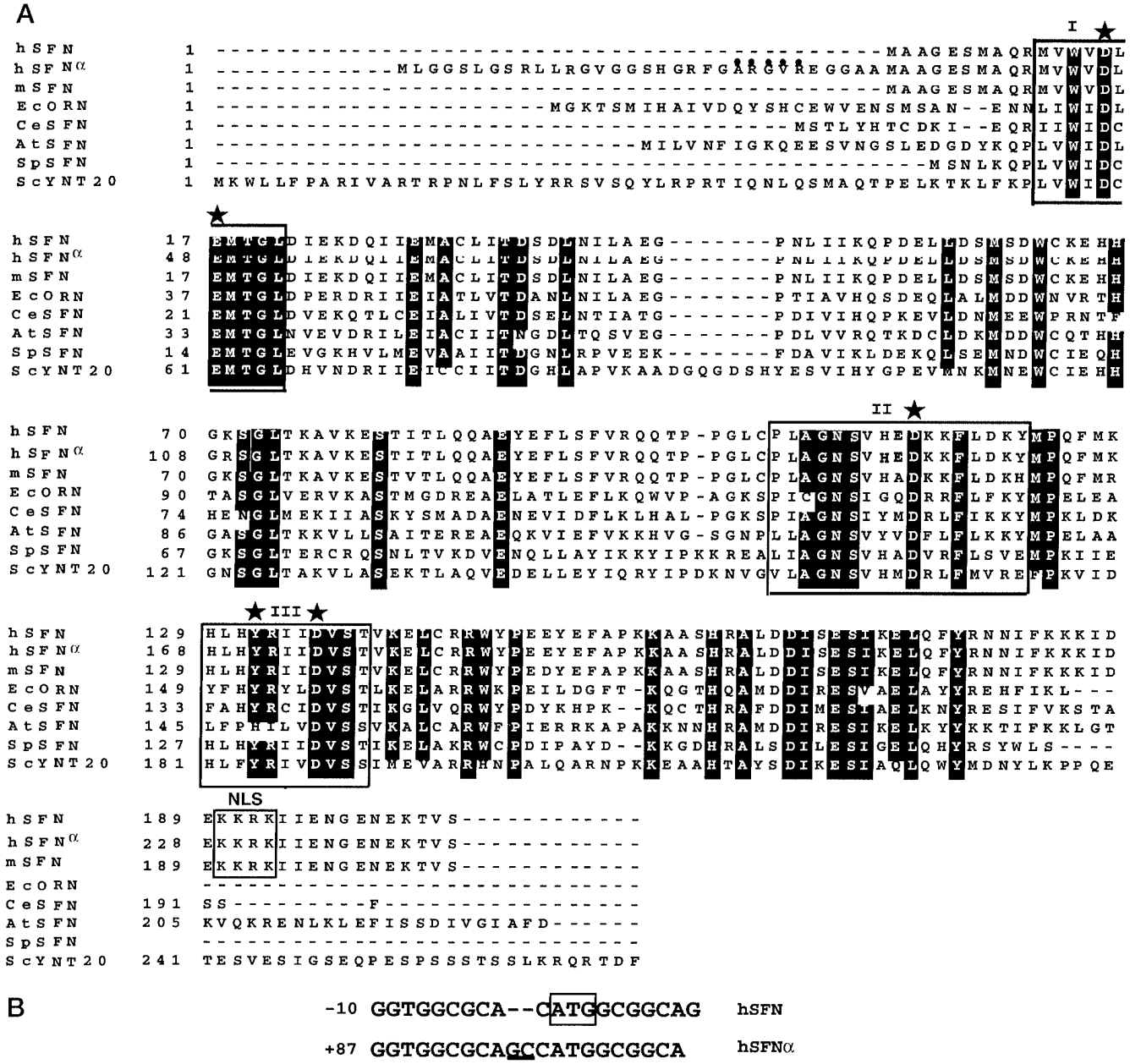

FIG. 1. **Comparison of amino acid and DNA sequences of the human *SFN*.** *A*, the amino acid sequence of the *SFN* subfamily. Amino acids in *black* are identical, *gray* are conserved, and *white* are non-conserved. This alignment was produced with the Boxshade program. *hSFN* is the *Homo sapiens* Sfn protein sequence (accession number Q9Y3B8); *hSFNα*, *H. sapiens* Ynt20 (CAB53690); *mSFN*, *Mus musculus* Sfn; *EcORN*, *E. coli* Orn (P39287); *CeSFN*, *Caenorhabditis elegans* Sfn (CAA96590); *AtSFN*, *Arabidopsis thaliana* Sfn (AAC77855); *SpSFN*, *Schizosaccharomyces pombe* Sfn (CAB37438); and *ScYNT20*, *S. cerevisiae* Ynt20 (P54964). The conserved exonuclease motifs of the 3′ to 5′ exonuclease superfamily (Exo I, II, and III) are shown as *boxes*. The *stars* indicate the catalytically important tyrosine and the four conserved negatively charged residues that are involved metal ion binding (1, 4). The nuclear localization signal (*NLS*), KKRK, is *boxed* (18). ● is used to mark the putative mitochondrial targeting signal, ARGVR, for *hSFNα* (17). *B*, sequences of the putative splice site in *hSFN* (accession number AF151872) and *hSFNα* (AL110239) mRNAs. The first nucleotide of the respective protein coding sequence is designated as +1. The first codon of *hSFN* is *boxed*. The differences in the two sequences are *underlined*.

EXPERIMENTAL PROCEDURES

Identification of SFN and SFNα cDNAs—The EST data base was searched using the TBLASTN program to identify human cDNA clones that encode a protein homologous to the *E. coli* Orn protein (GenBank accession number P39287). IMAGE clone 663460 was chosen, sequenced (11), and found to contain an open reading frame encoding a 205-amino acid protein. This protein is identical to CGI-114 protein (accession number is AF151872). The *SFNα* cDNA was found in the GenBank data base (accession number AL110239).

Chromosomal Localization of the Human SFN Gene—The sequence at the 5′ end (accession number AA224296) or the 3′ end (accession number AA224194) of the *SFN* gene, when compared with the "Sequenced Tagged Site" data base at National Cancer Biology Institute, identified STS-H98169 as the genetic locus of *SFN*. This sequence-tagged site is positioned at chromosome 11 in a region between markers D11S1347 and D11S939 (110.3–117.9 centimorgan), which corresponds to the region 11q23.1–11q23.2.

Buffers and Reagents—All reagents were purchased from Sigma unless otherwise indicated. Restriction enzymes were purchased from New England Biolabs. Labeled nucleotides were from Amersham Pharmacia Biotech. Spectrophotometric grade glycerol was obtained from Fisher. Olio(dT)$_{4-22}$ Ladder was purchased from Life Technologies, Inc. and consists of single-stranded DNA oligos from 4 to 22 nt in length, increasing by 1-nucleotide increments. DNA oligos were obtained from Operon Biotechnologies (Alameda, CA). Synthetic RNA was obtained from Dharmacon Research (Boulder, CO). L buffer (Lysis buffer) con-

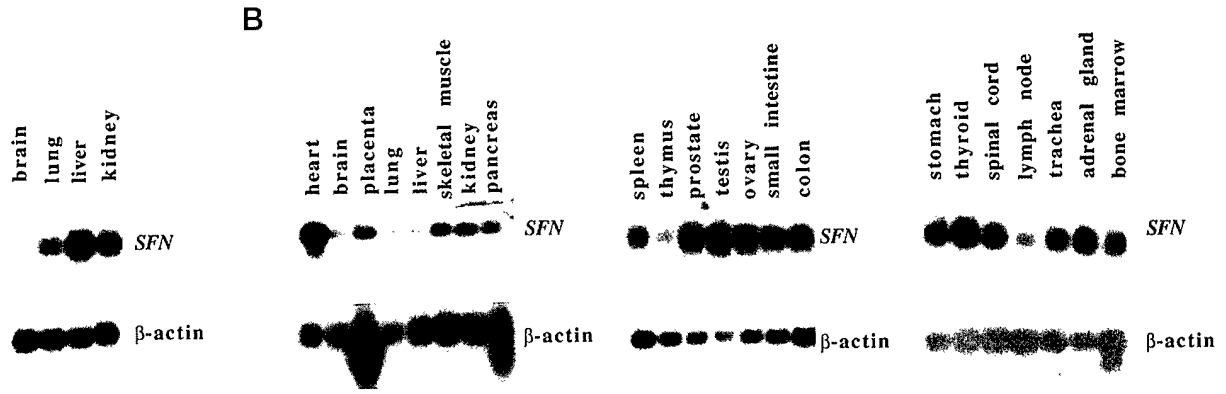

FIG. 2. **Expression pattern of *SFN* mRNA in fetal and adult human tissues.** Shown are Northern blot hybridization signals detected by autoradiography. Developmental stage, tissue type, and transcript type are indicated. β-Actin transcript was used for normalization. *Panel A* is an mRNA blot of fetal tissues. *Panel B* shows three mRNA blots of adult tissues.

tains 50 mM Tris-HCl, pH 7.9, 50 mM KCl, 20% glycerol, and 1 mM phenylmethylsulfonyl fluoride. W5 buffer is 50 mM Tris-HCl, pH 7.9, 500 mM NaCl, 20% glycerol, 5 mM imidazole, and 1 mM phenylmethylsulfonyl fluoride. W40 is 50 mM Tris-HCl, pH 7.9, 500 mM NaCl, 20% glycerol, 40 mM imidazole, and 1 mM phenylmethylsulfonyl fluoride. E250 buffer is 50 mM Tris-HCl, pH 7.9, 250 mM NaCl, 20% glycerol, 250 mM imidazole, and 1 mM phenylmethylsulfonyl fluoride. All pH values were determined at 21 °C.

Purification of Recombinant Sfn-His Protein—The *SFN* coding region was PCR amplified using primers NCO5′HYJER (5′-GCATGCCTGGCGGCAGGGGAGAGCAT) and HIND3′YJER (3′-GCAGTAAGCTTACTCACGGTCTTCTCAT), and subcloned after digestion into the *Nco*I and *Hin*dIII sites of pET28d (Novagen, Madison, WI) to generate phyjeR-His. This construct allows for expression of six histidine residues on the carboxyl terminus under the control of a T7 RNA polymerase promoter. phyjeR-His plasmid was sequenced and no PCR errors were found.

The phyjeR-His plasmid was transformed into BL21(DE3)/pLysS *E. coli* strain (Novagen). An overnight culture of 100 ml was grown at 37 °C in LB (1% bactotryptone, 0.5% bactoyeast extract, and 1% NaCl) with 50 μg/ml kanamycin and 25 μg/ml chloramphenicol. The overnight culture was used to inoculate 1 liter of the same medium. This culture was grown at 37 °C with vigorous aeration until the $A_{550\ nm}$ was 0.8. Isopropyl-1-thio-β-galactopyranoside (final concentration of 1 mM) was then added to induce Sfn-His protein expression. At 4 h after induction, cells were harvested. The cell paste was resuspended in 30 ml of L buffer. The cell suspension was sonicated using a Misonix XL sonicator by three 1-min bursts with a microtip at the maximum setting. The cell lysate was centrifuged at 27,000 × *g* for 30 min at 4 °C. To the supernatant, polyethyleneimine was added slowly with constant stirring to a final concentration of 0.25% to remove nucleic acids (12). The suspension was centrifuged and the supernatant was loaded at 1.5 ml/min onto a 2-ml S2 cation exchange column equilibrated with L buffer using the BioLogic Workstation FPLC system (Bio-Rad). Fractionation over the cation exchange column removed the contaminating proteins found to bind nonspecifically to the subsequent Ni affinity column. The S2 flow-through was collected, and NaCl and imidazole were added to final concentrations of 500 and 5 mM, respectively. The S2 flow-through was then incubated with 2 ml of Ni-NTA resin (Qiagen, Santa Clarita, CA) for 1 h at 4 °C with gentle rocking. This suspension was centrifuged, and the resin was washed 2 times each with 20 ml of W5 buffer, followed by 4 washes each with 10 ml of W40 buffer. Sfn-His proteins were then eluted from the Ni-NTA resin 4 times, each with 2 ml of E250 buffer, dialyzed overnight against L buffer containing 0.1 mM dithiothreitol, and stored at −70 °C. Concentrations of protein solutions were determined by measuring the absorbance at 280 nm and using the theoretical molar extinction coefficient $E_{280\ nm}$ of 25,940 $M^{-1}\ cm^{-1}$ calculated for Sfn-His (13).

Analytical Gel Filtration Chromatography—Sfn-His protein was separated on a 7.8 × 300-mm BioSil SEC 125–5 gel filtration column from Bio-Rad. The running buffer was 50 mM Tris-HCl, pH 7.9, 100 mM ammonium sulfate, 5% glycerol, 0.1 mM EDTA, and 0.1 mM dithiothreitol. The flow rate was 0.25 ml/min. Size markers used for calibration were thyroglobulin (670 kDa), γ-globulin (158 kDa), ovalbumin (44 kDa), myoglobin (17 kDa), and vitamin B-12 (1.35 kDa). Proteins were detected by ultraviolet absorbance at 280 nm.

Site-directed Mutagenesis of the SFN cDNA—Mutagenesis was performed using the overlapped PCR method as described (14). The site-specific mutant oligo used was D136A, 5′-TATAGAATAATTGCTGTGAGCACTGTTAAG-3′, with the mutated codon underlined. We chose to mutate Asp^{136} because a structurally equivalent mutation in *E. coli* DNA pol I (D501A) caused a 13,000-fold decrease in 3′-5′ exonuclease activity (15). The final *SFN* mutant PCR product was digested with *Nco*I and *Hin*dIII and subcloned into the same restriction sites of pET28d. This construct was sequenced as described (11).

Nuclease Assays—Various DNA and RNA substrates were labeled at the 5′ end by T4 polynucleotide kinase with [γ-^{32}P]ATP (16). RNA5 is 5′-GAUCG-3′. DNA5 is 5′-GATCG-3′. DNA8 is 5′-CACGAGCC-3′. 100 fmol of nucleic acid substrate was incubated with 100–2000 fmol of Sfn-His protein at 37 °C in 10 μl of 50 mM HEPES-KDH, pH 7.4, 10% glycerol, 50 mM KCl, 10 mM $MnCl_2$ (unless otherwise noted), 0.01% Triton X-100, and 0.1 mM dithiothreitol. The reactions were stopped with 10 μl of 80% formamide dye solution, heated at 80 °C for 3 min, and then fractionated on a 20 or a 22.5% 8 M urea polyacrylamide gel. The gel was exposed to x-ray film. Visualization of the labeled substrate on the gels was also achieved using a Molecular Dynamics (Sunnyvale, CA) STORM 860 Phosphorimager and quantitative analysis was performed using Molecular Dynamics ImageQuant v1.11 software.

Kinetics of Sfn Exonuclease Activity on Single-Stranded DNA and RNA Substrates—Nuclease assays were performed under standard buffer conditions as described above at 37 °C, with Sfn at a final concentration of 10 nM. The reaction was incubated for 5 min with RNA5 or 40 min with DNA5, and was within the linear range of enzymatic activity (*i.e.* ≤15% of the substrate was converted to product). The substrate concentration range was 0.1–3.2 μM. The apparent Michaelis-Menten constant (K_m) and maximal velocity (V_{max}) were obtained from a double-reciprocal Lineweaver-Burk plot. A linear plot of 1/[S] *versus* 1/*V* (where [S] is the substrate concentration in μM and *V* is the velocity in μM min^{-1} units) produces a slope of K_m/V_{max} and a *y* intercept of $1/V_{max}$. k_{cat} was calculated from the equation $(k_{cat})(E_t) = V_{max}$, where E_t is the total concentration of enzyme in the assay. Linear regression analysis was performed using CricketGraph software (Cricket Software, Philadelphia, PA).

Northern Blot Analysis—Northern blots were prehybridized for 3 h at 65 °C in ExpressHyb Solution (CLONTECH, Palo Alto, CA). The cDNA probe (SFN PCR product described above) was labeled using the Megaprime DNA Labeling System (Amersham Pharmacia Biotech) and [α-^{32}P]dCTP (Amersham Pharmacia Biotech), and hybridized in ExpressHyb Solution at 65 °C for 2–3 h. Blots were washed once at room temperature for 30 min and twice at 50 °C for 30 min with 50 mM $NaPO_4$, pH 7.4, 0.5% SDS, and 1 mM EDTA. Images were exposed on Kodak Bio-Max MS film for 16 h and developed. Blots were normalized with β-actin transcripts.

RESULTS

The SFN cDNA, Genomic Location, and mRNA Expression Pattern—A cDNA containing the *SFN* coding region was obtained from the EST data base (see "Experimental Procedures"). By blasting the sequence of the 5′ end (accession number AA224296) or the 3′ end (accession number AA224194) of the *SFN* cDNA against the NCBI UniGene data base, we found

that the human *SFN* gene mapped to chromosome 11 at position 11q23.1–11q23.2. Four additional genes also map within this vicinity: apolipoprotein A-I (*apoA-I*), human serotonin receptor 3 (*HTR3*), human nicotinamide *N*-methyltransferase (*NNMT*), and zinc finger protein ZNF259 (*PLZF*).

The *SFN* cDNA codes for a 205-amino acid protein of 23,754 daltons, with a theoretical pI of 5.6. *SFN* belongs to the *YjeR/ORN* family, which is a distinct subgroup of the 3′ to 5′ exonuclease superfamily (1, 5). Fig. 1 shows a comparison of the amino acid sequence of the Sfn-like proteins from bacteria, yeast, plant, worm, mouse, and human. The human Sfn protein is ~50% identical to its *E. coli* counterpart, the Orn protein (5). Sfn and *E. coli* Orn possess the three characteristic sequence motifs, termed Exo I, II, and III (2), of the 3′ to 5′ exonuclease superfamily (1) (Fig. 1*A*). Four conserved negatively charged residues within these three Exo motifs (shown in Fig. 1*A*) are involved in positioning of the two divalent cations required for catalysis and phosphodiester bond cleavage (reviewed in Ref. 4).

Upon further examination of the GenBank data base, an identical protein to hSfn, but with an extended NH_2-terminal domain, was identified (Fig. 1*A*). This protein, which we propose to call Sfnα, appears to be the human equivalent to the yeast Ynt20 protein and to have arisen from an alternative RNA splicing event where two additional nucleotides were introduced (Fig. 1*B*). Using the PSORT II computer search program, a putative consensus cleavage site motif for mitochondrial processing proteases (ARGVR) (17) was identified within the unique NH_2-terminal portion of Sfnα. Both Sfn and Sfnα contain a consensus nuclear localization signal (KKRK) (18) (Fig. 1*A*). It seems logical that Sfn would be targeted to the nucleus and that Sfnα would translocate predominantly to the mitochondria.

Northern blotting revealed that the *SFN* cDNA probe detects a single transcript of ~1 kilobase in all fetal and adult tissues examined (Fig. 2). Comparatively, relatively low mRNA levels are observed in adult lymph nodes, brain, lung, liver, spleen, and thymus, with highest levels observed in heart. Since the human *SFN* and *SFN*α cDNAs appear to differ by only two nucleotides, it was not possible to distinguish the two transcripts here. Of the 10 human ESTs found in the data base, 8 contained a sequence identical to the *SFN* cDNA and two maintained a sequence identical to SFNα.

Purification of Overproduced SFN-His Fusion Protein—We have characterized here Sfn, and expect that Sfnα will exhibit similar substrate specificity as it maintains the same core nuclease domain (Fig. 1*A*). The *SFN* gene was subcloned into the pET28d plasmid to produce a COOH-terminal-tagged Sfn-His fusion protein, and the recombinant protein was purified as described under "Experimental Procedures." From 1 liter of induced bacterial culture (about 5 g of wet cell pellet), we obtained ~4 mg of Sfn-His fusion protein of >95% purity (Fig. 3*A*). As shown in Fig. 3*B*, the Sfn-His fusion protein migrates as a single symmetrical peak on an analytical gel filtration column that corresponds to a globular protein with a molecular mass of ~90 kDa. Since the calculated molecular weight of Sfn is 24,000, Sfn-His fusion protein appears to migrate as a tetramer. However, since the elution position on a gel filtration column is dependent on size and shape of the protein, it is possible that the Sfn-His fusion protein exists in solution as a rod-shaped protein of lower oligomeric state, since rod-shaped proteins are known to migrate slower than expected for their molecular weight.[2] Unlike the human Sfn-His protein, the *E. coli* Orn protein was reported to be a dimer based on its gel filtration chromatographic profile, although it should be noted that the experimental conditions differed slightly from those used here (6).

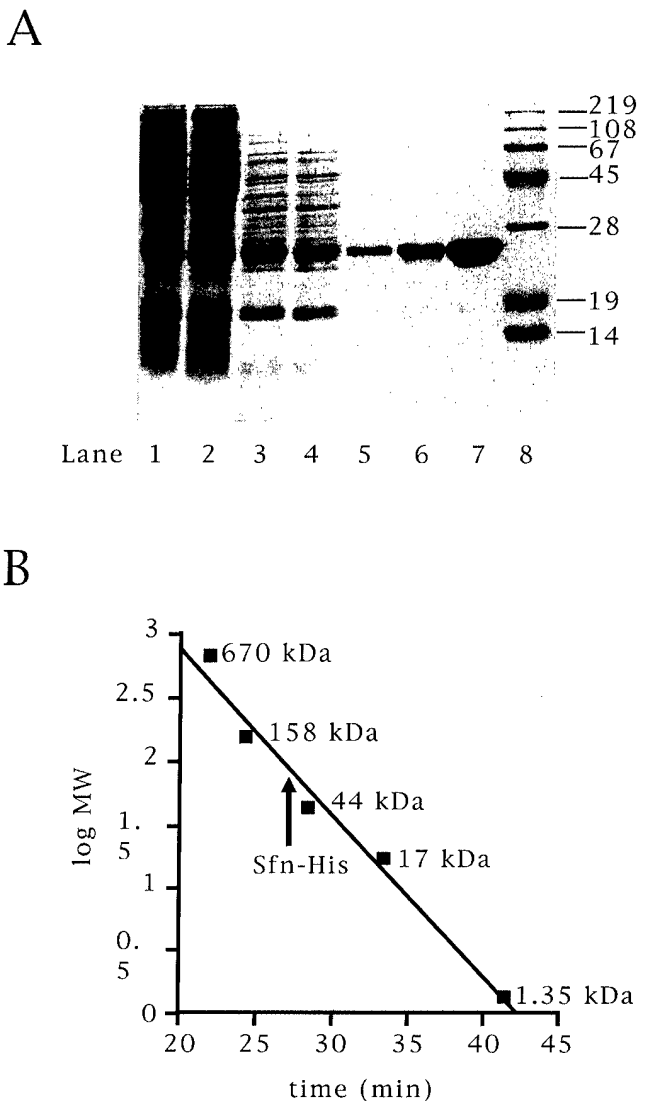

FIG. 3. **Purification of Sfn-His protein.** *A*, a 15% polyacrylamide SDS gel containing fractions of the various purification steps. *Lane 1* is 10 μl of whole cell extract (30 ml); *lane 2* is 10 μl of whole cell supernatant (30 ml); *lane 3* is 10 μl of the supernatant after 0.25% polyethyleneimine precipitation (30 ml); *lane 4* is 14 μl of the S2 cation exchange column flow-through (40 ml); *lanes 5–7* are 2.4, 7.2, and 21.6 μg of Ni-affinity purified Sfn-His (6 ml); and *lane 8* is protein markers. Protein marker sizes in kDa are indicated. The gel was stained with Coomassie Blue R-250. *B*, gel filtration column analysis of Ni-purified Sfn-His. The *x* axis is the retention time (in min) of marker proteins. The *y* axis is log of molecular weight (log MW) of proteins. The positions of the marker proteins are indicated on the calibration curve by their molecular weights. The retention time of Sfn-His is indicated by the *arrow* on the calibration curve.

Exonuclease Activity of Sfn-His Protein—Short fragments of ≤5 ribonucleotides were shown to be the optimal substrate for *E. coli* Orn protein (6, 10). Using a 5-nucleotide RNA (RNA5), labeled at the 5′ end, as the substrate, we determined the divalent metal cation preference of the human Sfn. At metal concentrations of 0.01, 0.05, 0.1, 0.5, 1, 5, and 10 mM, only Mg^{2+} and Mn^{2+} had any stimulatory effect on Sfn-His exonuclease activity, with Mg^{2+} being ~10-fold less effective than Mn^{2+} at 10 mM (Fig. 4*A* and data not shown). Both human Sfn-His and *E. coli* Orn enzymatic activities have a strong dependence on

[2] Dr. R. Burgess, University of Wisconsin-Madison, personal communication.

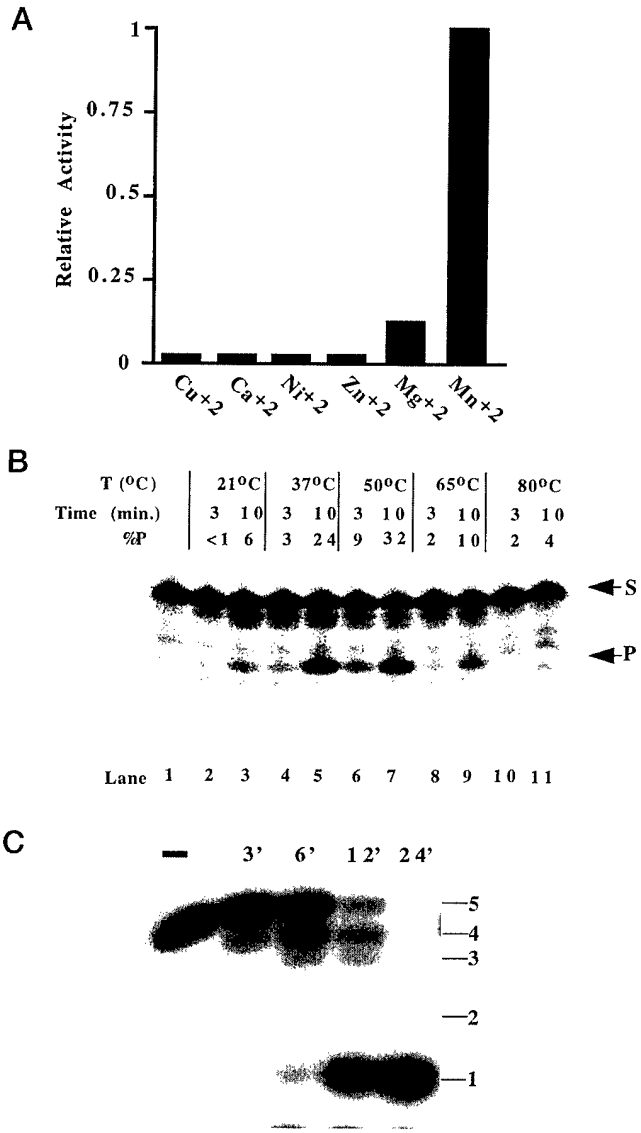

FIG. 4. **Metal cofactor requirement, temperature optimum, and time course of Sfn-His RNase activity.** *A*, metal preference of Sfn-His. 100 fmol of labeled RNA5 was incubated with 1 pmol of Sfn-His at 37 °C for 30 min in the presence of 10 mM of the different divalent metal cations as indicated. The *y* axis is relative exonuclease activity. Minimal detection for this assay was ≤1 fmol of product which is equivalent to ~2.5% of the activity detected with Mn^{2+} as shown for Cu^{2+}, Ca^{2+}, Ni^{2+}, and Zn^{2+}. *B*, temperature optimum of Sfn-His. 100 fmol of labeled RNA5 was incubated with 500 fmol of Sfn-His for 3 or 10 min at the temperature indicated. *Lane 1* is no protein control. *Lanes 2* and *3* represent reactions performed at 21 °C; *lanes 4* and *5*, 37 °C; *lanes 6* and *7*, 50 °C; *lanes 8* and *9*, 65 °C; and *lanes 10* and *11*, 80 °C. *%P* is the percentage of labeled substrate that has been converted to the final mononucleotide product. *S* is the labeled RNA5 substrate. *P* is the final product. Shown is a representative of three experiments. *C*, a time course of Sfn-His RNase activity with 5 mM $MnCl_2$ at 37 °C. *Lane 1* is the no protein control. *Lanes 2–5* are 0.2 μM RNA5 incubated with 0.02 μM Sfn-His for various times (in minutes) as indicated on *top* of the figure.

(and a preference for) Mn^{2+} (Fig. 4*A*; Ref. 10). The RNase activity of Sfn-His also has a temperature optimum around 50 °C (Fig. 4*B*), similar to that of *E. coli* Orn protein (10). Thus both proteins are quite thermostable. The RNA-specific degradation activity of Sfn at 37 °C is ~2-fold less than that at 50 °C (Fig. 4*B*). Since we observed degraded 4-mer products prior to detecting mononucleotide products (Fig. 4*C*), Sfn-His appears, as expected, to be a 3′ to 5′ exonuclease.

To determine whether short single-stranded DNA can serve

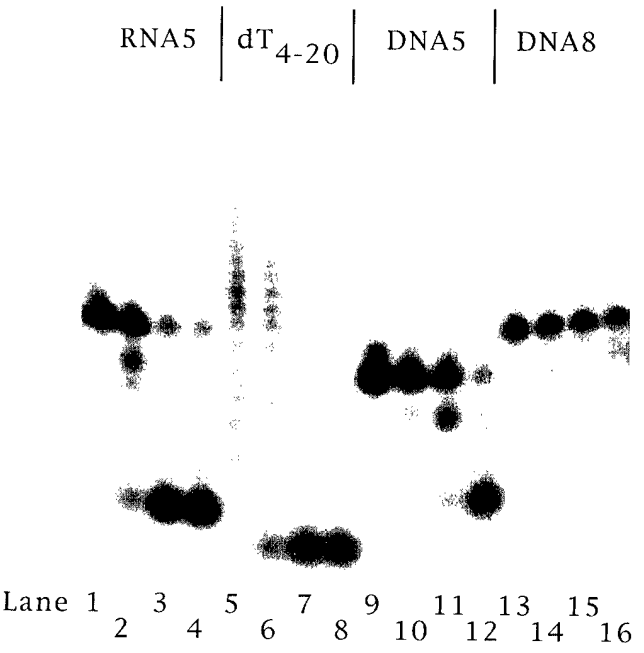

FIG. 5. **Sfn-His degrades small single-stranded RNAs and DNAs.** All substrates were labeled at the 5′ end. 0.01 μM of each substrate was incubated with 0.2 μM Sfn-His protein for 1 h at 37 °C in the presence of 5 mM $MnCl_2$ for RNAs and 5 mM $MgCl_2$ for DNAs. Oligo$(dT)_{4-22}$ ladder consists of single-stranded DNA oligos from 4 to 22 bases long, increasing by 1 base increments. DNA5 and DNA8 are single-stranded DNA of 5 and 8 bases in length. *Lanes 1, 5, 9,* and *13* are the no protein controls. *Lanes 2, 6, 10,* and *14*, 5-min incubations with Sfn-His; *lanes 3, 7, 11,* and *15*, 15-min incubations; and *lanes 4, 8, 12,* and *16*, 45-min incubations.

as substrate for Sfn-His, we used a single-stranded oligo(dT) ladder from 4 to 22 bases in length, and single-stranded DNA oligos of 5 and 8 nt. As shown in Fig. 5, Sfn-His is capable of degrading short single-stranded DNA, although with less efficiency than 5-mer RNAs. Furthermore, its DNase activity is inversely related to the length of the DNA oligo, as seen for the RNase activity of *E. coli* Orn (19). The data above is also consistent with the lack of DNase activity reported for Orn on double stranded T7 chromosomal (large) DNA (10).

The DNase and RNase Activities Are Intrinsic to Sfn-His—To confirm that the observed DNase and RNase activities are intrinsic to the Sfn-His protein, a catalytically inactive Sfn-His mutant was constructed. Amino acid residue Asp^{136} (Fig. 1, in Exo III motif) was selected because an aspartate to alanine mutation at the structurally equivalent residue (5) in *E. coli* DNA pol I causes a 13,000-fold decrease in 3′ to 5′ exonuclease activity (14). The D136A Sfn-His mutant was purified using the same procedure as described for wild type Sfn-His protein (Fig. 6*A*). When compared with wild type Sfn-His, D136A Sfn-His mutant displayed a ≥50-fold reduced exonuclease activity for both RNA5 and DNA5 substrates (Fig. 6*B*). These data are consistent with both nuclease activities being intrinsic to the Sfn-His protein, and not being the result of protein contaminants. The results also demonstrate the importance of this acidic residue in the enzymatic function of the 3′ to 5′ exonuclease family members (1).

We subsequently examined Sfn nuclease activity on DNA structures known to be products/substrates of DNA repair processes. As might be expected from the results above, in the presence of Mn^{2+} or Mg^{2+}, we did not detect any protein-dependent degradation of 42-base pair double-stranded DNAs of different configurations, including gapped, nicked, 4-nucleotide recessed or overhanged 3′ ends, or flap structures (data not shown; substrates described in Ref. 20).

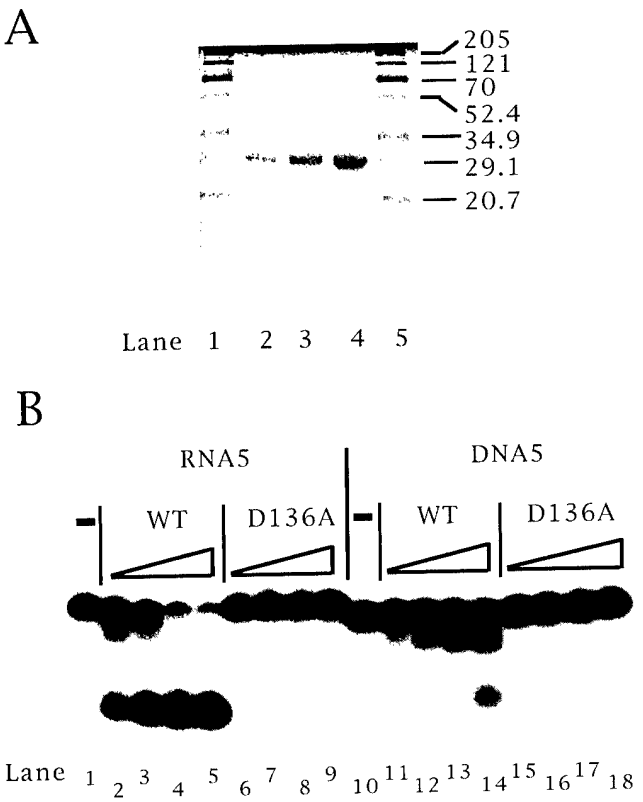

FIG. 6. **The effect of a D136A mutation on the DNase and RNase activities of Sfn-His.** *A*, purity of D136A Sfn-His mutant as determined on a 15% polyacrylamide SDS gel stained with Coomassie Blue R-250 dye. *Lanes 1* and *5* are protein markers; and *lanes 2–4* are 2.5, 5, and 10 μg of Ni-affinity purified D136A Sfn-His. Protein marker sizes in kilodaltons are indicated to the *right*. *B*, exonuclease activity of D136A Sfn-His mutant with RNA5 and DNA5 single-stranded substrates. *Lanes 1–9* are with RNA5, and *lanes 10–18* are with DNA5 substrates. The substrate concentration is 200 nM. *Lanes 1* and *10* are the no protein control. *Lanes 2–5* and *11–14* are 12, 24, 48, and 96 nM of purified wild type Sfn-His (WT). *Lanes 6–9* and *15–18* are 12, 24, 48, and 96 nM of purified D136A Sfn-His mutant. The reactions were incubated at 37 °C for 20 min.

Kinetic Parameters of the Sfn Nuclease Activities—To determine the reason(s) for the different nuclease efficiencies of Sfn-His, we determined the Michaelis-Menten constant (K_m), maximal velocity (V_{max}), and the apparent rate of catalysis (k_{cat}) for comparable RNA and DNA substrates (Fig. 7). The K_m of RNA5 (K_m = 1.56 μM) is essentially identical to that of DNA5 (K_m = 1.51 μM). In contrast, the V_{max} and k_{cat} values were ~4-fold higher for RNA5 (V_{max} = 0.015 μM min^{-1}, k_{cat} = 1.5 min^{-1}) than for DNA5 (V_{max} = 0.004 μM min^{-1}, k_{cat} = 0.39 min^{-1}). Our K_m value for RNA5 is consistent with the micromolar range reported for *E. coli* Orn on p(A)$_5$ single-stranded RNA substrates (19).

DISCUSSION

The human *SFN* gene belongs to the *YjeR/ORN* subfamily of the 3′ to 5′ exonuclease superfamily previously described (1, 5). Some of the members of this superfamily, most notably the Werner syndrome gene product and the polymyositis-scleroderma overlap syndrome 100-kDa autoantigen (PM-Scl 100), are associated with human disease (21, 22). While a connection of *SFN* to a specific human disease is not obvious, the ubiquitous expression of its transcript may suggest a general and essential role for the encoded protein in mammalian cells. Notably, the human *SFN* gene maps to chromosome position 11q23.1–11q23.2, a region that undergoes translocation events

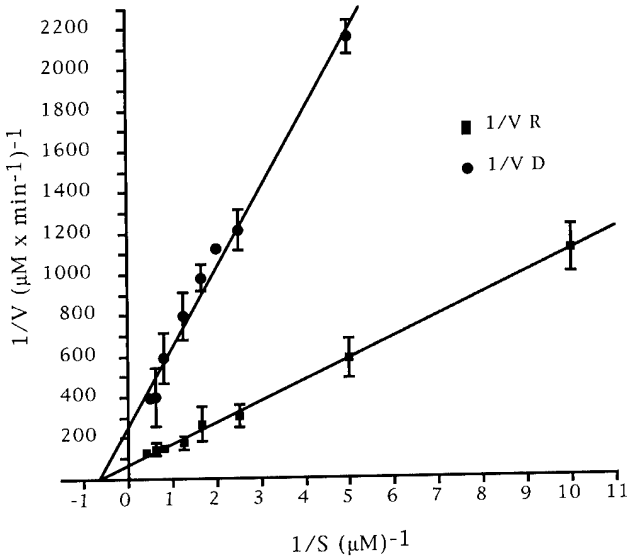

FIG. 7. **Double reciprocal Lineweaver-Burk plot of Sfn exonuclease activity on 5-nt single-stranded RNA5 and DNA5.** The *x* axis is the reciprocal of substrate (1/S) in (μM)$^{-1}$ units. The *y* axis is the reciprocal of velocity (1/V) in (μM × min^{-1})$^{-1}$ units. ■ represents RNA5; ●, DNA5 substrate. The data presented here is the average of five independent experiments for RNA5 and of four independent experiments for DNA5 in the presence of its preferred metal cation Mn^{2+}. *Error bars* represent the standard deviation. Linear regression analysis showed a correlation coefficient of 0.997 for RNA5 and 0.986 for DNA5.

in several leukemias (23, 24), although none of these translocation breakpoints have been finely mapped to *SFN*.

The unique NH_2 terminus of hSfnα contains a consensus cleavage site pattern for mitochondrial processing proteases (17), whereas both Sfnα and Sfn possess a nuclear targeting signal in their COOH-terminal domains. This observation suggests that an alternative splicing event has evolved to give rise to a mitochondrial (Sfnα) and a nuclear (Sfn) version of the Ynt20/Orn equivalents in human. However, at present, the genomic DNA sequence of the entire *hSFN* gene is not available, and thus the alternatively spliced products cannot be confirmed. Notably, in the mouse EST data base, there are also multiple transcripts, suggesting that alternatively spliced murine *SFN* transcripts exist as well. Future studies will need to address whether there is tissue-specific expression of the mRNA splice variants found in mammals. Interestingly, while *S. cerevisiae* maintains a homologue to *hSFN*α (called *YNT20* or *REX2*), we were unable to find a homologue to *SFN* in the NCBI data base using the Blastp search program.

A knockout of the *E. coli SFN* homologue, the *ORN* gene, results in cellular lethality (7). An *E. coli* temperature-sensitive mutant is not only lethal at the nonpermissive temperature (*i.e.* where Orn is inactive), but accumulates small oligoribonucleotides, indicating that Orn maintains an essential activity to degrade RNA (8). Three possibilities were provided as to why *ORN* deletion mutants are inviable (8): 1) accumulation of oligoribonucleotides results in a depletion of cellular mononucleotides; 2) accumulated oligoribonucleotides inhibit certain enzymes and interfere with essential metabolic processes; or 3) Orn has an additional unknown function that is responsible for the growth cessation. Since Sfn is capable of degrading both RNA and DNA, we propose that the human protein operates to remove not only short RNAs (likely resulting from RNA degradation processes) (25, 26), but also short single-stranded DNAs that might arise as products of DNA repair and recombination. Thus, by extension (8), Sfn would function globally to recycle nucleotides or to remove nucleic acids that may interfere with essential cellular processes. How

the nuclease activities of the Orn/Ynt20 proteins would function in mitochondrial DNA escape, a process that involves translocation of mitochondrial DNA to the nucleus (9) and is possibly linked to cellular aging or senescence (27), is presently unclear. Furthermore, although unlikely, whether the NH_2-terminal differences between these proteins affect substrate specificity will need to be determined.

Not surprisingly, Sfn-His, which shares ~50% identity in amino acid sequence to its bacterial counterpart, has very similar biochemical properties to Orn (5). In particular, both proteins degrade short RNAs in a 3′ to 5′ direction, prefer Mn^{2+} as its metal cofactor, and have an enzymatic activity temperature optimum of ~50 °C. However, gel filtration chromatography suggests that the human Sfn-His fusion protein is a tetramer, in contrast to *E. coli* Orn, which exists as a homodimer (6), suggesting that these proteins may maintain differing activities as well.

The nuclease activities of both Sfn and Orn (19) are inversely proportional to the length of the single-stranded substrate. Furthermore, previous kinetic data of *E. coli* Orn has shown that the K_m values for short and long single-stranded RNAs are similar (19). We observed that Sfn has a similar K_m for short single-stranded RNAs and DNAs, but that such short RNAs are degraded ~4-fold more efficiently than DNAs. Such experimental observations raise questions of how the substrate length or the nucleic acid chemistry influences Sfn/Orn enzymatic activity. To answer these questions will require determining which step(s) is influenced by nucleotide length or nucleic acid composition. High resolution structural data of Sfn, alone and in complex with RNA and DNA, would also shed light on the recognition and catalytic mechanisms of these proteins. Lastly, our studies emphasize that future experiments should pay particular attention to the potential range of substrate diversity recognized by the other 3′ to 5′ exonuclease superfamily members.

REFERENCES

1. Moser, M. J., Holley, W. R., Chatterjee, A., and Mian, I. S. (1997) *Nucleic Acids Res.* **25,** 5110–5118
2. Bernad, A., Blanco, L., Lazaro, J. M., Martin, G., and Salas, M. (1989) *Cell* **59,** 219–228
3. Koonin, E. V., and Deutscher, M. P. (1993) *Nucleic Acids Res.* **21,** 2521–2522
4. Joyce, C., and Steitz, T. (1994) *Annu. Rev. Biochem.* **63,** 777–822
5. Koonin, E. V. (1997) *Curr. Biol.* **7,** R604–R606
6. Zhang, X., Zhu, L., and Deutscher, M. P. (1998) *J. Bacteriol.* **180,** 2779–2781
7. Deutscher, M. P. (1993) *J. Bacteriol.* **175,** 4577–4583
8. Ghosh, S., and Deutscher, M. P. (1999) *Proc. Natl. Acad. Sci. U. S. A.* **96,** 4372–4377
9. Shafer, K. S., Hanekamp, T., White, K. H., and Thorsness, P. E. (1999) *Curr. Genet.* **34,** 438–448
10. Niyogi, S. K., and Datta, A. K. (1975) *J. Biol. Chem.* **250,** 7307–7312
11. Wilson, D. M., III, Carney, J. P., Coleman, M. A., Adamson, A. W., Christensen, M., and Lamerdin, J. E. (1998) *Nucleic Acids Res.* **26,** 3762–3768
12. Burgess, R. R. (1991) *Methods Enzymol.* **208,** 3–10
13. Pace, C. N., Vajdos, F., Fee, L., Grimsley, G., and Gray, T. (1995) *Protein Sci.* **4,** 2411–2423
14. Erzberger, J. P., and Wilson, D. M., III (1999) *J. Mol. Biol.* **290,** 447–457
15. Derbyshire, V., Grindley, N. D., and Joyce, C. M. (1991) *EMBO J.* **10,** 17–24
16. Sambrook, J., Fritsch, E. F., and Maniatis, T. (1989) *Molecular Cloning: A Laboratory Manual,* 2nd Ed., Cold Spring Harbor Laboratory, Cold Spring Harbor, NY
17. Gavel, Y., and von Heijne, G. (1990) *Protein Eng.* **4,** 33–40
18. Hicks, G. R., and Raikhel, N. V. (1995) *Annu. Rev. Cell Dev. Biol.* **11,** 155–188
19. Datta, A. K., and Niyogi, S. K. (1975) *J. Biol. Chem.* **250,** 7313–7319
20. Lee, B. I., and Wilson, D. M., III (1999) *J. Biol. Chem.* **274,** 37763–37769
21. Shen, J. C., Gray, M. D., Oshima, J., Kamath-Loeb, A. S., Fry, M., and Loeb, L. A. (1998) *J. Biol. Chem.* **273,** 34139–34144
22. Bluthner, M., and Bautz, F. A. (1992) *J. Exp. Med.* **176,** 973–980
23. Ziemin, L., van der Poel, S., McCabe, N. R., Gill, H. J., Espinosa, R., III, Patel, Y., Harden, A., Rubinelli, P., Smith, S. D., Le Beau, M. M., Rowley, J. D., and Diaz, M. O. *Proc. Natl. Acad. Sci. U. S. A.* **88,** 10735–10739
24. Chen, Z., Brand, N. J., Chen, A., Chen, S. J., Tong, J. H., Wang, Z.-Y., Waxman, S., and Zelent, A. (1993) *EMBO J.* **12,** 1161–1167
25. Morrissey, J. P., and Tollervey, D. (1995) *Trends Biochem. Sci.* **20,** 78–82
26. Jacobson, A., and Peltz, S. W. (1996) *Annu. Rev. Biochem.* **65,** 693–739
27. Shafer, K. S., Hanckamp, T., White, K. H., and Thorsness, P. E. (1999) *Curr. Genet.* **36,** 183–194

The Human Interferon- and Estrogen-Regulated *ISG20/HEM45* Gene Product Degrades Single-Stranded RNA and DNA in Vitro

Lam H. Nguyen, Lucile Espert, Nadir Mechti, and David M. Wilson, III

Molecular and Structural Biology Division, Lawrence Livermore National Laboratory, P.O. Box 808, L-441, Livermore, California 94551, and U475 INSERM, 99 rue du Puech Villa, 34197 Montpellier Cedex 5, France

Biochemistry®

Reprinted from
Volume 40, Number 24, Pages 7174–7179

The Human Interferon- and Estrogen-Regulated *ISG20/HEM45* Gene Product Degrades Single-Stranded RNA and DNA in Vitro†

Lam H. Nguyen,‡ Lucile Espert,§ Nadir Mechti,*,§ and David M. Wilson, III*,‡

Molecular and Structural Biology Division, Lawrence Livermore National Laboratory, P.O. Box 808, L-441, Livermore, California 94551, and U475 INSERM, 99 rue du Puech Villa, 34197 Montpellier Cedex 5, France

Received January 22, 2001; Revised Manuscript Received April 19, 2001

ABSTRACT: The human *ISG20/HEM45* gene was identified independently on the basis of its increased level of expression in response to either interferon or estrogen hormone. Notably, the encoded protein is homologous with members of the 3′ to 5′ exonuclease superfamily that includes RNases T and D, and the proofreading domain of *Escherichia coli* DNA polymerase I. We provide here direct biochemical evidence that Isg20 acts as a 3′ to 5′ exonuclease in vitro. This protein displays a pH optimum of ~7.0, prefers Mn^{2+} as a metal cofactor, and degrades RNA at a rate that is ~35-fold higher than its rate for single-stranded DNA. Along with RNase L, Isg20 is the second known RNase regulated by interferon. Previous data showed that Isg20 is located in promyelocytic leukemia (PML) nuclear bodies, known sites of hormone-dependent RNA polymerase II transcription and oncogenic DNA viral transcription and replication. The combined data suggest a potential role for Isg20 in degrading viral RNAs as part of the interferon-regulated antiviral response and/or cellular mRNAs as a regulatory component of interferon and estrogen signaling.

Interferons (IFNs)[1] make up a family of secreted cellular proteins involved in regulating cell proliferation, cellular differentiation, immune response, and the general antiviral response (reviewed in refs *1*−*3*). Estrogen is a hormone that promotes mitogenic responses in a number of cell types, particularly female reproductive tissue (*4*). The *ISG20* (interferon-stimulated gene product of 20 kDa) gene, also called *HEM45* (HeLa estrogen-modulated, band 45), was identified on the basis of transcript induction following exposure to either IFN or estrogen (*4*, *5*). These observations suggested a role for Isg20 in mediating the regulatory and/or developmental activities of such agents.

Isg20, like some other IFN-induced proteins, is located in spherical nuclear particles termed promyelocytic leukemia protein oncogenic domains (PODs) (also known as nuclear domain 10 or the Kr body; reviewed in refs *6* and *7*). PODs are large multiprotein complexes associated with the nuclear matrix (*6*). Although the precise function of these substructures is unknown, certain observations suggest that they may be preferential targets for viral infection and thus could play a mechanistic role in the antiviral action of IFNs (reviewed in ref *7*). In addition, PODs have been implicated in transcriptional regulation (*8*), apoptosis (*9*), maintenance of genomic stability (*10*) and telomere length by a telomerase-independent process (*11*), p53 acetylation, and p53-dependent cellular senescence upon oncogene expression (*12*). Notably, the number and morphology of PODs vary through the cell cycle and in some pathological contexts, including leukemia and viral infections (reviewed in ref *7*).

Recently, Isg20 was placed into the 3′ to 5′ exonuclease superfamily (*13*). This superfamily includes RNases (such as RNase T and D), the proofreading domains of the Pol I family of DNA polymerases, and DNases that exist as independent proteins (such as *Escherichia coli* Exo I) or as domains within larger polypeptides (such as a region within the Werner's syndrome helicase) (*13*−*15*). Homology within the superfamily is concentrated at three conserved exonuclease motifs termed *Exo*I, *Exo*II, and *Exo*III (*13*, *14*). In this report, we present the first biochemical evidence that Isg20 is a 3′ to 5′ exonuclease with a preference for RNA over single-stranded DNA.

EXPERIMENTAL PROCEDURES

Buffers and Reagents. All reagents were purchased from Sigma unless otherwise indicated. Restriction enzymes were purchased from New England Biolabs. Labeled nucleotides were from Amersham. Spectrophotometric-grade glycerol was obtained from Fisher. pET vectors were from Novagen (Madison, WI). DNA oligos were obtained from Operon Biotechnologies (Alameda, CA). Synthetic RNA was obtained from Dharmacon Research (Boulder, CO). L buffer (lysis buffer) contains 50 mM Tris-HCl (pH 7.0), 50 mM NaCl, 20% glycerol, 20 mM β-mercaptoethanol, and 1 mM phenylmethanesulfonyl fluoride (PMSF). W5 buffer is 50 mM Tris-HCl (pH 7.9), 500 mM NaCl, 20% glycerol, 5 mM

† This work was carried out under the auspices of the U.S. Department of Energy by Lawrence Livermore National Laboratory under Contract W-7405-ENG-48 and supported by U.S. Army US-AMRMC (BC980514) and NIH (CA79056) grants to D.M.W. L.E. and N.M. are supported by grants from the Association pour la Recherche contre le Cancer, the Ligue Contre le Cancer, the Federation pour la Recherche Medicale, and the INSERM and CNRS.

* To whom correspondence should be addressed. D.M.W.: e-mail, wilson61@llnl.gov; phone, (925) 423-0695; fax, (925) 422-2282. N.M.: e-mail, mechti@montp.inserm.fr; phone, 04-67-63-62-71; fax, 04-67-04-18-63.

‡ Lawrence Livermore National Laboratory.

§ U475 INSERM.

[1] Abbreviations: IFN, interferon; PML, promyelocytic leukemia; POD, promyelocytic leukemia protein oncogenic domain; PMSF, phenylmethanesulfonyl fluoride.

10.1021/bi010141t CCC: $20.00
Published on Web 05/19/2001

imidazole, 10 mM β-mercaptocthanol, and 1 mM PMSF. W20 is identical to W5, but with 20 mM imidazole. E250 buffer is identical to W5 except it contains 250 mM NaCl and 250 mM imidazole. All pH values were determined at 21 °C.

Purification of Recombinant Isg20 Proteins. To generate pIsg20-His, the *ISG20* coding region was PCR amplified using primers NCO5′ (5′-GCATGCCATGGCTGGGAGC-CGTGAG-3′) and 3′XHO (3′-CGAGTCTCGAGGTCTGA-CACAGCCAGG-5′), partially digested with *Nco*I and *Xho*I, and subcloned into these sites of pET28a (Novagen). This construct allows for expression of a carboxyl-terminal six-histidine-tagged Isg20 fusion protein under the control of the T7 RNA polymerase promoter. To generate a pIsg20D94G plasmid that expresses a D94G (located within the *Exo*II exonuclease motif; *13*) histidine-tagged mutant protein, a 145 bp *Pst*I fragment containing this mutation was gel isolated from the *Pst*I-digested pGST-Isg20ExoII plasmid (see below) and subcloned into the internal *Pst*I sites of pIsg20-His.

The pGST-Isg20 was generated by first PCR amplifying the *ISG20* cDNA coding region with GST 5′ (5′-GTC GGA ATT CAA CTC GAG ATG GCT GGG AGC CGT-3′) and GST 3′ (5′-ACG GTC GAA TTC TAG AGA AAA TAT AGA GCC-3′). The PCR product was then subcloned into the *Eco*RI site (underlined above) of pGEX2T (Amersham/Pharmacia) in the same open reading frame as the GST domain. Site-specific mutants were created using the procedure of the QuickChange Site-Directed Mutagenesis Kit (Stratagene). The following primer sets were employed for PCR amplification (the mutated codon is underlined): for the D11G mutation in the *Exo*I motif, EXO IA (5′-GAG GTG GTG GCC ATG GGC TGC GAG ATG GTG GGG CTG GGG-3′) and EXO IB (5′-CCC CAG CCC CAC CAT CTC GCA GCC CAT GGC CAC CAC CTC-3′); for the D94G mutation in the *Exo*II motif, EXO IIA (5′-CAT GAC CTG AAG CAC GGC TTC CAG GCA CTG AAA GAG GAC-3′) and EXO IIB (5′-GTC CTC TTT CAG TGC CTG GAA GCC GTG CTT CAG GTC ATG-3′); and for the D154G mutation in the *Exo*III motif, EXO IIIA (5′-CAC AGC TCG GTG GAA GGT GCG AGG GCA ACG ATG-3′) and EXO IIIB (5′-CAT CGT TGC CCT CGC ACC TTC CAC CGA GCT GTG-3′). Appropriate PCR products were subsequently cloned into the pGST-Isg20 to generate pGST-Isg20*Exo*I, pGST-Isg20*Exo*II, and pGST-Isg20*Exo*III.

To generate the His-tagged Isg20 protein, pIsg20-His was transformed into the BL21(DE3)/pLysS *E. coli* strain (Novagen). An overnight culture of 100 mL was subsequently grown at 37 °C in LB (1% bacto-tryptone, 0.5% bacto-yeast extract, and 1% NaCl) with 30 μg/mL kanamycin and 25 μg/mL chloramphenicol. The overnight culture was used to inoculate 2 L of the same medium. This culture was grown at 37 °C with vigorous aeration until the A_{550} was ~0.6. Isopropyl 1-thio-β-galactopyranoside was then added (final concentration of 1 mM) to induce Isg20-His protein expression. After induction for 4 h, cells were harvested, and cell pellets were frozen at −20 °C. Notably, the pIsg20-His plasmid, but not the pIsg20D94G plasmid, causes a 2−3-fold decrease in the rate of growth of BL21(DE3) cells (in the uninduced state and with the pLysS plasmid; data not shown), suggesting that the nuclease activity of Isg20 reduces the growth rate. The cell pellet was thawed and resuspended in 30 mL of L buffer. The cell suspension was sonicated using a Misonix XL sonicator with a macrotip at the maximum setting with two 1 min bursts. The cell lysate was centrifuged at 27000*g* for 30 min at 4 °C. To the supernatant was added slowly polyethyleneimine with constant stirring to a final concentration of 0.3% to remove nucleic acids (*16*). The suspension was centrifuged, and to the supernatant were added NaCl and imidazole to final concentrations of 500 and 5 mM, respectively. The soluble protein extract was then incubated with 2 mL of Ni−NTA resin (Qiagen, Santa Clarita, CA) for 1 h at 4 °C with gentle rocking. This suspension was centrifuged, and the resin was washed two times each with 20 mL of W5 buffer, followed by two washes each with 20 mL of W20 buffer. Isg20-His proteins were then eluted from the Ni−NTA resin four times, each with 2 mL of E250 buffer. These eluants were pooled. Imidazole was removed by two rounds of concentration with Centricon 30 concentrators and dilution with L buffer containing 0.1 mM DTT. Glycerol was then added to the retentate to a final concentration of 50%, and these protein samples were stored at −20 °C, as Isg20-His appears to be sensitive to multiple freeze−thaw cycles. Under such storage conditions, Isg20-His is stable for ~3 months. Concentrations of protein solutions were determined by measuring the absorbance at 280 nm and using the theoretical molar extinction coefficient E_{280} of 13 325 M^{-1} cm^{-1} calculated for Isg20-His (*17*). From 2 L of induced bacterial culture, we obtained ~0.5 mg of Isg20-His fusion protein. GST-Isg20, GST-Isg20*Exo*I, GST-Isg20*Exo*II, and GST-Isg20*Exo*III fusion proteins were generated and partially purified according to the protocol of Pharmacia.

Nuclease Assays. Various DNA and RNA substrates were labeled at the 5′ end with T4 polynucleotide kinase and [γ-^{32}P]ATP (*18*). RNA5 is 5′-GAUCG-3′. DNA5 is 5′-GATCG-3′. Supercoiled pET-28a was used as the promoter DNA template to produce a 343-nucleotide RNA with a 15-base stem and 6-base loop structure (TΦ transcription terminator) at the 3′ end (*19*). For the 210-nucleotide RNA, the transcription template was the pET-28a plasmid linearized with *Xho*I, a restriction enzyme that cuts specifically between the T7 promoter and the TΦ transcription terminator. Uniformly labeled RNA substrates were synthesized with T7 RNA polymerase and [α-^{32}P]GTP according to the instructions of the manufacturer (Gibco-BRL).

Labeled nucleic acid substrate (200−400 fmol) was incubated with 40−1000 fmol of Isg20-His protein at 37 °C in 10 μL of 50 mM HEPES-KOH (pH 7.0) 10% glycerol, 50 mM NaCl, 1 mM $MnCl_2$, 0.01% Triton X-100, and 1 mM DTT. The reactions were stopped with 10 μL of an 80% formamide dye solution, and the mixtures were heated at 80 °C for 3 min and then fractionated on a 20 or 22.5% urea (8 M)−polyacrylamide gel. Visualization of the labeled substrate and product was achieved using a Molecular Dynamics (Sunnyvale, CA) STORM 860 Phosphorimager, and quantitative analysis was performed using Molecular Dynamics ImageQuant version 1.11 software. For the pH titrations, instead of 50 mM HEPES-KOH (pH 7.0), different pHs were obtained using a buffer mixture of constant ionic strength consisting of 25 mM acetic acid and MES, and 50 mM Trizma base (*20*). Specific activity is defined as units per microgram of Isg20-His, with 1 unit being 1 pmol of RNA5 or DNA5 substrate degraded to mononucleotides in 1 min at 37 °C.

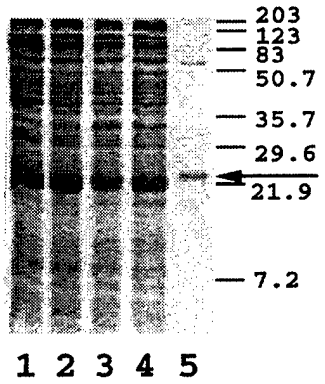

FIGURE 1: Isg20-His protein. Aliquots of protein fractions from the various purification steps separated on a 15% polyacrylamide–SDS gel: lane 1, whole cell extract; lane 2, whole cell supernatant; lane 3, 0.3% polyethyleneimine supernatant; lane 4, flow-through from Ni affinity chromatography; and lane 5, Ni affinity-purified fraction. Sizes of protein standards are indicated in kilodaltons on the right. The gel was stained with Coomassie Blue R250. The arrow indicates the position of Isg20-His.

To search for potential inhibitory effects of the three GST-Isg20 mutant proteins (D11G, D94G, or D154G), 0.1 nM RNA5 was preincubated on ice for 20 min with either of the mutants at 1 nM. Subsequently, 0.05 nM WT Isg20-His protein (which by itself degrades ~100% of the RNA5 substrate) was added to the mutant-containing reaction mixtures and the mixture incubated at 37 °C for 10 min. RNA5 degradation was then evaluated as described above.

RESULTS

Isg20 Is a 3′ to 5′ Exonuclease. The *ISG20* cDNA encodes a 181-amino acid protein of 20 363 Da with a theoretical pI of 9.5. This protein belongs to the 3′ to 5′ exonuclease superfamily (*13*) based on the presence of the three characteristic *Exo*I, -II, and -III motifs (*14*). To examine experimentally the possibility of nuclease activity, the *ISG20* gene was subcloned into the pET28a plasmid to produce a C-terminally tagged Isg20-His fusion protein. The recombinant protein was partially purified as described in Experimental Procedures (Figure 1). As shown in Figure 2 A, this Isg20-His preparation degraded RNA5, DNA5, and the single-stranded region of a 3′ DNA flap, stopping at the double-stranded DNA junction. Isg20-His was ~35-fold more active on single-stranded RNA than DNA (Figure 2A), with a specific activity of 4.21 ± 0.80 units/μg for RNA5 and 0.12 ± 0.01 unit/μg for DNA5. We observed degraded 4-mer products prior to detecting mononucleotides during the time course experiments with both substrates (Figure 2A), consistent with a 3′ to 5′ exonuclease activity.

To determine if the observed DNase and RNase activities are intrinsic to Isg20, particularly in light of the ~65 kDa contaminating band seen in Figure 1, a mutant in a presumed catalytic residue was constructed to obtain an inactive protein. Aspartate 94 of Isg20 was selected because an aspartate to alanine mutation at the structurally equivalent residue in *E. coli* DNA polymerase I causes a significant decrease in its 3′ to 5′ exonuclease activity (*21*). When compared to the wild-type protein, the Isg20D94G mutant (purified using the same procedure; see Experimental Procedures) displayed a >90% reduction in specific activity to degrade RNA5 and DNA5 substrates (Figure 2B). Moreover, a GST-Isg20 fusion

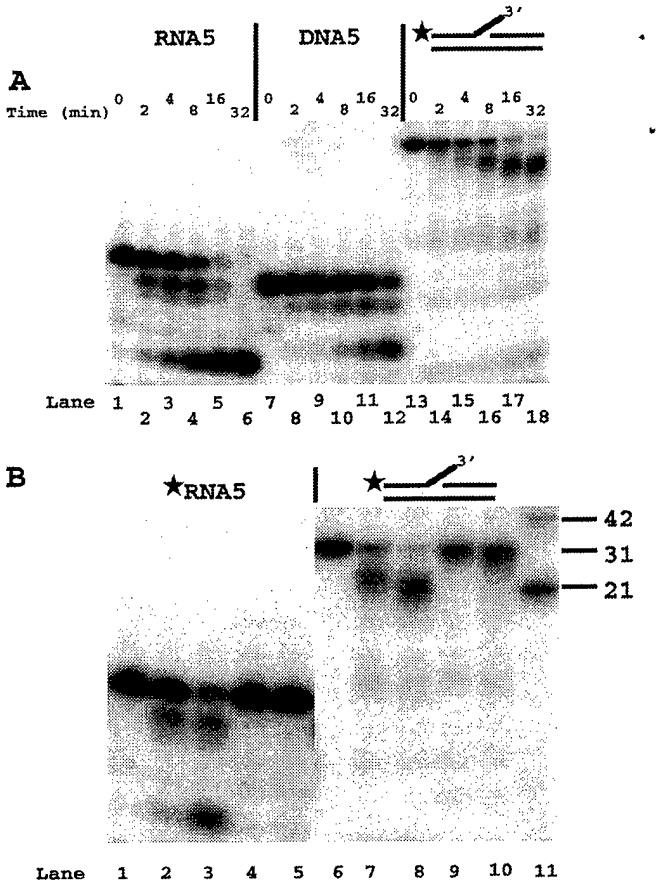

FIGURE 2: Isg20-His is a 3′ to 5′ exonuclease. (A) Isg20-His degrades single-stranded RNA and DNA. RNA5 (40 nM) or a DNA substrate, DNA5 or 3′ flap (40 nM), was incubated with 20 or 200 nM Isg20-His protein, respectively, for various times at 37 °C. RNA5, DNA5, and the strand containing the flap (as indicated by the star) were labeled at the 5′ end. The 3′ flap DNA substrate is described in ref *23*. Lanes 1–6 show reactions performed with RNA5; lanes 7–12, DNA5; and lanes 13–18, 3′ flap DNA substrate of 42 nucleotides in length with a 10-nucleotide flap. Lanes 1, 7, and 13 are the no protein controls; lanes 2, 8, and 14, 2 min incubations with Isg20-His; lanes 3, 9, and 15, 4 min incubations; lanes 4, 10, and 16, 8 min incubations; lanes 5, 11 and 17, 16 min incubations; and lanes 6, 12, and 18, 32 min incubations. (B) The D94G mutation abolishes the DNase and RNase activities of Isg20-His. Lanes 1–5 are the RNA5 (40 nM) reactions, and lanes 6–10 are with the 3′ flap substrate (40 nM). Reactions were performed at 37 °C for 20 min. Lane 1 is RNA5 untreated control. Lanes 2 and 3 correspond to RNA5 incubated with 5 and 15 nM wild-type Isg20-His (WT), respectively. Lanes 4 and 5 correspond to RNA5 incubated with 5 and 15 nM Isg20-D94G (D94G mutant), respectively. Lane 6 corresponds to the 3′ flap DNA undigested control. Lanes 7 and 8 correspond to 50 and 150 nM WT enzyme, respectively. Lanes 9 and 10 correspond to 50 and 150 nM D94G mutant, respectively. Lane 11 contains 42-nucleotide and 21-nucleotide DNA markers. The data presented here are representative of three independent experiments.

protein exhibited RNase and DNase activities similar to that of wild-type Isg20-His (under slightly different in vitro conditions), and site-specific mutations of D11G (in the *Exo*I motif), D94G (*Exo*II), and D154G (*Exo*III) in the GST fusion led to ≥85, ≥87, and ≥87% reductions, respectively, in RNase activity. These data are consistent with both nuclease activities being intrinsic to Isg20, and indicate the importance of these conserved residues. Notably, nucleases that are not members of the 3′ to 5′ exonuclease superfamily, specifically, human Ape1 (an abasic endonuclease of the *E. coli* exonuclease III family; *22*), *E. coli* endonuclease IV (a representa-

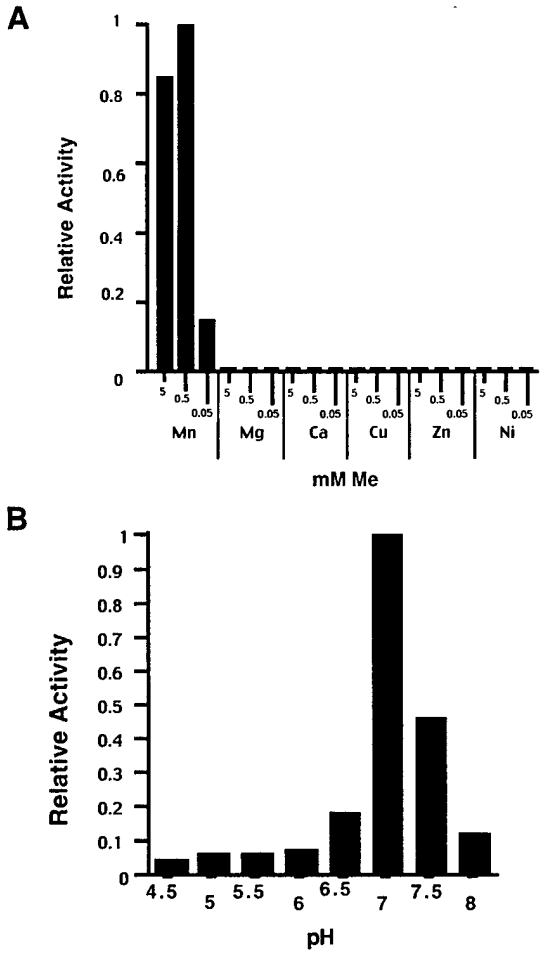

FIGURE 3: Metal cofactor requirement and pH optimum of Isg20-His exonuclease activity. (A) Metal cofactor requirement. The labeled RNA5 substrate (40 nM) was incubated with 2 nM Isg20-His enzyme for 10 min at 37 °C with different concentrations (5, 0.5, and 0.05 mM) of the various divalent metal cations, with chloride as the anion. Exonuclease activity is represented by the amount of labeled RNA5 substrate converted to the final mononucleotide product. The highest activity was designated as 1. At all the concentrations tested here, the relative activity was <0.01 for $MgCl_2$, $CaCl_2$, $CuCl_2$, $NiCl_2$, and $ZnCl_2$. Shown is a representative of three independent experiments. (B) pH optimum. 5′-labeled RNA5 (40 nM) was incubated with 2 nM Isg20-His for 10 min at 37 °C at the various pHs. The pH was maintained with a mixture of 25 mM acetic acid, 25 mM MES, and 50 mM Tris-HCl (*20*). The relative exonuclease activities were determined as described for panel A.

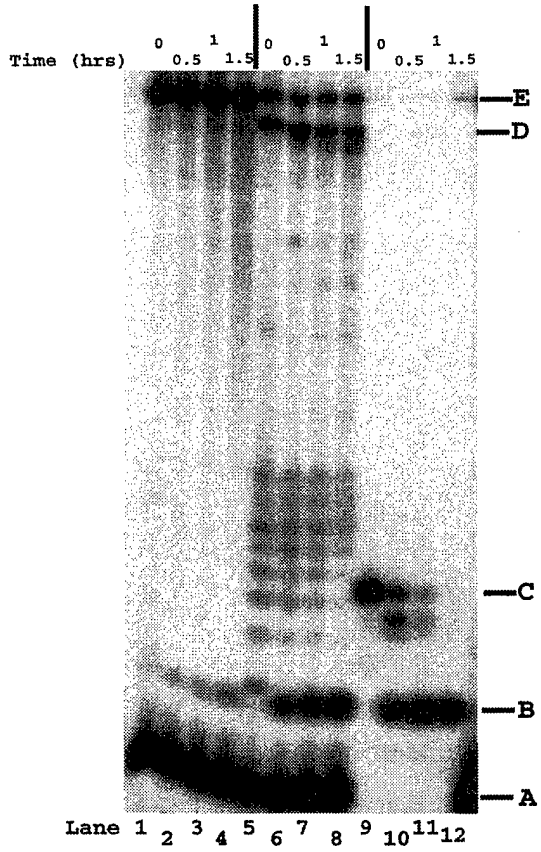

FIGURE 4: Isg20-His nuclease activity on long RNA substrates with or without a stem−loop structure at the 3′ end. Lanes 1−4 are reactions with uniformly labeled 343-base RNA with the TΦ transcription terminator stem−loop structure at the 3′ end, lanes 5−8 uniformly labeled 210-base RNA, and lanes 9−12 RNA5 labeled at the 5′ end. Lanes 1, 5, and 9 are the no protein controls. All the other lanes are reactions with 10 nM Isg20-His. Lanes 2, 6, and 10 are 30 min reactions at 37 °C; lanes 3, 7, and 11, 60 min reactions; and lanes 4, 8, and 12, 90 min reactions. On the right of the figure, band A is unincorporated [α-P^{32}]GTP; band B, Isg20-His degraded mononucleotide products; band C, RNA5 substrate; band D, 210-base RNA; and band E, 343-base RNA with a 3′ end stem−loop structure. The intermediate products observed in lanes 5−8 (including the no protein control) likely represent abortive initiation RNA products obtained with the linearized DNA promoter template, but not the supercoiled promoter template (*29*). Band E in lanes 5−8 is the RNA product generated from residual supercoiled promoter DNA, due to incomplete linearization of the promoter DNA template by *Xho*I.

tive of an independent abasic endonuclease family; *22*), and the human 5′-nucleases Fen1 and Exo1 (members of the RAD2 nuclease family; *23*), did not degrade DNA5 or RNA5 substrates (data not shown). Last, we found that preincubation of any of the three GST-Isg20 mutant proteins (1 nM) with 0.1 nM RNA5 substrate (see Experimental Procedures) inhibited the WT Isg20-His protein RNase activity by ≥90% in vitro, suggesting that these three GST-Isg20 fusion mutants bind the RNA5 substrate effectively and may exhibit dominant-negative effects in vivo.

Optimal Conditions for the Exonuclease Activity of Isg20. Using a 5′ end-labeled RNA5 as the substrate, we determined the divalent metal cation preference of the human Isg20-His protein. At metal concentrations of 0.05, 0.5, and 5 mM, only Mn^{2+} had a stimulatory effect on the exoribonuclease activity of Isg20-His, whereas Mg^{2+}, Ca^{2+}, Cu^{2+}, Zn^{2+}, and Ni^{2+} had virtually no effect (Figure 3A). The DNase activity of Isg20-His, as determined with the 3′ flap DNA substrate used in Figure 2, exhibited the same metal dependence (data not shown). Moreover, the RNase and DNase activities of Isg20-His on RNA5 and 3′ flap DNA substrates, respectively, exhibited the same pH response, with an optimum of ~7.0 (Figure 3B and data not shown).

Substrate Preference of Isg20. In addition to RNA5, DNA5, and 3′ flap DNA substrates, we examined Isg20-His nuclease activity on longer RNA substrates, with or without a stem−loop structure at the 3′ end. As shown in Figure 4, Isg20-His degrades not only short RNAs, such as RNA5, but also RNAs 210 nucleotides in length. However, the presence of a stem−loop structure at the 3′ end of a long RNA substrate caused a ~40-fold reduction in RNase activity (Figure 4). Such data are consistent with the above results indicating that Isg20-His degrades RNA in a 3′ to 5′

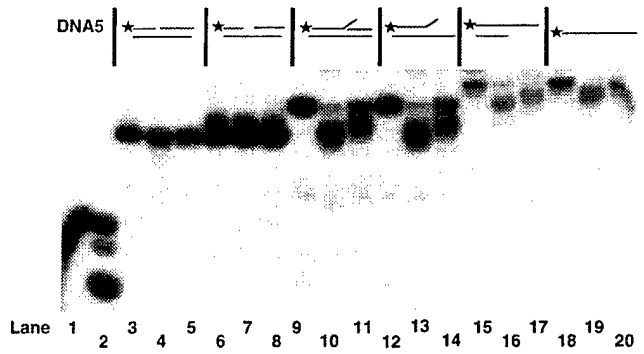

FIGURE 5: DNA substrate preference of Isg20-His. All substrates were labeled at the 5′ end as indicated by the star. Various DNA substrates (shown here and described in ref *23*) at a concentration of 40 nM were incubated with Isg20-His protein for 20 min at 37 °C. Lanes 1, 3, 6, 9, 12, 15, and 18 are the no protein controls. Lanes 1 and 2 are reactions with DNA5; lanes 3−5, nicked DNA; lanes 6−8, one-nucleotide gap DNA; lanes 9−11, 3′ flap DNA; lanes 12−14, 3′ pseudoflap DNA; lanes 15−17, 3′ overhang DNA; and lanes 18−20, single-stranded DNA 42 nucleotides in length. Lanes 2, 4, 7, 10, 13, 16, and 19 are reactions with 256 nM Isg20-His protein, while lanes 5, 8, 11, 14, 17, and 20 are reactions with 64 nM Isg20-His protein.

direction, and operates poorly on double-stranded regions. Results from Figure 4 also suggest that the exonuclease activity of Isg20-His is processive and not distributive on long RNA substrates, since, in a time course, we did not detect any intermediate-sized products between the starting RNA substrate and the final mononucleotide product.

Last, we examined Isg20 nuclease activity on other DNA structures known to be products and/or substrates of DNA repair processes (the various double-stranded DNA substrates used are described in ref *23*). We did not detect significant (<1% of DNA5 specific activity) protein-dependent degradation of 42 bp double-stranded DNAs of 5′ flap, gapped, nicked, or flushed structures (Figure 5 and data not shown). From Figure 5, Isg20 did exhibit weak 3′ to 5′ exonuclease activity (at least 10-fold lower than its RNase activity) on single-stranded DNAs of 42 nucleotides, and the single-stranded DNA regions of 3′ flaps, 3′ pseudoflaps, and 3′ overhangs.

DISCUSSION

We present here biochemical evidence that Isg20 is a 3′ to 5′ exonuclease, with a preference for single-stranded RNA over single-stranded DNA. Notably, Isg20 is the second known RNase regulated by IFN. RNase L, the first IFN-activated RNase, is normally a dormant, cytosolic endoribonuclease. However, upon viral infection or IFN exposure, 2′−5′ oligoadenylate (2−5A) synthetase is activated, increasing the intracellular concentration of short oligoadenylates (reviewed in refs *1*−*3*). These 2−5A oligoadenylates bind RNase L and promote its nuclease activity and, thus in turn, the degradation of cellular 18S and 28S rRNAs as well as viral RNAs, inhibiting cellular protein synthesis and viral propagation. Nevertheless, RNase L (−/−) knockout embryonic fibroblasts are able to develop an IFN-induced antiviral state, suggesting that alternative antiviral mechanisms exist (*24*). Given its localization to PODs, known sites of transcription and replication of oncogenic DNA viruses (e.g., simian virus 40, adenovirus, and herpes simplex virus; *7*), and substrate preferences, the Isg20 protein may act selectively to degrade viral mRNAs as part of an IFN-stimulated antiviral defense mechanism. Such a specialized function is also consistent with the fact that the *Saccharomyces cerevisiae* Isg20 homologue, Rex4p (which is not essential for viability), does not play a prominent role in processing many cellular RNA types (*25*).

The role of the weak DNase activity of Isg20 is less foreseeable. Since it was recently shown that proteins with roles in DNA recombination and telomere maintenance, such as the disease-related proteins Nbs1 and Mre11, are localized to PODs (*10*, *12*), the DNase function of Isg20 may contribute to telomere length maintenance in telomerase-negative immortal cells (*11*).

POD substructures have also been shown to play a role in regulating hormone-dependent transcriptional activity (*26*, *27*). It is conceivable that a function of Isg20, which is induced by estrogen and localized to PODs, is to downregulate the estrogen-dependent transcriptional response by degrading estrogen-induced mRNAs within these substructures. Notably, the estrogen-specific increase in the level of *ISG20* mRNA in immature rat uterus occurs after the enhanced expression of several estrogen early response genes, e.g., c-jun, c-fos, and zif-268 (*4*). Moreover, the downregulation of c-myc expression by IFN occurs through specific degradation of c-myc mRNA (*28*). Future in vivo studies are needed to determine the precise roles of the nuclease activities of Isg20, and the specific contributions of this protein to the cellular IFN-dependent response and the estrogen hormone signaling pathway.

ACKNOWLEDGMENT

We thank Dr. Robert Tebbs for his input.

REFERENCES

1. Lengyel, P. (1993) *Proc. Natl. Acad. Sci. U.S.A. 90*, 5893−5895.
2. Stark, G. R., Kerr, I. M., Williams, B. R., Silverman, R. H., and Schreiber, R. D. (1998) *Annu. Rev. Biochem. 67*, 227−264.
3. Player, M. R., and Torrence, P. F. (1998) *Pharmacol. Ther. 78*, 55−113.
4. Pentecost, B. T. (1998) *Steroid Biochem. Mol. Biol. 64*, 25−33.
5. Gongora, C., David, G., Pintard, L., Tissot, C., Hua, T. D., Dejean, A., and Mechti, N. (1997) *J. Biol. Chem. 272*, 19457−19463.
6. Seeler, J. S., and Dejean, A. (1999) *Curr. Opin. Genet. Dev. 9*, 362−367.
7. Maul, G. G. (1998) *BioEssays 20*, 660−667.
8. Zhong, S., Salomoni, P., and Pandolfi, P. P. (2000) *Nat. Cell Biol. 2*, E85−E90.
9. Guo, A., Salomoni, P., Luo, J., Shih, A., Zhong, S., Gu, W., Paolo, P., and Pandolfi, P. (2000) *Nat. Cell Biol. 2*, 730−736.
10. Lombard, D. B., and Guarente, L. (2000) *Cancer Res. 60*, 2331−2334.
11. Wu, G., Lee, W. H., and Chen, P. L. (2000) *J. Biol. Chem. 275*, 30618−30622.
12. Pearson, M., Carbone, R., Sebastiani, C., Cioce, M., Fagioli, M., Saito, S., Higashimoto, Y., Appella, E., Minucci, S., Pandolfi, P. P., and Pelicci, P. G. (2000) *Nature 406*, 207−210.
13. Moser, M. J., Holley, W. R., Chatterjee, A., and Mian, I. S. (1997) *Nucleic Acids Res. 25*, 5110−5118.
14. Moser, M. J., Holley, W. R., Chatterjee, Bernad, A., Blanco, L., Lazaro, J. M., Martin, G., and Salas, M. (1989) *Cell 59*, 219−228.

15. Joyce, C., and Steitz, T. (1994) *Annu. Rev. Biochem. 63*, 777−822.
16. Burgess, R. R. (1991) *Methods Enzymol. 208*, 3−10.
17. Pace, C. N., Vajdos, F., Fee, L., Grimsley, G., and Gray, T. (1995) *Protein Sci. 4*, 2411−2423.
18. Erzberger, J. P., and Wilson, D. M., III (1999) *J. Mol. Biol. 290*, 447−457.
19. Studier, F. W., Rosenberg, A. H., Dunn, J. J., and Dubendorff, J. W. (1990) *Methods Enzymol. 185*, 60−89.
20. Ellis, K. J., and Morrison, J. F. (1982) *Methods Enzymol. 87*, 405−426.
21. Derbyshire, V., Grindley, N. D., and Joyce, C. M. (1991) *EMBO J. 10*, 17−24.
22. Hadi, M., and Wilson, D. M., III (2000) *Environ. Mol. Mutagen. 36*, 312−324.
23. Lee, B. I., and Wilson, D. M., III (1999) *J. Biol. Chem. 274*, 37763−37769.
24. Zhou, A., Paranjape, J. M., Der, S. D., Williams, B. R., and Silverman, R. H. (1999) *Virology 258*, 435−440.
25. van Hoof, A., Lennertz, P., and Parker, R. (2000) *EMBO J. 19*, 1357−1365.
26. Doucas, V., Tini, M., Egan, D. A., and Evans, R. M. (1999) *Proc. Natl. Acad. Sci. U.S.A. 96*, 2627−2632.
27. LaMorte, V. J., Dyck, J. A., Ochs, R. L., and Evans, R. M. (1998) *Proc. Natl. Acad. Sci. U.S.A. 95*, 4991−4996.
28. Dani, C., Mechti, N., Piechaczyk, M., Lebleu, B., Jeanteur, P., and Blanchard, J. M. (1985) *Proc. Natl. Acad. Sci. U.S.A. 82*, 4896−4899.
29. Diaz, G. A., Rong, M., McAllister, W. T., and Durbin, R. K. (1996) *Biochemistry 35*, 10837−10843.

BI010141T

ELSEVIER

Mutation Research 485 (2001) 283–307

DNA Repair

www.elsevier.com/locate/dnarepair
Community address: www.elsevier.com/locate/mutres

The major human abasic endonuclease: formation, consequences and repair of abasic lesions in DNA

David M. Wilson III*, Daniel Barsky

Molecular and Structural Biology Division, Biology and Biotechnology Research Program, L-441, Lawrence Livermore National Laboratory, 7000 East Avenue, Livermore, CA 94551, USA

Received 7 September 2000; received in revised form 2 January 2001; accepted 5 January 2001

Abstract

DNA continuously suffers the loss of its constituent bases, and thereby, a loss of potentially vital genetic information. Sites of missing bases — termed abasic or apurinic/apyrimidinic (AP) sites — form spontaneously, through damage-induced hydrolytic base release, or by enzyme-catalyzed removal of modified or mismatched bases during base excision repair (BER). In this review, we discuss the structural and biological consequences of abasic lesions in DNA, as well as the multiple repair pathways for such damage, while emphasizing the mechanistic operation of the multi-functional human abasic endonuclease APE1 (or REF-1) and its potential relationship to disease.

Keywords: APE1; REF-1; Abasic DNA; AP endonuclease; Base excision repair; Apurinic/apyrimidinic site

1. Abasic sites in DNA

1.1. Formation

Apurinic/apyrimidinic (AP) sites (Fig. 1) are non-coding lesions that are generated via the spontaneous, chemically-induced, or enzyme-catalyzed hydrolysis of the *N*-glycosyl bond, severing the information-containing purine or pyrimidine base from the deoxyribose sugar of the DNA backbone. In 1972, knowing that bases are released from DNA in detectable amounts [1], Lindahl and Nyberg [2] measured the quantitative release of radiolabeled purine bases from double-stranded DNA as a function of temperature, pH and ionic strength. In a Mg^{2+}-containing buffer, they determined the rate constant for spontaneous in vitro depurination to be $4 \times 10^{-9}\,s^{-1}$ at 70°C and physiological pH (7.4). Extrapolating these data to a mammalian cell environment, it was estimated that ~12,000 purines would be lost spontaneously per genome per cell generation (20 h), in the absence of the protective effects of chromatin packaging. It was subsequently shown that depyrimidination occurs at a rate ~100 times slower than depurination [3], for reasons that are not obvious. In good agreement with these findings, studies using a biotin-tagged, aldehyde reactive probe (that covalently links to ring-opened AP sites) to monitor in vitro spontaneous AP site formation in purified calf thymus DNA projected roughly 9000 AP sites would be generated in each cell per day under normal physiological conditions [4].

To add to the burden of spontaneous AP sites, damaging chemicals — e.g. free radicals and alkylating agents — promote base release, often by introducing base modifications that destabilize the *N*-glycosyl linkage by generating a better leaving group moiety

* Corresponding author. Tel.: +1-925-423-0695; fax: +1-925-422-2282.
E-mail address: wilson61@llnl.gov (D.M. Wilson III).

0921-8777/01/$ – see front matter
PII: S0921-8777(01)00063-5

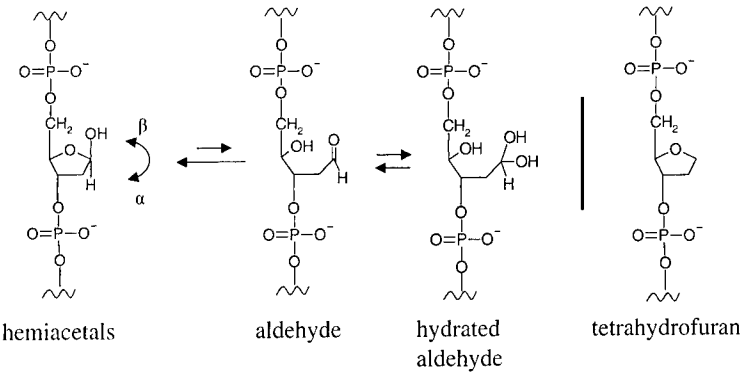

Fig. 1. Chemical form(s) of the natural abasic site and the abasic site analog, tetrahydrofuran. Natural AP sites (left of vertical bar) are in an equilibrium mixture of racemeric α- and β-hemiacetals (2-deoxy-D-*erythro*-pentofuranoses), an aldehyde form, and a hydrated aldehyde form. In vitro experiments indicate that the hemiacetal forms predominate, in roughly equal number, with ~1% aldehyde forms being present [64,65,201]. Tetrahydrofuran is commonly used as an abasic site analog (right of vertical bar), due to its chemical resistance to spontaneous strand cleavage [202].

(reviewed in [5,6]). For instance, alkylation of the N_7 position of purine residues accelerates base loss as much as six orders of magnitude. In addition, damaged or mismatched bases are excised from DNA by repair glycosylases, which hydrolyze the substrate *N*-glycosyl bond (reviewed in [7,8]).

Using a procedure involving the aldehyde reactive probe, Atamna et al. [9] found that roughly 2 million AP sites are produced in a *living* mammalian cell during a 20 h period. This value presumably reflects AP sites formed by spontaneous decomposition, endogenous chemical-induction and the repair activity of DNA glycosylases. Atamna et al. [9] measured the in vivo steady-state level of abasic sites to be <0.67 per 10^6 nucleotides, which corresponds to <4500 AP sites in a 3 billion nucleotide genome. This number differs dramatically from the steady-state value of 50,000 to 200,000 reported by Nakamura and Swenberg [10]. While the precise reason for the large discrepancy is unknown, it has been suggested that during the in vitro isolation of DNA (in the procedure employed by Nakamura and Swenberg), additional abasic sites were produced prior to AP site number determination. The differences in the estimated AP site levels may also reflect, to some degree, differences in the source of DNA, i.e. the type and age of the target cell [9]. Additional research and methodology development should help clarify the existing discrepancies.

1.2. Biological consequences

Non-coding AP sites are mutagenic and cytotoxic, and thus, represent a major threat to the integrity and survival of the cell. Their cytotoxicity is perhaps best exemplified by bacterial cells that contain a temperature-sensitive mutation in the gene encoding dUTPase (deoxyuridine triphosphatase) and lack full repair capacity for AP sites [11]. At non-permissive temperature, where dUTPase is inactive, intracellular dUTP levels are elevated, and thus, uracil is incorporated at high frequency (in place of thymine) into chromosomal DNA during replication. Subsequent removal of the uracil bases by uracil DNA glycosylase generates an increased number of AP sites in the genome. When accompanied by a defect in AP site repair, dUTPase-deficient cells are inviable, presumably due to the accumulation of these cytotoxic lesions. Consistent with this result, Schaaper and Loeb [12] found that the main outcome of introducing AP sites into φX174 *am*3 DNA is loss of biological activity as measured by phage viability in a transfection assay. Thus, it is presumed that in many instances, DNA (and RNA) polymerases pause and dissociate upon encountering an AP site, leading to the formation of replicative chromosome strand breaks (or abortive, non-productive transcriptional events), which at high enough frequency result in lethality or cellular dysfunction. Cytotoxicity of AP sites may also be related

to their ability to promote or inhibit (depending on their proximity to the cutting site) the DNA cleavage activity of topoisomerases (reviewed in [13]), and/or to irreversibly trap topoisomerase-DNA covalent complexes (e.g. seen with mammalian Topoisomerase I [14]).

The mutagenic potency of AP sites was first realized when it was found that noncomplementary nucleotides (e.g. guanine) are incorporated at higher than normal frequency during the in vitro copying of poly(dAdT) substrates treated with acid to promote base release [15]. It was subsequently shown that DNA and RNA polymerases, if able to bypass the lesion, preferentially incorporate an adenine opposite the abasic site (with there being some sequence-context effects) both in vitro and in vivo (referred to as the "A-rule" [16–26]). Occasionally, DNA polymerases bypass the lesion altogether by "skipping" the abasic site (presumably due to collapse of the DNA in specific sequence contexts; see below), an event that results in nucleotide deletion. It was recently been demonstrated in vitro that, in certain sequence arrangements, a single AP site can induce triplet repeat expansion — a phenomenon associated with neurological and neuromuscular diseases including Fragile X syndrome and myotonic dystrophy — presumably by replication slippage [27].

In *Escherichia coli*, AP site-directed mutagenesis requires activation of the SOS response system [12]. This damage-inducible pathway involves the induction of several genes that promote a transient mutator phenotype by altering the fidelity of replication, recombination and repair (reviewed in [28]). Notably, DNA polymerases that lack exonuclease proof-reading ability are activated during the SOS response, and such error-prone polymerases are more capable of bypassing an AP site in vitro than polymerases of high fidelity (i.e. those that maintain proof-reading capacity [18]). It has been postulated that apurinic sites are responsible for the G:C → T:A transversions associated with SOS activation [29].

Whereas *E. coli* exhibit a clear preference for incorporation of adenine opposite an abasic site (presumably mediated by polIV and polV during the SOS response [30]), a precise eukaryotic mutagenic pattern has not emerged. Specifically, yeast lacking efficient AP site repair exhibit an increased frequency of A:T to C:G transversions [31], suggesting that guanine is inserted opposite the apurinic lesion. In another study involving yeast, which used a recoverable shuttle vector system containing a site-specific abasic site, cytosine was found to be preferentially incorporated opposite the damage [32]. This latter finding is consistent with the activities of yeast Rev1, a protein that adds cytosine opposite abasic sites as a terminal transferase to facilitate translesion synthesis by the Rev3/Rev7 DNA polymerase complex (Polζ) (reviewed in [33,34]). In simian kidney (COS) cells, adenine, cytosine and thymine were found to be incorporated opposite AP sites at roughly the same frequency [35–38]. Conversely, in a separate study involving COS cells [39], preferential incorporation of adenine was observed opposite the abasic site analog, tetrahydrofuran (Fig. 1). In human lymphoblastoid cells, guanine was most commonly inserted opposite the abasic lesion [40]. The reason(s) for the wide variety of AP site-directed mutational outcomes in eukaryotes is unknown, but may reflect differences in the employed vector systems or the existence of multiple translesion replication machines.

Consistent with the mutagenesis pattern observed by Takeshita and Eisenberg [39], the recently discovered human Polη (XPV or RAD30A) and Polκ (Polθ or DINB1) translesion synthesis polymerases preferentially incorporate adenine opposite an abasic lesion in vitro, albeit inefficiently [41–46]. Similarly, both calf thymus DNA polymerase α and calf thymus DNA polymerase δ (in the presence of the processivity factor PCNA) predominantly incorporate dAMP opposite a model abasic site template [26,47]. Although cytosine was not found to be preferentially incorporated opposite the AP site in any of the mammalian cell line studies described above, in vitro biochemical experiments have shown that the human Rev1 protein exhibits dCMP transferase activity opposite an AP lesion [48]. In a more recent study, it was found that DNA polymerases Polι and Polζ act sequentially to bypass DNA lesions, with Polι preferentially inserting G or T opposite an abasic site, to facilitate damage bypass (i.e. "mispair" extension) by Polζ [49]. How these and other AP site bypass pathways are called upon (perhaps by damage-inducibility) and ultimately affect the mutagenic profile of abasic lesions in mammals is under investigation.

1.3. Structural considerations

The structural aspects of AP-DNA have been examined to gain insights into their mutagenic and cytotoxic effects. Under typical experimental conditions (1–3 mM DNA, pH 7–7.5, 10–20 mM $NaPO_4$, 100–150 mM NaCl, and 0.05–2.0 mM EDTA), two-dimensional nuclear magnetic resonance (NMR) spectroscopy, using relatively short oligonucleotides (9 to 11-mers), reveals that the helix of AP-DNA assumes more or less canonical B-DNA form [50–53]. However, sequence-specific conformational effects have been observed. For instance, a purine base opposite an abasic site remains stacked within the AP-DNA helix [54], whereas an "orphan" pyrimidine exists in both intra and extrahelical configurations, depending upon the chemical nature of the abasic site and the neighboring base sequence context [50,52,53,55–58]. Furthermore, purine residues flanking an AP site have a propensity to stack, which can give rise to the sugar and/or the orphan base being excluded from the double helix. While most studies indicate that the abasic site disrupts only the structure of neighboring base pairs, structural differences have been observed as many as four base pairs from the abasic site when positioned in the middle of a dA tract [58]. Several of the NMR studies, and a fluorescence study [59], have also indicated increased flexibility in abasic DNA.

Two computational methods have been applied to the prediction and characterization of abasic DNA. A conformational sampling approach, using internal coordinate molecular mechanics, showed sequence-dependent helix kinking and flexibility [60,61], that agreed well with the experimental data concerning intrahelical versus extrahelical orphan base conformations [62]. A molecular dynamics (MD) approach, where all the atoms of a 12-mer DNA, water and salt system are simulated under standard conditions for 1–2 ns, revealed unique kinking and increased molecular motion near the abasic site, relative to unmodified DNA controls (Fig. 2) [63]. The abasic sugar itself "flipped out" of the double helix, and displayed an

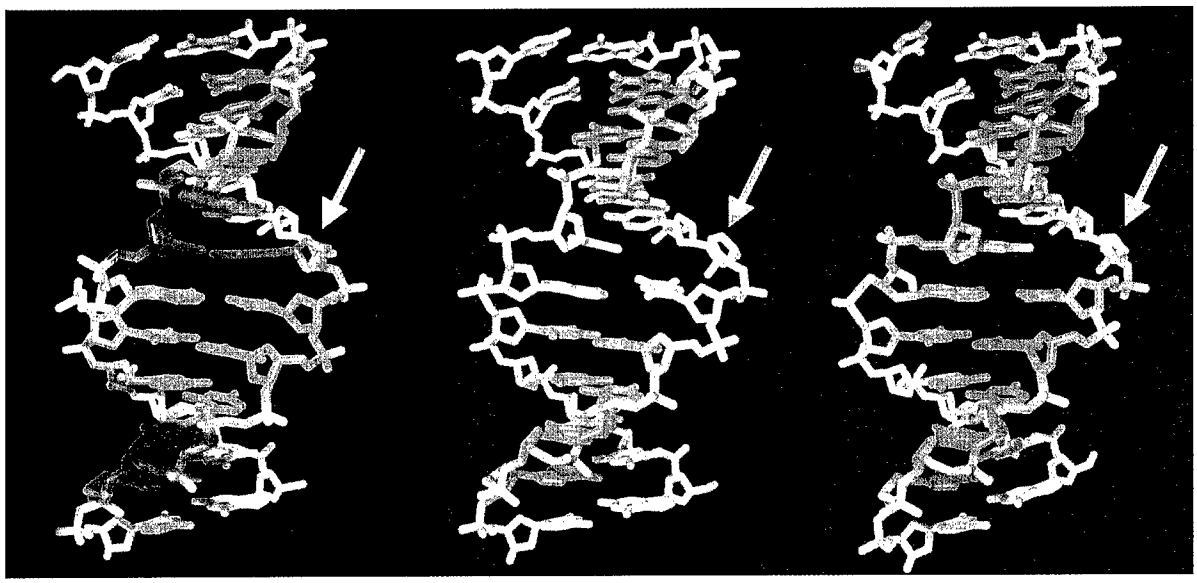

Fig. 2. Identical views of average DNA structures from MD simulations of essentially identical dodecamer duplexes with no abasic site (left), an abasic site opposite an orphan C base (middle), or an abasic site opposite an orphan G base (right). Shown are all non-hydrogen atoms (as capped-sticks), colored by the degree of internal movement where blue indicates the largest movement (5.0 Å) and red the smallest (0.7 Å). A blue arrow points to the 6th sugar, which is abasic in the middle and right models. Notice that atoms near the abasic site show more movement than the same atoms in the control (left), and that the "melted" nature of the region surrounding the C-orphan abasic site is visible (middle). The average structures were created by performing a root-mean-square (RMS) fit over all atoms for 0.5 ps sampling within a 1.5 ns MD trajectory. The isotropic RMS fluctuations were used to color each atom. The gap created by the missing base was filled mainly by water, or with a neighboring base when the sequence context makes pairing with the orphan base favorable [63].

unusually broad range of northern sugar puckers, beyond that of A-form DNA. Although some degree of "roll" is often found at pyrimidine-purine steps, the bending at the abasic site in these simulations was about twice as large, and involved both roll and tilt, which is unusual since tilt requires contortions of the DNA backbone.

The natural abasic ribose exists as an equilibrium mixture between four species — 99% as two hemiacetal enantiomers (α- and β-2-deoxy-D-ribofuranose) and ~1% as ring-opened aldehyde and hydrated aldehyde forms [64,65] (Fig. 1); the ring-opened forms are subject to beta-elimination that results in DNA strand scission [66]. Thus, in many structural, thermodynamic and biochemical studies, a prototypical abasic residue, tetrahydrofuran, has been employed due to its more stable, non-racemic nature. For the most part, structural studies involving the natural abasic ribose have yielded similar results to those using the analog. However, there have been observed effects of AP site chemistry on DNA structure. For instance, NMR indicates that the β-form of the sugar remains intrahelical while the α-form flips out [52]. Additionally, a chemical form of abasic damage, 2-deoxyribonolactone, results in an unkinked double helix [67]. Given the chemical instability (and consequent difficulties in synthesizing) of many of the natural AP site forms, determination of sequence- or chemistry-dependent effects on the structural and thus biological consequences of certain abasic sites may require inferences from additional computational modeling.

In spite of its modest effect on the overall helical structure of DNA, a single abasic site has a surprisingly strong destabilizing effect on double helices as determined by spectroscopic and calorimetric methods [68]. This observation agrees well with MD studies of AP-DNA showing distortion of the canonical structure near the abasic site, with mild disruption of Watson–Crick hydrogen bonds throughout the helix [63]. Depending on local sequence, calorimetric destabilization energies range widely from 6 to 14 kcal/mol [69], which is up to three times greater than the destabilization energy of the worst base-pair mismatch [70].

It is worth considering the connection between the structure/stability of AP-DNA and its handling by repair enzymes and polymerases. Although there is no understood molecular basis for the thermodynamic instability of AP-DNA, a lower duplex melting temperature (i.e. more structural disorder) has been shown to correspond to a reduced AP site incision efficiency for *E. coli* endonuclease IV ([71]; EndoIV, alternatively called Nfo, see next section). In regards to the molecular mechanism of AP site-bypass polymerization, scientists have for more than a decade postulated that the larger free energy of base–base stacking for purines (i.e. their "stickiness"), relative to that of the pyrimidines, would favor the insertion of purines opposite a non-coding site [56]. Purines were further argued to be incorporated preferentially opposite an AP site due to their space-filling capacity, as this characteristic helps stabilize the double helical structure [69]. This concept was recently bolstered by a study showing that a large, pyrene nucleotide analogue is preferentially inserted opposite an abasic site over natural DNA nucleotides [72]. Yet, even though the pyrene completely fills the abasic gap, and thus, maintains the native double helical structure, DNA polymerase (polI) stalling still occurs after the abasic site, as it does when adenine is inserted. This observation indicates that the polymerase must discriminate beyond the simple maintenance of the DNA helical structure when deciding whether to continue elongation, possibly by probing for key hydrogen bonds in the minor groove of the emerging duplex.

While space-filling and stacking interactions may give rise to preferential insertion of purines over pyrimidines, it may be the differential solvation that favors adenine over guanine incorporation opposite the abasic lesion. A recent theoretical study suggested that, in the absence of hydrogen bonds with the template, bases with lower solvation energies are preferentially inserted [73]. Thus, adenine, with roughly half the calculated solvation free energy of guanine, would be preferred for insertion opposite an abasic lesion (in accordance with the A-rule). This also concurs with the favored insertion of pyrene, since the solvation energy of pyrene is even lower than that of adenine.

2. The AP endonuclease families

To cope with the large number of mutagenic and cytotoxic abasic lesions in DNA, organisms are equipped with enzymes, termed AP endonucleases, that incise at the first phosphate 5′ to the AP site,

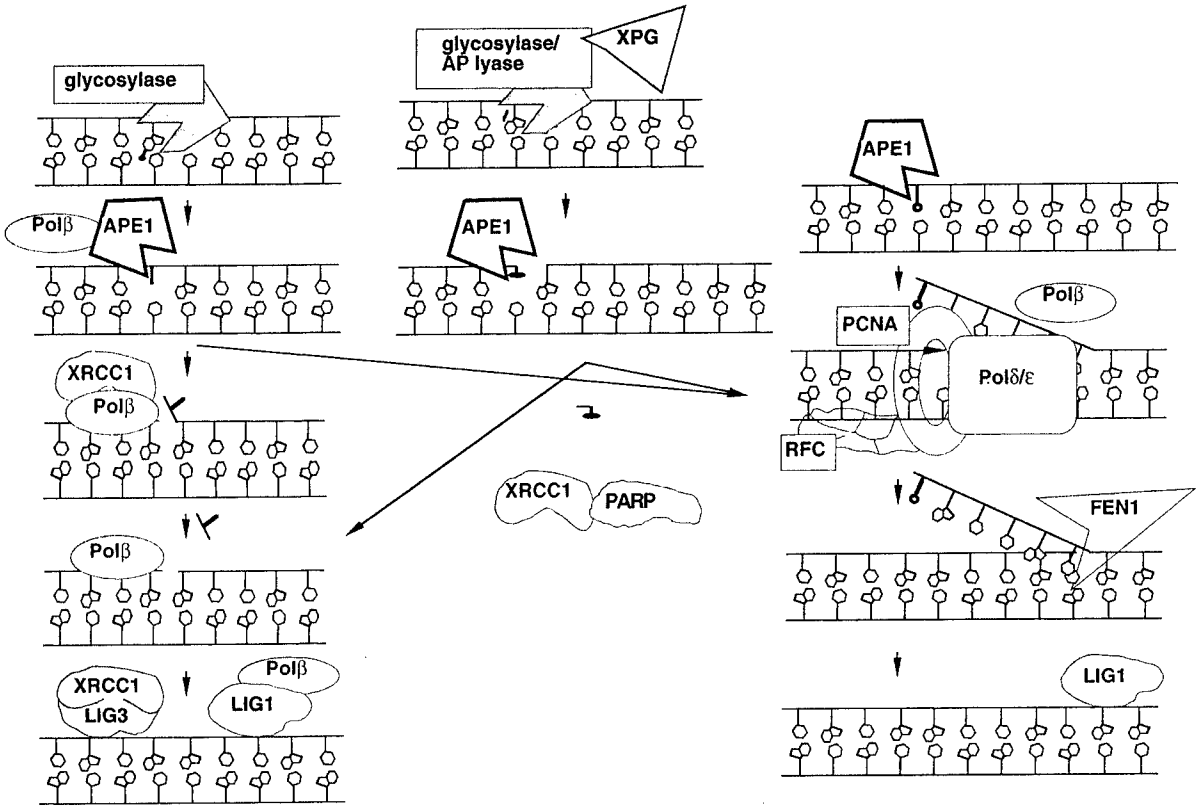

Fig. 3. The alternative pathways of mammalian BER. The short-patch (or single nucleotide, left) and the long-patch (or multiple nucleotide, right) pathways are depicted. Protein factors are shown and labeled, and overlapping symbols indicate protein–protein communication or stable interactions. For comprehensive reviews on BER see [203–206]. APE1 has a central role in that it incises at abasic sites and removes 3′-unsaturated aldehyde/3′-phosphate groups left behind by the AP lyase activity of bifunctional DNA glycosylases (center). XRCC1 and PARP can presumably bind and function at any stage involving strand breaks (reviewed in [207,208]). Abbreviations: xeroderma pigmentosum group G, XPG; polymerase β, Polβ; AP endonuclease, APE1; X-ray cross complementing, XRCC1; poly(ADP-ribose) polymerase, PARP; proliferating cellular nuclear antigen, PCNA; replication factor C, RFC; polymerase α/ε, Polδ/ε; flap endonuclease 1, FEN1; ligase 1 and 3, Lig1 and Lig3.

initiating a repair cascade that involves several proteins of the base excision repair (BER) pathway (Fig. 3). AP endonucleases have been divided into two families based on their amino acid sequence identity to either exonuclease III (ExoIII, alternatively called Xth) or EndoIV, the major abasic endonucleases of *E. coli* (Table 1). Under normal physiological conditions, ExoIII comprises ~90% of the total cellular AP endonuclease activity in *E. coli* [74]. However, during periods of oxidative stress, EndoIV is induced to protein levels that are comparable to ExoIII as a part of the SoxRS regulon, a response mechanism designed to prevent the deleterious effects of elevated intracellular concentrations of superoxide anions ([75]; reviewed in [76]). In mammals, the predominant AP endonuclease is APE1 (also called HAP1 or APEX), an enzyme that belongs to the ExoIII family [77–79]. Based on biochemical projections, APE1 comprises >95% of the total cellular AP site incision activity in human cell extracts [80]. A mammalian EndoIV counterpart has not yet been identified.

In contrast to both *E. coli* and humans, the major AP endonuclease of *Saccharomyces cerevisiae*, Apn1, is an EndoIV homolog [81]. Apn2/Eth1, the ExoIII equivalent in *S. cerevisiae* [82,83], exhibits a weak AP site-specific incision activity [84], and constitutes

Table 1
The major AP endonuclease family classifications[a]

Taxomony	ExoIII family		EndoIV family
Eukaryota			
Homo sapiens	APE1	APE2	?
Mus musculus	Apex	*	?
Caenorhabditis elegans	T42391	?	Apn1#
Drosophila	Rrp1	–	–
Arabidopsis thaliana	Arp	*	–
Schizosaccharomyces pombe	–	Apn2/Eth1#	Apn1
Saccharomyces cerevisiae	–	Eth1	Apn1
Archaea			
Methanobacterium thermoautotrophicum	B69126	–	G69001
Bacteria			
Escherichia coli	ExoIII (Xth)	–	EndoIV (Nfo)

[a] The "*" indicates that a likely or candidate sequence homolog was found in the expressed sequence tagged (EST) database. The "–" indicates that a sequence homolog was not detected in complete genome sequence. The "?" indicates that it is presently unknown whether there exists a sequence homolog. Those proteins listed by accession number or indicated by a "#" are database sequence homologs that have not been shown experimentally to exhibit relevant functional activities. It is noteworthy that *Schizosaccharomyces pombe* appears to lack AP endonuclease repair activity [214], and that *Arabidopsis thaliana* may possess two APE-1-like proteins, and a single APE-2-like protein [215].

<5% of the total cellular AP endonuclease activity. The reason for the reversal in AP endonuclease prevalence may reflect the nature of the DNA damage profiles (and, in turn, the most common environmental exposures) of the organism and/or the substrate specificities of the AP endonuclease families. While displaying significant overlap, the ExoIII and EndoIV members do indeed exhibit marked differences in their substrate preferences (reviewed in [85]).

In addition to AP site incision activity, AP endonucleases possess varying levels of 3′-phosphodiesterase activity for common free radical-induced DNA products, e.g. 3′-phosphates and 3′-phosphoglycolates, which require removal prior to repair synthesis or ligation. The bacterial proteins ExoIII and EndoIV, in addition to yeast Apn1, exhibit nearly equal 3′-repair and AP endonuclease activities (reviewed in [86]). Conversely, in vitro biochemical and in vivo complementation studies reveal that APE1 exhibits a relatively poor activity on 3′-blocking termini (>100-fold less efficient than its AP endonuclease activity) [77,78,80,87,88]. Thus, while in vitro reconstitution experiments indicate that APE1 can remove obstructive 3′-termini, including those produced by the AP lyase activity of bifunctional DNA glycosylases (Fig. 3; [89]), its poor 3′-repair activity suggests alternative repair proteins or processing mechanisms. It has also been suggested that, to overcome the weak 3′-repair activity and this apparently rate-limiting step in DNA strand break repair [90], mammalian cells have evolved a reactive oxygen species-dependent adaptive response (not observed with UV light or alkylating agent treatment [91,92]) that increases APE1 protein and mRNA, and promotes translocation of the protein to the nucleus. Interestingly, APE1 was recently found to remove the deoxyribonucleoside analog, β-L-dioxolane-cytidine — a replication chain terminator used in some anti-viral and anti-cancer treatment schemes — from the 3′-terminus of duplex DNA substrates [93].

The recent identification of human APE2 [84,94], which differs from APE1 at the N- and C-terminal ends, but retains many of the essential active site residues, marks the existence of a second subfamily of ExoIII-like proteins, which includes yeast Apn2/Eth1 (Table 1). The emergence of this additional sub-family raises questions regarding the relative biological contributions of APE1 and APE2 in mammals. Moreover, the reasons for the apparent weak nuclease activity of APE2 [84,94], once found, may suggest an alternative role for this protein, further expanding the biological repertoire of these enzymes.

3. The major mammalian AP endonuclease — APE1

Given its poor 3′-repair diesterase activity, it is somewhat surprising that, while APE1 was originally identified as an enzyme that incises at AP sites in DNA [95,96], the encoding cDNA was cloned via reverse genetics or immunoscreens following purification of a protein that removes 3′-damages [77,97,98]. The APE1 protein has a molecular mass of 35.5 kDa (excluding post-translational modifications), a theoretical pI of 8.3 and three consensus nuclear localization signals in the N-terminus. Partial proteolysis studies and crystallography results indicate that the human protein consists of a tight globular nuclease domain, and a flexible, disordered N-terminal region [99–102]. The core nuclease domain shares structural homology to not only ExoIII, but also to the non-specific endonuclease, DNase I [99,103]. Recently, it was found that the highly conserved core α/β sandwich motif of these Mg^{2+}-dependent endonucleases is also present in phosphatases and proteins involved in cell cycle regulation and signal transduction [104].

3.1. Substrate discrimination

The crystal structure of ExoIII bound to a single dCTP, and the contemporaneous structure determination of several proteins bound to a flipped out (extrahelical) base (reviewed in [105]), fostered the hypothesis that the ExoIII family members might bind specifically to abasic site-containing DNA by complexing with the flipped-out, unpaired "orphan" base [103]. However, placing an abasic site opposite another abasic site resulted in only a two- to three-fold reduction in the enzymatic activity of either ExoIII or APE1 [106,107], indicating a non-essential role for a base opposite in recognition and incision. Furthermore, replacement of a natural nucleotide (purine or pyrimidine) with a non-polar base analogue (which should be more strongly retained within the duplex structure) opposite an abasic site had no effect on APE1 or ExoIII incision activity [108]. Lastly, "bulged" DNA, which contains an additional, unpaired, extrahelical base, was neither bound nor incised, suggesting that a flipped-out base alone is not sufficient for recognition.

Soon thereafter, upon determination of the APE1 crystal structure, it was proposed that targeted recognition was accomplished by a specific hydrophobic interaction of a phenylalanine residue (Phe266) in the protein active site with the ring structure of the abasic moiety [99]. This proposal was at odds, however, with previous studies employing a propane acyclic abasic site analog that demonstrated that the absence of a ribose ring had little effect on the cleavage efficiency of APE1 or ExoIII [106,107,109]. Subsequent studies showed that catalytically-inactive APE1 mutant proteins bind acyclic AP site-containing DNAs with similar affinity to cyclic (tetrahydrofuran abasic site analogs) AP site substrates [110]. Furthermore, it has been shown that APE1 binds even single nucleotide-gapped DNA, indicating that the entire sugar of the abasic site is unnecessary for protein–DNA complex formation and stability [111].

Mutating Phe266 of APE1 to alanine imparted only a six-fold reduction in DNA binding or incision activity [108], suggesting a non-essential role for this residue as well. This result also argued against the hypothesis that substrate selectivity is mediated by insertion of a hydrophobic residue (Phe266 in APE1; Trp212 in ExoIII) into the abasic 'gap' [112], as occurs with the tripeptide Lys–Trp–Lys [113]. In ExoIII, however, Shida et al. [114] found that mutating Trp212 to serine generated a protein that exhibited no detectable AP site incision or binding activity. One possible explanation is that the non-conservative replacement of Trp212 with a hydrophilic residue [114] had a more severe affect on the structural integrity of the important recognition loop (i.e. the peptide region between β_V and β_{VI} of ExoIII or β_{10}/α_{11} of APE1) than replacement of Phe266 in APE1 with alanine [108] — neither study examined protein structure. Another interpretation is that disruption of the tight hydrophobic binding pocket of ExoIII (composed of a single aromatic residue Trp212, and Leu226 and Ile228)/APE1 (composed of two aromatic residues Phe266, Trp280 and Leu282; Fig. 4A) interferes with complex formation.

Weiss proposed in 1976 [74] that AP endonuclease specificity is mediated through the targeted recognition of the vacated abasic space within the duplex. From data described above, it is apparent that the gap per se does not play a direct role in specific binding and moreover that abasic-DNA does not take on a particular structure (i.e. does not form a structural "beacon") in the absence of the protein. However, as previously noted, MD simulations and NMR studies

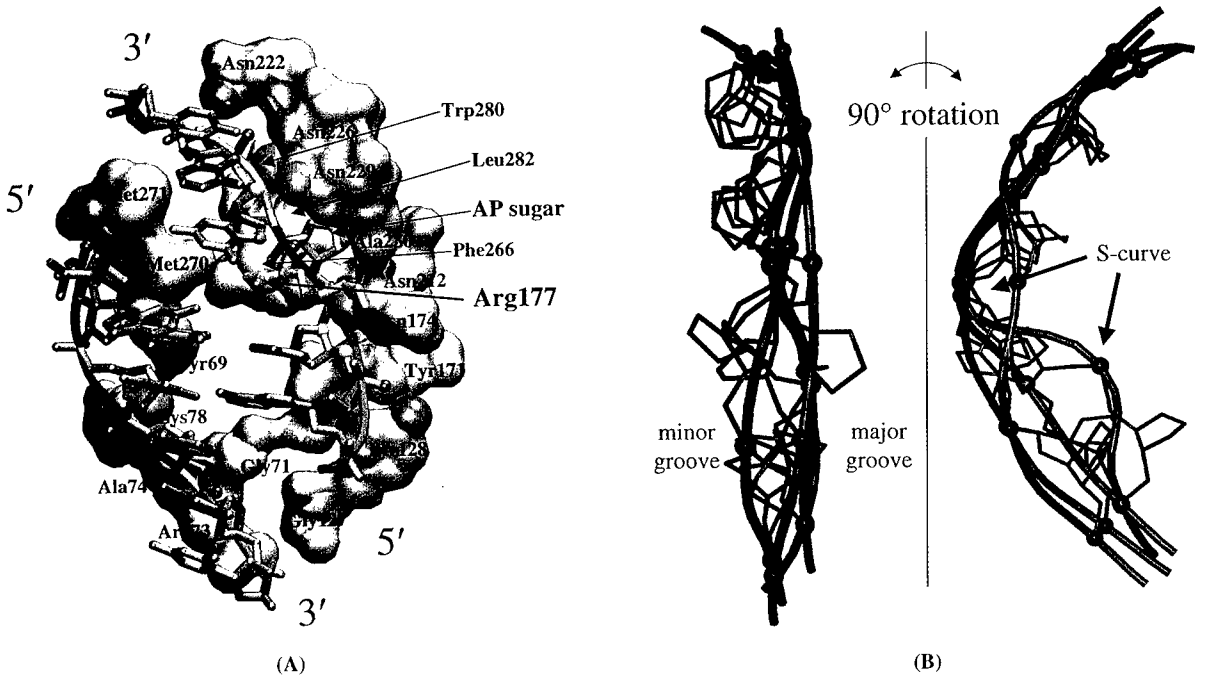

Fig. 4. (A) Contacts in the APE1-DNA crystal complex (Protein Data Bank entry 1DE8; [101]). The solvent accessible surface area of APE1 (green) is shown for all residues containing an atom within 3 Å of the double-stranded AP-DNA (gray). The contacting atoms are shown as red (oxygen), blue (nitrogen), and cyan/sky blue (carbon) space-filled atoms in the protein and smaller ball-and-stick atoms in the DNA. The hydrophobic pocket (orange), comprised of residues Trp280, Leu282, and Phe266, is within 4 Å of the DNA. (B) AP-DNA conformational changes. Comparison of the abasic site-containing DNA strands from molecular dynamics simulations, at 0 ns (black, canonical B-DNA), 1 ns (blue), and 1.4 ns (green) [63]) and within the APE1 co-complex (red). Using a least squares fit, DNA strand conformations from the simulations were aligned by the flanking sugars. The DNA of the crystal structure was subsequently aligned by the corresponding phosphate atoms. The sugar in the MD simulation flipped out into the minor groove, while in the protein complex the AP-sugar is in the major groove (left). The 1 ns (blue) and 1.4 ns (green) conformations demonstrate flexibility in the DNA backbone, and the 1 ns conformation only partly follows the S-shaped kinking observed in the co-complex (right, 90° rotated from left).

have found unique kinking, melting, and structural fluctuations local to the abasic site gap. Similar increased structural flexibility has been observed with single nucleotide-gapped DNA [115], an oligonucleotide substrate that is likewise bound by APE1 [111]. Conversely, fully base-paired, nicked DNA, which retains an unkinked B-DNA conformation with only slight distortions at the lesion site, is not bound by APE1. Similarly, stable APE1:DNA complexes have not been observed with unmodified duplex DNA [108,116,117]. Biochemical footprinting studies have found that upon APE1 binding, AP-DNA undergoes a detectable and specific conformational change [117]. The compilation of these results suggests that APE1 probes for increased backbone flexibility, specific to AP sites or single nucleotide gaps. The recently determined crystal structures of APE1:AP-DNA complexes provide seemingly conclusive evidence that APE1 is indeed a structure-specific nuclease that locates and productively binds DNA that can adopt a unique, kinked conformation [101].

While the conformations of AP-DNA in solution during a 1.5 ns MD simulation showed kinking at the AP site and flipping out of the abasic sugar [63], the co-crystal structure of APE1:AP-DNA reveals a much larger extent of DNA deformation (Fig. 4B). This result suggests that APE1 plays an active role in generating the bound conformational state of AP-DNA, and that binding occurs by "strain" of the substrate — similar in concept to "induced-fit," except that it refers to the substrate rather than the enzyme [118]. Thus, an integrated view is that APE1 scans DNA in

a "quasi-processive" mechanism, searching more than 200 nucleotides for an abasic site before dissociating if unsuccessful in its search [119], and upon encountering a substrate lesion, forces and traps the highly flexible DNA molecule into the bound conformational state through specific hydrophobic and electrostatic intermolecular contacts near the abasic site. For details on the molecular nature of the APE1-AP-DNA co-complex, see [120].

3.2. *Enzyme specificity*

The crystal structures reveal that APE1 possesses a preformed DNA binding interface, which undergoes little conformational change upon AP-DNA complex formation and includes a hydrophobic pocket that accommodates the abasic sugar while excluding normal bases [99,101]. It was suggested that this hydrophobic pocket would exclude racemized β-anomer AP sites, however, the co-complex structure does not appear to support this on the basis of merely steric exclusion. Further sequence and structure comparison of ExoIII/APE1 with DNase I indicated that three loop regions, which are absent from DNase I, may be important in AP site specificity (Fig. 5). It was shown by Cal and colleagues [121] that transposition of one of these "loops" (the α_M helix of ExoIII, which is positionally equivalent to APE1 α_8/Asn229 loop) from ExoIII into DNase I imparts AP site selectivity to the chimeric protein. In the APE1 co-complex crystal structure [101], these loops are inserted selectively into the major and minor grooves of AP DNA. Notably, these unique protein elements exhibit significant flexibility in APE1 [102,122].

Human L1 retrotransposon encodes an endonuclease (L1 EN) with amino acid sequence homology to the ExoIII protein family [123]. It was, therefore, postulated that retrotransposons mobilize by inserting

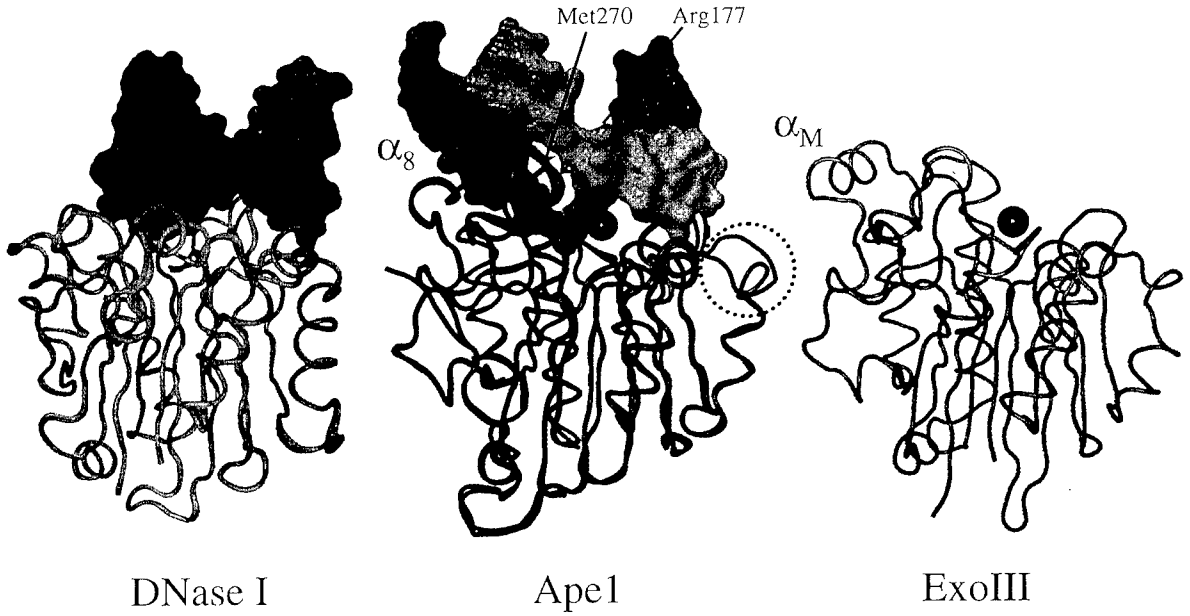

Fig. 5. Comparison of DNase I +/− DNA (green/yellow), APE1 +/− DNA (tan/red), and ExoIII (blue) from coordinates in PDB entries 1DNK [147]/3DNI [209], 1DE8 [101]/1BIX [99], and 1AKO [103], respectively. The metal ion (red sphere) coordinates are that of Sm^{3+} in 1BIX. Using an APE1-ExoIII alignment, the same relative position was used to place a metal ion in ExoIII. The dotted circle denotes a region (residues 100–104) of APE1 that changes from coil to α-helical upon DNA binding. The specificity loops (Arg 177, Met 270 and α_8 of APE1 are indicated. The α_M region of ExoIII (comparable to α_8/Asn229 loop of APE1) is also depicted. These specificity loops are notably absent from DNase I. The DNA double helices (left and center) are shown by solvent accessible surface area, using the SURF routine [210] within the VMD molecular graphics program [211], rendered by Raster3D [212]. Protein alignments were done through the LGA facility at the Protein Structure Prediction Center [213].

at DNA breaks generated by L1 EN cleavage. Despite its homology to ExoIII, L1 does not cleave at AP sites, but instead incises at unusual DNA structures found at the TpA junction of 5′(dT_n – dA_n):5′(dT_n – dA_n) duplex tracts [124]. Consistently, the loop domains that impart AP site specificity to APE1 and ExoIII are absent from L1 [99]. In this regard, there is similarity between L1 and DNase I, although DNase I appears to be even less specific in nature (reviewed in [125]). Recently, it was reported that open reading frame 1 of the L1Tc retrotransposon of *Trypanosoma cruzi* encodes a protein with AP endonuclease activity [126]. This result is surprising since it lacks the aforementioned AP site-specificity loops, particularly α_M of ExoIII [127], but could suggest structural similarity between abasic DNA and possible sequence-specific targets of this nuclease.

Despite the sequence and structural similarity between ExoIII and APE1 (28% identity across the conserved repair domain), these proteins exhibit significant differences in the scope of their nuclease capacities. ExoIII exhibits a powerful 3′ to 5′ exonuclease activity, which is comparable to its endonuclease activity [128], whereas APE1 displays only a minor exonuclease activity (<0.03% its endonuclease function) that appears to be substrate dependent [79,107]. Furthermore, unlike APE1 [107,108], ExoIII has been reported to bind and incise at AP sites in single-stranded DNA [112]. The observation that APE1 is more effective at removing 3′-damages from single-strand nicks or gaps of duplex DNA, than from blunt or 3′-overhang double-stranded ends [88] is consistent with APE1 interacting with both DNA strands around the damage [101,117,122] — this property of APE1 may also explain why others have been unable to detect significant 3′ to 5′ exonuclease activity on the blunt-ended duplex substrates typically used [80,129].

The structural basis for the ExoIII family of enzymes possessing both a 3′ nuclease and AP-specific endonuclease activity, albeit at varying capacities, is not known. It is possible that the specificity loops of APE1 and ExoIII permit binding only to DNAs that exhibit sufficient flexibility or to DNA ends, where no substrate bending is required. Notably, there is significant similarity between the destabilized region of an abasic site and the instability (or fraying) of the last base pair in double stranded DNA. Thus, DNA end-specific exonuclease and AP site-specific endonuclease activities may require disrupted regions of a DNA duplex. It would be interesting to know if certain sequence contexts, which promote DNA instability, permit low level "non-specific" APE1 endonuclease cleavage. Since APE1 demonstrates a 10-fold higher AP site incision activity and a 10-fold lower 3′-diesterase activity than ExoIII, there must exist differences in amino acid sequence and structural content (e.g. in the loop domains) that impart distinct enzymatic properties.

It is surprising that the AP endonucleases APE1, ExoIII and EndoIV all recognize and cleave 5′ to bulky exocyclic base adducts formed by *p*-benzoquinone (*p*-BQ) (reviewed in [130]). *E. coli* EndoIV consists of an $\alpha_8\beta_8$ TIM barrel fold that is similar to the structural framework of several sugar isomerases [131,132]. The EndoIV:AP-DNA crystal structure reveals that targeted recognition of AP-DNA occurs through unique loop domains that intercalate specific side chains into the abasic gap, compress the DNA backbone, bend the DNA ~90°, and promote "double-nucleotide flipping" by capturing the orphan base in an extrahelical conformation and sequestering the extrahelical AP site in an enzyme pocket that excludes undamaged nucleotides [132]. Though similar in many respects to APE1, EndoIV promotes a more severe DNA structural change and, unlike APE1, undergoes major conformational movements to accommodate DNA binding. Phosphodiester bond cleavage by EndoIV appears to involve three Zn^{2+} ions bound within the protein crystal. The divergent mechanisms of damage recognition and phosphodiester bond hydrolysis between the two AP endonuclease families likely explains their notable substrate specificity differences [106,107,133–138]. Still, how AP endonucleases recognize base adducts is presently unclear, particularly since AP sites and *p*-BQ-dC appear to cause different conformational changes in DNA as visualized by molecular modeling [139].

3.3. The catalytic reaction

The phosphodiester linkages of RNA and DNA are extremely resistant to spontaneous hydrolysis (reviewed in [140]). This resistance is in part attributed to the electrostatic repulsion of an approaching nucleophile by the negatively-charged oxygens of the phosphodiester backbone. Thus, neutralization of this

negative charge is thought to be a contributing factor in promoting phosphate hydrolysis. In the situation of an enzyme-catalyzed reaction, the remainder of the rate acceleration (which can be as great as 10^9) is probably manifested by the unique physical properties of the protein's active site, which likely facilitates the formation of the appropriate attack conformation.

The members of the ExoIII family incise the phosphodiester backbone via a divalent metal cation-facilitated acid–base $S_N2(P)$ catalytic mechanism. In this hydrolytic reaction, three events need to take place: (1) formation of the active site nucleophile; (2) neutralization and orientation of the negatively charged oxygens of the target phosphodiester bond, and establishment of the trigonal bypyramidal, pentacoordinate phosphorane transition state/intermediate; and (3) stabilization of the reaction product phosphomonoester leaving group [140]. Depending on the enzyme, the divalent metal ion cofactor (simply "metal" hereafter) is thought to play a role in all or some of the phases of the catalytic reaction. The finding that acyclic AP site analogs are incised in the absence of a metal cofactor suggests that the major role of the divalent metal in APE1 is in the establishment of the DNA transition state intermediate when faced with a ribose ring, and not in the chemistry of the catalytic reaction [110].

In the published crystal structures of ExoIII and APE1, a single metal ion is bound within the active site, with the metal being principally complexed to glutamate 96 of APE1 [99,103]. Consistent with the hypothesis that more than a single residue coordinates the metal [141], site-specific mutagenesis, metal-titration studies, metal-footprinting experiments, and molecular dynamics simulations indicate either a direct or indirect (i.e. through a water molecule) role for three amino acids of APE1 (Asp70, Glu96 and Asp308) in binding of the active site metal cofactor [122,142–144]. However, tight metal binding to APE1 has not been detected by atomic absorption spectroscopy [141,142], suggesting that stable APE1-metal binary complexes do not readily exist in solution and that the metal is not an integral component of the APE1 protein. Consistent with poor metal binding, APE1 is most active at magnesium concentrations (~5 mM) that are nearly six orders of magnitude higher than protein or DNA [95,142] — at even higher Mg^{2+} concentrations (>10 mM), where the charge density of the substrate is perturbed [145], APE1 incision activity is reduced. Importantly, APE1 incubated in the presence of EDTA still retains strong site-specific AP-DNA binding affinity in the 10^{-9} M range [117], indicating that a metal ion is not essential for protein conformational integrity or protein–DNA complex formation, and thus that the primary role of the metal is in the cleavage event. Addition of magnesium ions to protein–substrate complexes pre-formed in EDTA promotes APE1 incision, revealing that the divalent metal is successfully recruited to the catalytic active site, even when the protein is first bound. Thus, divalent metal acquisition by APE1 appears to occur in cooperation with DNA, and probably involves displacement of a monovalent metal ion. The specific activity of APE1 is highest with the divalent metal Mg^{2+}, $A_{Mg^{2+}}$, decreasing as follows: $A_{Mg^{2+}} > A_{Mn^{2+}} \gg A_{Ni^{2+}} > A_{Zn^{2+}} \gg A_{Ca^{2+}} = A_{K^+}$ [142].

APE1, and presumably ExoIII, appear to utilize the same mechanism for catalyzing incision adjacent to either a bulky adduct or an abasic site [139], indicating a single functional nuclease pocket. Initially, it was suggested that His309 of APE1, in cooperation with Asp283, acts as the general base to abstract a hydrogen from an active site water molecule to form the required nucleophile (Fig. 6, Scheme 1; [99,103,142]). The electron withdrawing metal cofactor was proposed to facilitate nucleophilic attack by orienting the phosphate group, stabilizing the transition state intermediate, and/or polarizing the target P–O 3′ bond [99,103]. This mechanism was similar in many ways to the initial endonuclease reaction of DNAse I [146,147]. Subsequent studies showing that APE1 was more active when Asp210 was mutated to a histidine relative to an alanine suggested that this residue operates as a proton donor, and thus, to stabilize the leaving group [110]. Consistent with Scheme 1, site-directed mutagenesis studies indicated that both Asp210 and His309 maintain an essential role in the incision reaction, but little or no role in AP-DNA complex formation [110,111,142,144,148].

Recent crystal structures of APE1 bound to either intact AP-DNA, or incised AP-DNA with Mn^{2+}, suggested a modified reaction scheme [101]. In this scheme Asp210 operates as the base to generate the active site nucleophile, His309 functions to orient and polarize the target P–O3′ bond, and the metal ion acts primarily to stabilize the leaving group (Fig. 6,

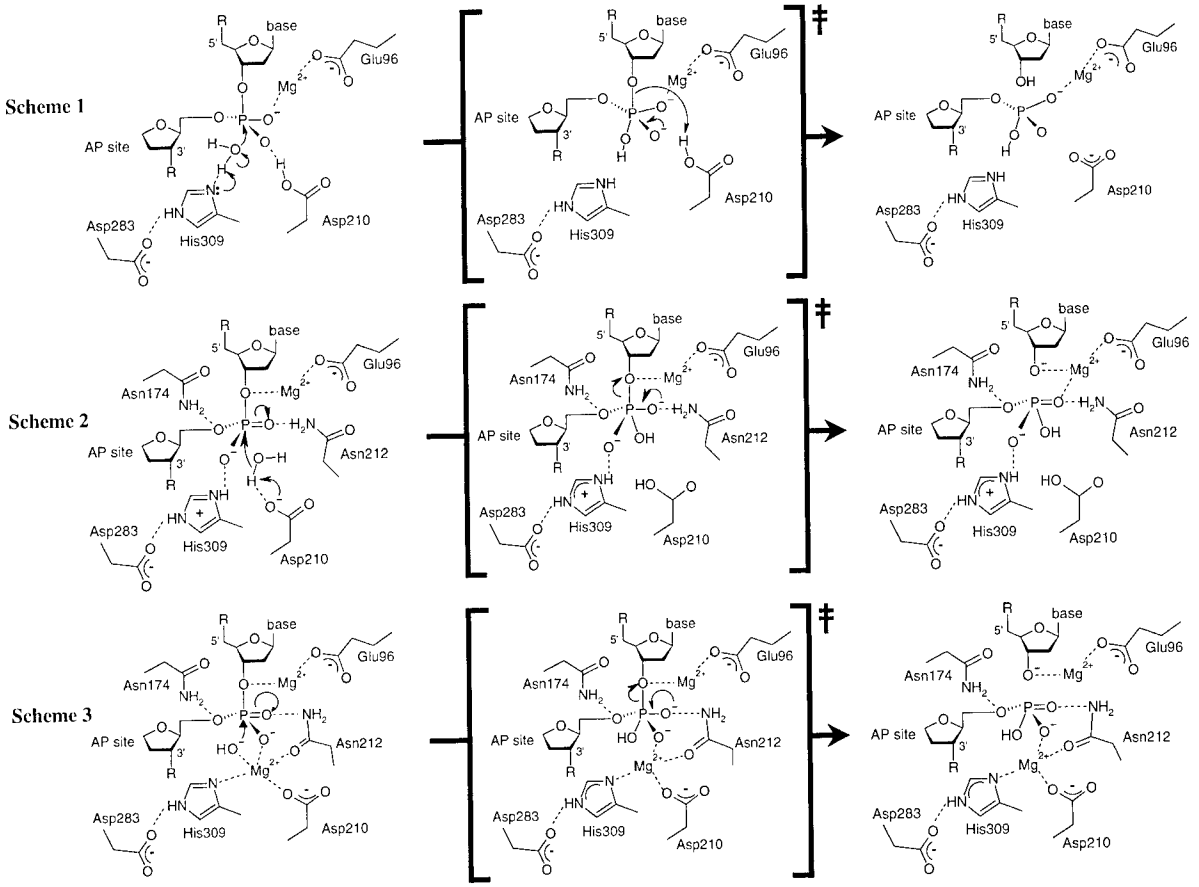

Fig. 6. Proposed catalytic reaction schemes for APE1. In Scheme 1, His309 abstracts a proton from a water molecule to generate a nucleophile (OH^-), while the Mg^{2+} has an electron withdrawing and likely an orienting effect on the phosphate [142]. A protonated Asp210 has been proposed to stabilize the leaving group [110]. In Scheme 2, Asp210 abstracts a proton from a water molecule to generate a nucleophile (OH^-), while a protonated His309 orients the phosphate, and Mg^{2+} stabilizes the leaving group [101]. In Scheme 3, the Mg^{2+} in Site A (Asp70 and Glu96) coordinates a hydroxyl ion, which carries out nucleophilic attack on the phosphorous 5′ to the abasic nucleotide [102]. The Mg^{2+} in Site B (Asp210, Asn212 and His309) acts to neutralize the charge of the pentacovalent intermediate and/or stabilize the 3′ leaving group. The transition state/intermediate of each reaction is indicated in the bracketed center.

Scheme 2). The observation that the metal ion concentration influences the rate of APE1 dissociation from incised AP-DNA [143] is consistent with the metal participating in leaving group stabilization.

While complicated by the effects of pH on protein–DNA complex formation, a series of pH titration experiments with site-specific APE1 mutants Asp210Asn/Lys/His suggested that this residue does not operate as the general base (Lam Nguyen and DMWIII, unpublished observations). Similar titration experiments also revealed that the pH profiles of Asp283Asn and His309Ser APE1 derivatives are not shifted as would be expected for His309 to operate as the base. Moreover, the previously published APE1 crystal structures were obtained at pH 6.2, a pH value outside of the range of APE1 activity (6.5–9.0, with a pH optimum of 7.5; [95]), raising potential concerns about the previously proposed reaction schemes. Since, a new APE1 crystal form at pH 7.5 has been solved with two lead (Pb^{2+}) ions in the active site [102], suggesting yet another reaction scheme involving two divalent metal ions (Fig. 6, Scheme 3) — more similar to what has been proposed recently for DNase I [149] and previously for the proofreading

domain of DNA polymerase I [150]. Future work towards conclusively elucidating the chemical details of the catalytic reaction, and identifying the precise role of the metal cation(s), will provide not only important mechanistic information, but may permit the design of structure–function based inhibitors. Such inhibitors (of a specific DNA repair protein) could have value in elucidating the biological function of the target protein (as a surrogate to genetic knockouts) or in sensitizing cells during anti-cancer treatment schemes, since most anti-cancer agents elicit their cytotoxicity through the introduction of lethal genetic damage.

3.4. BER pathway coordination

BER corrects most spontaneous-decomposition, alkylation and oxidative lesions (Fig. 3). The finding that APE1 facilitates binding of Polβ to DNA and stimulates the deoxyribose phosphodiesterase activity of Polβ in vitro [151] provided the first evidence that the BER pathway is coordinated. More recently, it has been shown that APE1 promotes the dissociation and in turn the turnover efficiency of the uracil (Udg) and thymine (Tdg) DNA glycosylases, indicating that the initial step of BER is also coupled [152,153]. Glycosylases have, thus, been suggested to bind tightly to abasic sites to provide protection to the chemically unstable AP site or prevent mutagenic bypass, and/or serve as a beacon for subsequent APE1 binding (and perhaps BER pathway selection) or alternative cellular responses. However, whether the in vitro BER "interactions" thus far observed affect the in vivo biology of BER has, in most cases, not been determined.

Interestingly, much of the BER communication appears to occur without tight protein–protein associations. For instance, stable protein complexes have not been observed with APE1/Polβ, APE1/Udg or APE1/Tdg [151–154]. Recent crystallography and biochemical studies [101] have instead suggested that BER coordination is facilitated through strategic bending or manipulation of the DNA by the initial protein factor, promoting subsequent DNA binding by the downstream enzyme in a "passing the baton" manner [155]. In these structure–function experiments [101], site-specific mutation of an arginine residue (Arg177Ala) in a DNA binding loop of APE1 was found to improve the enzyme's catalytic efficiency (i.e. increases k_{cat}/K_m), suggesting that APE1, and perhaps other proteins of DNA repair, evolved not for turnover efficiency, but for the kinetic effectiveness of the pathway as a whole. Thus, it was proposed that tight binding of APE1 to its incised product, and subsequent manipulation of the DNA structure, would promote the dowstream steps of BER. However, Strauss and colleagues previously reported that APE1 rapidly releases its product [116]. In these studies, steady-state and transient-state kinetic analysis indicated that the minimal scheme for APE1 endonuclease activity entails a Briggs–Haldane mechanism, implying that APE1 is a perfectly-evolved enzyme operating near the diffusion-controlled limit of its reaction. More recent experiments have found that APE1 is inhibited by its incised product [143], and can in fact form stable complexes with 5′-cleaved AP-DNAs [153], supporting the "passing the baton" mechanism.

It is worth pointing out that APE1 undergoes subtle, but significant, conformational changes upon binding AP-DNA (Fig. 5), but whether these alterations permit post-complex contacts with proteins of BER (e.g. Polβ) remains to be determined. Clarification of whether there are important protein interactions of APE1 may also require structural information on the first (N-terminal) 41 residues, which have hitherto been unobservable in structure determination experiments. Spectroscopic methods (e.g. NMR) and MD simulations, capable of illuminating the dynamical aspects of protein–protein and protein–DNA interactions, may also shed light on molecular movements potentially relevant to pathway coordination.

3.5. Additional biological contributions

It is worth noting that APE1 (also referred to as REF-1; [156]) was independently purified based on its ability to stimulate the sequence-specific DNA binding activity of Fos–Jun heterodimers (also called AP-1, a complex that functions as an intermediary transcriptional regulator in signal transduction processes) in vitro. Subsequently, it was determined that this binding activation was mediated by reduction of a specific cysteine residue within the DNA binding domain of the target transcription factor. The in vivo significance of such a regulatory mechanism was inferred from the fact that a Jun viral oncoprotein containing a Cys to Ser substitution was insensitive

to redox modification, and thus, constitutively active ([157] and references within). It has since been found that APE1 potentiates the DNA binding activity of several transcription factors, including NF-kB, Myb, members of the ATF/CREB and BSAP/Pax families, Egr-1, HIF-1α and p53, through both redox-dependent and -independent mechanisms [158–163]. The redox state of APE1 itself appears to be modulated by the ubiquitous thioredoxin system [164,165].

Truncation analysis has shown that the redox regulatory and nuclease regions of APE1 overlap, yet are distinct, functional entities (Fig. 7A). Consistently, the two activities can be separately inactivated by strategic site-directed mutagenesis or partial truncation

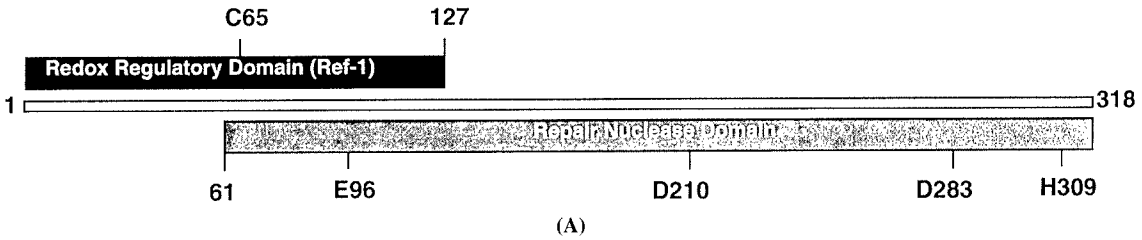

(A)

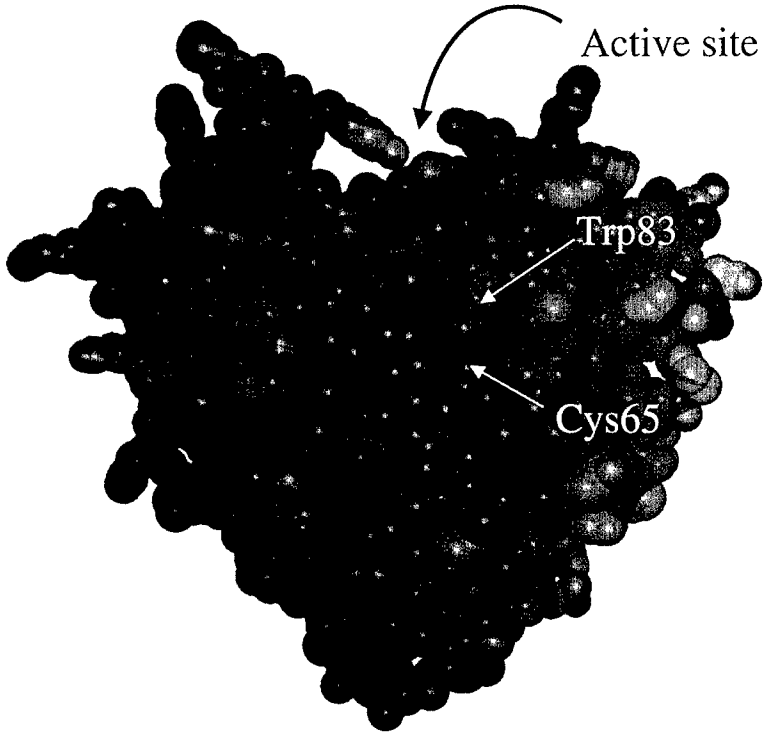

(B)

Fig. 7. (A) The functional domains of APE1. APE1 is separable into two structural and functional domains, a nuclease (residues 61 through 318) and a redox regulatory (residues 1 through 127) domain. These domains were identified by terminal deletion studies [166,167] and partial proteolysis [100]. Residues proposed to be important for the redox (Cys65) or nuclease activities (Glu96, Asp210, Asp283 and His309) of APE1 are shown. (B) Space-filled representation of APE1 coordinates (non-hydrogen atoms) from MD simulation, color coded by motion as in Fig. 2 [122]. The APE1 protein molecule depicted here lacks the first 43 N-terminal amino acids [99]. The buried Cys65 (purple) is behind residue Trp83, which is rather mobile. The position of these residues, and the APE1 catalytic pocket (active site) is indicated.

([148,166,167] and references therein). Studies have also revealed that the nuclease and regulatory activities of APE1 may be modulated in vivo by post-translational modification (e.g. phosphorylation) or by differential compartmentalization [168–171].

While Cys65 was initially inferred by site-specific mutagenesis and in vitro biochemical analysis to be critical for the redox function of APE1 [172], the crystal structure solved by Gorman and colleagues [99] suggested that this residue was buried within the protein core, and thus, inaccessible. It was, therefore, proposed either that, in the previous study, the Cys65Ala mutant induced a gross structural change which indirectly disrupted the protein's modulatory function, or that APE1 undergoes a conformational change, permitting Cys65 availability. Our recent MD simulations and crystallography results suggest that the helical regions surrounding Cys65 may not be rigidly fixed, and that outward rotation of a mobile tryptophan side chain could expose Cys65, permitting access to thioredoxin or target transcription factors (Fig. 7B) [102,122]. Alternatively, the redox mechanism may involve a relay system from the protein surface to a redox core in APE1 comprised of Cys65. Whatever the case, the precise details of the regulatory mechanism remain unresolved.

Lastly, APE1 appears to function as part of a multiprotein regulatory complex that binds to a calcium-responsive element (nCaRE) in response to changes in the intracellular calcium homeostasis, and regulates the expression of the parathyroid gene [173,174]. APE1 similarly negatively regulates its own gene expression in an nCaRE-dependent fashion [175]. The compilation of the results suggest that the APE1-mediated genetic responses may be facilitated by a Ca^{2+}-dependent signaling process, as intracellular Ca^{2+} levels are also influenced by the oxidative status of the cell [176]. For more details on the biological properties and the additional cellular complexities of APE1/REF-1, see [177].

4. Cellular role(s) of AP endonucleases and potential relationship to disease

Knockout studies indicate an absolute requirement for APE1 in normal embryonic development and animal survival. Specifically, mice lacking both APE1 alleles die following blastocyst formation, shortly after implantation, with degeneration of the mutant embryos clearly visible as early as embryonic day E5.5 [178]. Heterozygous animals on the other hand display no gross anatomical abnormalities up to 9 months of age, exhibiting normal size, fertility and no behavioral defects. In a separate study, homozygous null APE1 embryos were found to exhibit successful implantation and nearly normal developmental progression until E7.5, followed by morphogenetic failure and adsorption of embryos by day E9.5 [179]. This animal inviability appears to stem from embryonic lineage-specific cell lethality, as these cells, and not the extra-embryonic sections (e.g. the ectoplacental core), were pycnotic at day E8.5. Explanted homozygous APE1 null blastocysts display increased sensitivity to γ-irradiation, indicating an involvement of this protein in ionizing radiation resistance. To our knowledge, cells deficient in APE1 have not been derived or generated. Thus, APE1 may be required for cell viability, and therefore, definitive analysis into the biological roles of the encoded protein may require the construction of conditional-null or site-specifically altered animals or cell lines — of particular interest will be the specific contributions of the various APE1activities.

Targeted anti-sense experiments in mammalian cells indicate that reduced APE1 levels increase cellular sensitivity to MMS, hydrogen peroxide, menadione, paraquat and ionizing radiation, but not to UV irradiation [180–182]. Consistently, bacteria or yeast deficient in AP endonuclease activity exhibit elevated sensitivity to the oxidizing agent hydrogen peroxide and the alkylating agent MMS [183–185]. Elimination of the major yeast AP endonuclease (APN1) has also been shown to result in an elevated spontaneous mutation frequency [185], indicating that impaired function in this repair activity can lead to genetic instability in eukaryotes. Thus, reduction in AP endonuclease activity (and BER capacity) in humans could like wise lead to increased mutation frequencies and cancer proneness, as well as to disorders related to the accumulation of DNA damage, such as premature aging and neurodegeneration. As measured by in vitro crude cell extract assays, an approximately three-fold variation has been reported in the total AP endonuclease incision activity among a subset of healthy individuals [186]. When crossed with XPC−/− mice, the loss of a single APE1 allele (i.e. a

+/− heterozygous state) increased the predisposition of these animals to UV radiation-induced skin cancer, demonstrating that gene dosage (i.e. reduced function) in APE1 can be related to cancer susceptibility (note: this effect appears to operate genetically through p53 (aka Trp53) activity, and thus, presumably the redox regulatory function of APE1 [187]).

Analysis of APE1 transcripts from nine patients with the oxidative stress-related, neurodegenerative disorder amyotrophic lateral sclerosis (ALS; Lou Gehrig's disease) and two individuals (twins) with familial ALS uncovered five amino acid variants in APE1: Leu104Arg, Glu126Asp, Asp148Glu, Asp283Gly and Gly306Ala [188]. Each of these substitutions was observed only once, excluding Glu126Asp, which was observed in each twin. Since no amino acid changes were identified in five healthy controls, it was proposed that alterations and corresponding defects in APE1 may be related to the pathogenesis of ALS. Supportively, a separate study found that AP endonuclease activity was significantly lower in the brain tissue of ALS patients relative to age-matched controls [189]. In yet another study, the Asp148Glu variant was found to associate more frequently with individuals suffering from sporadic ALS ($P = 0.027$), but not with familial ALS. However, no other amino acid substitutions were identified (although a premature stop variant was identified in a single sporadic ALS patient) in screening 153 ALS samples [190]. More recent analysis of DNA from the CNS tissue of 84 ALS patients revealed only three genetic differences in APE1 (a four base deletion in the 3′ UTR, a less common polymorphism Gln51His, and the Asp148Glu polymorphism in exon 5), arguing that APE1 mutations do not account for a large number of ALS cases [191]. Lastly, while in most of the above studies the zygosity was not determined, it is likely that the rare polymorphisms exist in the heterozygous state, and in this condition, the potential for dominant-negative effects must be considered.

Combining the data from the ALS studies, with genomic DNA resequencing and interrogation of the DNA sequence databases, a total of 11 APE1 substitution variants have been identified [192]. Of the seven amino acid changes found in the nuclease domain of APE1, four (Leu104Arg, Glu126Asp, Arg237Ala/Cys, and Asp283Gly) were shown to reduce AP site-specific endonuclease activity 40 to 90% as assessed by in vitro biochemical assays. These reduced-function variants represent potential disease susceptibility alleles for cancer and neurodegenerative disorders, although in all cases, they appear to be rare.

While APE1 is generally thought to be a ubiquitous enzyme predominantly localized to the nucleus, several recent studies have discovered striking differences in either APE1 intracellular compartmentalization or expression levels in several cancer types ([193–196]; and reviewed in [177]). Notably, several of these localization and expression differences appear to correlate with specific cancer forms, perhaps providing a means for diagnosing cancer type and/or stage of progression. Moreover, while the reasons for and biological impact of the differential expression is unknown, it has been suggested that the cytoplasmic localization observed for APE1 may be related to the oxygen tension of the cell, and thus, may reflect the complex functions of APE1/REF-1. It will be interesting to determine if any of these "abnormal" cellular observations correlate with variant APE1 protein molecules.

5. Alternative pathways for AP site repair/tolerance

While most abasic sites are repaired via an AP endonuclease-directed pathway, in the absence of such repair activity, alternative corrective mechanisms have been observed. One genetic study found that in yeast the AP lyase activity of the bifunctional DNA glycosylases Ntg1 and Ntg2 contributes to suppression of the hyperrecombination phenotype associated with *apn1* mutants presumably caused by AP site accumulation [197]. Yet, as noted above, AP lyase incision requires a 3′-repair diesterase activity to excise the remaining 3′-blocking moiety, a function that presumably would belong to Apn1, but must exist in another yeast protein(s), perhaps Eth1/Apn2. Furthermore, in *S. cerevisiae*, deletion of either the lesion bypass (Rev3-dependent) or recombination (Rad52-dependent) pathway enhances the hyper-recombination or mutator phenotype of AP site repair-defective strains, respectively, suggesting the involvement of these processes in tolerance or removal of abasic damages. In vitro and in vivo studies also indicate that nucleotide excision repair, which

typically copes with bulky DNA adducts such as those generated by ultraviolet radiation, is an alternative pathway for correcting abasic sites [197–200]. These results emphasize the emerging complexities and overlapping nature of the various protective, repair and damage-tolerance processes. Ultimately, our understanding of these interrelated pathways will require the identification of the signals and components that direct pathway selection.

Acknowledgements

We thank our LLNL colleagues, Dr. Peter Beernink, Dr. Felice Lightstone, Dr. Lam Nguyen, Dr. Robert Tebbs and Dr. Larry Thompson, and external colleagues, Dr. Paul Doetsch (Emory University School of Medicine), Dr. Mark R. Kelley (Indiana University Medical Center) and Dr. Arthur P. Grollman (State University of New York, Stony Brook), as well as Mr. Jan Erzberger (University of California, Berkeley), for their insightful comments and suggestions. This work was performed under the auspices of the US Department of Energy by the University of California, Lawrence Livermore National Laboratory, under Contract No. W-7405-Eng-48, and supported by NIH (CA79056) and US Army (BC980514) grants to DMWIII.

References

[1] S. Greer, S. Zamenhof, Studies on depurination of DNA by heat, J. Mol. Biol. 4 (1962) 123.
[2] T. Lindahl, B. Nyberg, Rate of depurination of native deoxyribonucleic acid, Biochemistry 11 (1972) 3610–3618.
[3] T. Lindahl, O. Karlström, Heat-induced depyrimidination of deoxyribonucleic acid in neutral solution, Biochemistry 12 (1973) 5151–5154.
[4] J. Nakamura, V.E. Walker, P.B. Upton, S.Y. Chiang, Y.W. Kow, J.A. Swenberg, Highly sensitive apurinic/apyrimidinic site assay can detect spontaneous and chemically induced depurination under physiological conditions, Cancer Res. 58 (1998) 222–225.
[5] L.A. Loeb, B.D. Preston, Mutagenesis by apurinic/apyrimidinic sites, Annu. Rev. Genet. 20 (1986) 201–230.
[6] T. Lindahl, Instability and decay of the primary structure of DNA, Nature 362 (1993) 709–715.
[7] H.E. Krokan, R. Standal, G. Slupphaug, DNA glycosylases in the base excision repair of DNA, Biochem. J. 325 (1997) 1–16.
[8] A.K. McCullough, M.L. Dodson, R.S. Lloyd, Initiation of base excision repair: glycosylase mechanisms and structures, Annu. Rev. Biochem. 68 (1999) 255–285.
[9] H. Atamna, I. Cheung, B.N. Ames, A method for detecting abasic sites in living cells: age-dependent changes in base excision repair, Proc. Natl. Acad. Sci. U.S.A. 97 (2000) 686–691.
[10] J. Nakamura, J.A. Swenberg, Endogenous apurinic/apyrimidinic sites in genomic DNA of mammalian tissues, Cancer Res. 59 (1999) 2522–2526.
[11] A.F. Taylor, B. Weiss, Role of exonuclease III in the base excision repair of uracil-containing DNA, J. Bacteriol. 151 (1982) 351–357.
[12] R.M. Schaaper, L.A. Loeb, Depurination causes mutations in SOS-induced cells, Proc. Natl. Acad. Sci. U.S.A. 78 (1981) 1773–1777.
[13] P.S. Kingma, N. Osheroff, The response of eukaryotic topoisomerases to DNA damage, Biochim. Biophys. Acta. 1400 (1998) 223–232.
[14] P. Pourquier, L.M. Ueng, G. Kohlhagen, A. Mazumder, M. Gupta, K.W. Kohn, Y. Pommier, Effects of uracil incorporation, DNA mismatches, and abasic sites on cleavage and religation activities of mammalian topoisomerase I, J. Biol. Chem. 272 (1997) 7792–7796.
[15] C.W. Shearman, L.A. Loeb, Depurination decreases fidelity of DNA synthesis in vitro, Nature 270 (1977) 537–538.
[16] S. Boiteux, J. Laval, Coding properties of poly(deoxycytidylic acid) templates containing uracil or apyrimidinic sites: in vitro modulation of mutagenesis by deoxyribonucleic acid repair enzymes, Biochemistry 21 (1982) 6746–6751.
[17] D. Sagher, B. Strauss, Insertion of nucleotides opposite apurinic/apyrimidinic sites in deoxyribonucleic acid during in vitro synthesis: uniqueness of adenine nucleotides, Biochemistry 22 (1983) 4518–4526.
[18] T.A. Kunkel, R.M. Schaaper, L.A. Loeb, Depurination-induced infidelity of deoxyribonucleic acid synthesis with purified deoxyribonucleic acid replication proteins in vitro, Biochemistry 22 (1983) 2378–2384.
[19] R.M. Schaaper, T.A. Kunkel, L.A. Loeb, Infidelity of DNA synthesis associated with bypass of apurinic sites, Proc. Natl. Acad. Sci. U.S.A. 80 (1983) 487–491.
[20] T.A. Kunkel, Mutational specificity of depurination, Proc. Natl. Acad. Sci. U.S.A. 81 (1984) 1494–1498.
[21] S.K. Randall, R. Eritja, B.E. Kaplan, J. Petruska, M.F. Goodman, Nucleotide insertion kinetics opposite abasic lesions in DNA, J. Biol. Chem. 262 (1987) 6864–6870.
[22] C.W. Lawrence, A. Borden, S.K. Banerjee, J.E. LeClerc, Mutation frequency and spectrum resulting from a single abasic site in a single-stranded vector, Nucleic Acids Res. 18 (1990) 2153–2157.
[23] W. Zhou, P.W. Doetsch, Effects of abasic sites and DNA single-strand breaks on prokaryotic RNA polymerases, Proc. Natl. Acad. Sci. U.S.A. 90 (1993) 6601–6605.
[24] H. Ide, H. Murayama, S. Sakamoto, K. Makino, K. Honda, H. Nakamuta, M. Sasaki, N. Sugimoto, On the mechanism of preferential incorporation of dAMP at abasic sites in

translesional DNA synthesis. Role of proofreading activity of DNA polymerase and thermodynamic characterization of model template-primers containing an abasic site, Nucleic Acids Res. 23 (1995) 123–129.
[25] T. Paz-Elizur, M. Takeshita, Z. Livneh, Mechanism of bypass synthesis through an abasic site analog by DNA polymerase I, Biochemistry 36 (1997) 1766–1773.
[26] S. Shibutani, M. Takeshita, A.P. Grollman, Translesional synthesis on DNA templates containing a single abasic site. A mechanistic study of the "A rule", J. Biol. Chem. 272 (1997) 13916–13922.
[27] T. Lyons-Darden, M.D. Topal, Abasic sites induce triplet-repeat expansion during DNA replication in vitro, J. Biol. Chem. 274 (1999) 25975–25978.
[28] M.Z. Humayun, SOS and Mayday: multiple inducible mutagenic pathways in *Escherichia coli*, Mol. Microbiol. 30 (1998) 905–910.
[29] J.H. Miller, K.B. Low, Specificity of mutagenesis resulting from the induction of the SOS system in the absence of mutagenic treatment, Cell 37 (1984) 675–682.
[30] M. Tang, P. Pham, X. Shen, J.S. Taylor, M. O'Donnell, R. Woodgate, M.F. Goodman, Roles of *E. coli* DNA polymerases IV and V in lesion-targeted and untargeted SOS mutagenesis, Nature 404 (2000) 1014–1018.
[31] B.A. Kunz, E.S. Henson, H. Roche, D. Ramotar, T. Nunoshiba, B. Demple, Specificity of the mutator caused by deletion of the yeast structural gene (APN1) for the major apurinic endonuclease, Proc. Natl. Acad. Sci. U.S.A. 91 (1994) 8165–8169.
[32] P.E. Gibbs, C.W. Lawrence, Novel mutagenic properties of abasic sites in Saccharomyces cerevisiae, J. Mol. Biol. 251 (1995) 229–236.
[33] C.W. Lawrence, D.C. Hinkle, DNA polymerase zeta and the control of DNA damage induced mutagenesis in eukaryotes, Cancer Surv. 28 (1996) 21–31.
[34] K. Baynton, R.P. Fuchs, Lesions in DNA: hurdles for polymerases, Trends Biochem. Sci. 25 (2000) 74–79.
[35] A. Gentil, G. Renault, C. Madzak, A. Margot, J.B. Cabral-Neto, J.J. Vasseur, B. Rayner, J.L. Imbach, A. Sarasin, Mutagenic properties of a unique abasic site in mammalian cells, Biochem. Biophys. Res. Commun. 173 (1990) 704–710.
[36] A. Gentil, J.B. Cabral-Neto, R. Mariage-Samson, A. Margot, J.L. Imbach, B. Rayner, A. Sarasin, Mutagenicity of a unique apurinic/apyrimidinic site in mammalian cells, J. Mol. Biol. 227 (1992) 981–984.
[37] J.B. Neto, A. Gentil, R.E. Cabral, A. Sarasin, Mutation spectrum of heat-induced abasic sites on a single-stranded shuttle vector replicated in mammalian cells, J. Biol. Chem. 267 (1992) 19718–19723.
[38] J.B. Cabral Neto, R.E. Cabral, A. Margot, F. Le Page, A. Sarasin, A. Gentil, Coding properties of a unique apurinic/apyrimidinic site replicated in mammalian cells, J. Mol. Biol. 240 (1994) 416–420.
[39] M. Takeshita, W. Eisenberg, Mechanism of mutation on DNA templates containing synthetic abasic sites: study with a double strand vector, Nucleic Acids Res. 22 (1994) 1897–1902.
[40] D.K. Klinedinst, N.R. Drinkwater, Mutagenesis by apurinic sites in normal and ataxia telangiectasia human lymphoblastoid cells, Mol. Carcinogen. 6 (1992) 32–42.
[41] E. Ohashi, T. Ogi, R. Kusumoto, S. Iwai, C. Masutani, F. Hanaoka, H. Ohmori, Error-prone bypass of certain DNA lesions by the human DNA polymerase κ, Genes Dev. 14 (2000) 1589–1594.
[42] C. Masutani, R. Kusumoto, S. Iwai, F. Hanaoka, Mechanisms of accurate translesion synthesis by human DNA polymerase η, EMBO J. 19 (2000) 3100–3109.
[43] R.E. Johnson, S. Prakash, L. Prakash, The human DINB1 gene encodes the DNA polymerase Polθ, Proc. Natl. Acad. Sci. U.S.A. 97 (2000) 3838–3843.
[44] Y. Zhang, F. Yuan, X. Wu, O. Rechkoblit, J.S. Taylor, N.E. Geacintov, Z. Wang, Error-prone lesion bypass by human DNA polymerase eta, Nucleic Acids Res. 28 (2000) 4717–4724.
[45] Y. Zhang, F. Yuan, X. Wu, M. Wang, O. Rechkoblit, J.S. Taylor, N.E. Geacintov, Z. Wang, Error-free and error-prone lesion bypass by human DNA polymerase kappa in vitro, Nucleic Acids Res. 28 (2000) 4138–4146.
[46] L. Haracska, M.T. Washington, S. Prakash, L. Prakash, Inefficient bypass of an abasic site by DNA polymerase eta, J. Biol. Chem. (2000).
[47] D.J. Mozzherin, S. Shibutani, C.K. Tan, K.M. Downey, P.A. Fisher, Proliferating cell nuclear antigen promotes DNA synthesis past template lesions by mammalian DNA polymerase delta, Proc. Natl. Acad. Sci. U.S.A. 94 (1997) 6126–6131.
[48] W. Lin, H. Xin, Y. Zhang, X. Wu, F. Yuan, Z. Wang, The human REV1 gene codes for a DNA template-dependent dCMP transferase, Nucleic. Acids Res. 27 (1999) 4468–4475.
[49] R.E. Johnson, M.T. Washington, L. Haracska, S. Prakash, L. Prakash, Eukaryotic polymerases iota and zeta act sequentially to bypass DNA lesions, Nature 406 (2000) 1015–1019.
[50] P. Cuniasse, L.C. Sowers, R. Eritja, B. Kaplan, M.F. Goodman, J.A. Cognet, M. LeBret, W. Guschlbauer, G.V. Fazakerley, An abasic site in DNA. Solution conformation determined by proton NMR and molecular mechanics calculations, Nucleic Acids Res. 15 (1987) 8003–8022.
[51] M.W. Kalnik, C.N. Chang, F. Johnson, A.P. Grollman, D.J. Patel, NMR studies of abasic sites in DNA duplexes: deoxyadenosine stacks into the helix opposite acyclic lesions, Biochemistry 28 (1989) 3373–3383.
[52] I. Goljer, S. Kumar, P.H. Bolton, Refined solution structure of a DNA heteroduplex containing an aldehydic abasic site, J. Biol. Chem. 270 (1995) 22980–22987.
[53] Y. Coppel, N. Berthet, C. Coulombeau, J. Garcia, J. Lhomme, Solution conformation of an abasic DNA undecamer duplex d(CGCACXCACGC) × d(GCGTGTGTGCG): the unpaired thymine stacks inside the helix, Biochemistry 36 (1997) 4817–4830.
[54] M.W. Kalnik, C.N. Chang, A.P. Grollman, D.J. Patel, NMR studies of abasic sites in DNA duplexes: deoxyadenosine stacks into the helix opposite the cyclic analogue of 2-deoxyribose, Biochemistry 27 (1988) 924–931.

[55] K.M. Morden, Y.G. Chu, F.H. Martin, I. Tinoco Jr., Unpaired cytosine in the dexyoligonucleotide duplex dCA_3CA_3G/dCT_6G is outside of the helix, Biochemistry 22 (1983) 5557–5563.
[56] P. Cuniasse, G.V. Fazakerley, W. Guschlbauer, B.E. Kaplan, L.C. Sowers, The abasic site as a challenge to DNA polymerase. A nuclear magnetic resonance study of G, C and T opposite a model abasic site, J. Mol. Biol. 213 (1990) 303–314.
[57] M.P. Singh, G.C. Hill, D. Péoc'h, B. Rayner, J.L. Imbach, J.W. Lown, High-field NMR and restrained molecular modeling studies on a DNA heteroduplex containing a modified apurinic abasic site in the form of covalently linked 9-aminoellipticine, Biochemistry 33 (1994) 10271–10285.
[58] K.Y. Wang, S.A. Parker, I. Goljer, P.H. Bolton, Solution structure of a duplex DNA with an abasic site in a dA tract, Biochemistry 36 (1997) 11629–11639.
[59] J.T. Stivers, 2-Aminopurine fluorescence studies of base stacking interactions at abasic sites in DNA: metal-ion and base sequence effects, Nucleic Acids Res. 26 (1998) 3837–3844.
[60] L. Ayadi, M. Jourdan, C. Coulombeau, J. Garcia, R. Lavery, Experimental and theoretical studies of the conformational perturbations induced by an abasic site, J. Biomol. Struct. Dyn. 17 (1999) 245–257.
[61] L. Ayadi, C. Coulombeau, R. Lavery, The impact of abasic sites on DNA flexibility, J. Biomol. Struct. Dyn. 17 (2000) 645–653.
[62] L. Ayadi, C. Coulombeau, R. Lavery, Abasic sites in duplex DNA: molecular modeling of sequence-dependent effects on conformation, Biophys. J. 77 (1999) 3218–3226.
[63] D. Barsky, N. Foloppe, S. Ahmadia, D.M. Wilson III, A.D. MacKerell Jr., New insights into the structure of abasic DNA from molecular dynamics simulations, Nucleic Acids Res. 28 (2000) 2613–2626.
[64] J. Pierce, A.S. Serianni, R. Barker, Anomerization of furanose sugars and sugar phosphates, J. Am. Chem. Soc. 107 (1985) 2448–2456.
[65] J.A. Wilde, P.H. Bolton, A. Masumder, M. Manoharan, J.A. Gerlt, Characterization of the equilibrating forms of the aldehydic abasic site in duplex DNA by ^{17}O NMR, J. Am. Chem. Soc. 111 (1989) 1894–1896.
[66] B. Weiss, L. Grossman, Phosphodiesterases involved in DNA repair, Adv. Enzymol. Relat. Areas Mol. Biol. 60 (1987) 1–34.
[67] M. Jourdan, J. Garcia, E. Defrancq, M. Kotera, J. Lhomme, 2′-Deoxyribonolactone lesion in DNA: refined solution structure determined by nuclear magnetic resonance and molecular modeling, Biochemistry 38 (1999) 3985–3995.
[68] G. Vesnaver, C.N. Chang, M. Eisenberg, A.P. Grollman, K.J. Breslauer, Influence of abasic and anucleosidic sites on the stability, conformation, and melting behavior of a DNA duplex: correlations of thermodynamic and structural data, Proc. Natl. Acad. Sci. U.S.A. 86 (1989) 3614–3618.
[69] C.A. Gelfand, G.E. Plum, A.P. Grollman, F. Johnson, K.J. Breslauer, Thermodynamic consequences of an abasic lesion in duplex DNA are strongly dependent on base sequence, Biochemistry 37 (1998) 7321–7327.
[70] F. Aboul-ela, D. Koh, I. Tinoco Jr., F.H. Martin, Base–base mismatches. Thermodynamics of double helix formation for dCA3XA3G + dCT3YT3G (X, Y = A, C, G, T), Nucleic Acids Res. 13 (1985) 4811–4824.
[71] J. Sági, B. Hang, B. Singer, Sequence-dependent repair of synthetic AP sites in 15-mer and 35-mer oligonucleotides: role of thermodynamic stability imposed by neighbor bases, Chem. Res. Toxicol. 12 (1999) 917–923.
[72] T.J. Matray, E.T. Kool, A specific partner for abasic damage in DNA, Nature 399 (1999) 704–708.
[73] D. Barsky, E.T. Kool, M.E. Colvin, Interaction and solvation energies of nonpolar DNA base analogues and their role in polymerase insertion fidelity, J. Biomol. Struct. Dyn. 16 (1999) 1119–1134.
[74] B. Weiss, Endonuclease II of *Escherichia coli* is exonuclease III, J. Biol. Chem. 251 (1976) 1896–1901.
[75] E. Chan, B. Weiss, Endonuclease IV of *Escherichia coli* is induced by paraquat, Proc. Natl. Acad Sci. U.S.A. 84 (1987) 3189–3193.
[76] B. Demple, E. Hidalgo, H. Ding, Transcriptional regulation via redox-sensitive iron–sulphur centres in an oxidative stress response, Biochem. Soc. Symp. 64 (1999) 119–128.
[77] B. Demple, T. Herman, D.S. Chen, Cloning and expression of APE, the cDNA encoding the major human apurinic endonuclease: definition of a family of DNA repair enzymes, Proc. Natl. Acad. Sci. U.S.A. 88 (1991) 11450–11454.
[78] C.N. Robson, I.D. Hickson, Isolation of cDNA clones encoding a human apurinic/apyrimidinic endonuclease that corrects DNA repair and mutagenesis defects in *E. coli* Xth (exonuclease III) mutants, Nucleic Acids Res. 19 (1991) 5519–5523.
[79] S. Seki, M. Hatsushika, S. Watanabe, K. Akiyama, K. Nagao, K. Tsutsui, cDNA cloning, sequencing, expression and possible domain structure of human APEX nuclease homologous to *Escherichia coli* exonuclease III, Biochim. Biophys. Acta 1131 (1992) 287–299.
[80] D.S. Chen, T. Herman, B. Demple, Two distinct human DNA diesterases that hydrolyze 3′-blocking deoxyribose fragments from oxidized DNA, Nucleic Acids Res. 19 (1991) 5907–5914.
[81] S.C. Popoff, A.I. Spira, A.W. Johnson, B. Demple, Yeast structural gene (APN1) for the major apurinic endonuclease: homology to *Escherichia coli* endonuclease IV, Proc. Natl. Acad. Sci. U.S.A. 87 (1990) 4193–4197.
[82] R.E. Johnson, C.A. Torres-Ramos, T. Izumi, S. Mitra, S. Prakash, L. Prakash, Identification of APN2, the Saccharomyces cerevisiae homolog of the major human AP endonuclease HAP1, and its role in the repair of abasic sites, Genes Dev. 12 (1998) 3137–3143.
[83] R.A. Bennett, The Saccharomyces cerevisiae ETH1 gene, an inducible homolog of exonuclease III that provides resistance to DNA-damaging agents and limits spontaneous mutagenesis, Mol. Cell Biol. 19 (1999) 1800–1809.
[84] I. Unk, L. Haracska, R.E. Johnson, S. Prakash, L. Prakash, Apurinic endonuclease activity of yeast Apn2 protein, J. Biol. Chem. 21 (2000) 22427–22434.
[85] B. Demple, L. Harrison, D.M. Wilson III, R.A. Bennett, T. Takagi, A.G. Ascione, Regulation of eukaryotic abasic

endonucleases and their role in genetic stability, Environ. Health Perspect. 105 (Suppl. 4) (1997) 931–934.
[86] B. Demple, L. Harrison, Repair of oxidative damage to DNA: enzymology and biology, Annu. Rev. Biochem. 63 (1994) 915–948.
[87] T.A. Winters, W.D. Henner, P.S. Russell, A. McCullough, T.J. Jorgensen, Removal of 3′-phosphoglycolate from DNA strand-break damage in an oligonucleotide substrate by recombinant human apurinic/apyrimidinic endonuclease, Nucleic Acids Res. 22 (1994) 1866–1873.
[88] D. Suh, D.M. Wilson III, L.F. Povirk, 3′-Phosphodiesterase activity of human apurinic/apyrimidinic endonuclease at DNA double-strand break ends, Nucleic Acids Res. 25 (1997) 2495–2500.
[89] A. Klungland, M. Höss, D. Gunz, A. Constantinou, S.G. Clarkson, P.W. Doetsch, P.H. Bolton, R.D. Wood, T. Lindahl, Base excision repair of oxidative DNA damage activated by XPG protein, Mol. Cell. 3 (1999) 33–42.
[90] T. Izumi, T.K. Hazra, I. Boldogh, A.E. Tomkinson, M.S. Park, S. Ikeda, S. Mitra, Requirement of human AP endonuclease 1 for repair of 3′-blocking damage at DNA single-strand breaks induced by reaction oxygen species, Carcinogenesis 21 (2000) 1329–1334.
[91] C.V. Ramana, I. Boldogh, T. Izumi, S. Mitra, Activation of apurinic/apyrimidinic endonuclease in human cells by reactive oxygen species and its correlation with their adaptive response to genotoxicity of free radicals, Proc. Natl. Acad. Sci. U.S.A. 95 (1998) 5061–5066.
[92] S. Grösch, G. Fritz, B. Kaina, Apurinic endonuclease (REF-1) is induced in mammalian cells by oxidative stress and involved in clastogenic adaptation, Cancer Res. 58 (1998) 4410–4416.
[93] K.M. Chou, M. Kukhanova, Y.C. Cheng, A novel action of human Apurinic/Apyrimidinic endonuclease. Excision of l-configuration deoxyribonucleoside analogs from the 3(termini of DNA, J. Biol. Chem. 275 (2000) 31009–31015.
[94] M.Z. Hadi, D.M. Wilson III, A second human protein with homology to the *Escherichia coli* abasic endonuclease exonuclease III, Environ. Mol. Mutagen 36 (2000) 312–324.
[95] C.M. Kane, S. Linn, Purification and characterization of an apurinic/apyrimidinic endonuclease from HeLa cells, J. Biol. Chem. 256 (1981) 3405–3414.
[96] W.D. Henner, N.P. Kiker, T.J. Jorgensen, J.N. Munck, Purification and amino-terminal amino acid sequence of an apurinic/apyrimidinic endonuclease from calf thymus, Nucleic Acids Res. 15 (1987) 5529–5544.
[97] C.N. Robson, A.M. Milne, D.J. Pappin, I.D. Hickson, Isolation of cDNA clones encoding an enzyme from bovine cells that repairs oxidative DNA damage in vitro: homology with bacterial repair enzymes, Nucleic Acids Res. 19 (1991) 1087–1092.
[98] S. Seki, K. Akiyama, S. Watanabe, M. Hatsushika, S. Ikeda, K. Tsutsui, cDNA and deduced amino acid sequence of a mouse DNA repair enzyme (APEX nuclease) with significant homology to *Escherichia coli* exonuclease III, J. Biol. Chem. 266 (1991) 20797–20802.
[99] M.A. Gorman, S. Morera, D.G. Rothwell, E. de La Fortelle, C.D. Mol, J.A. Tainer, I.D. Hickson, P.S. Freemont, The crystal structure of the human DNA repair endonuclease HAP1 suggests the recognition of extra-helical deoxyribose at DNA abasic sites, EMBO J. 16 (1997) 6548–6558.
[100] P.R. Strauss, C.M. Holt, Domain mapping of human apurinic/apyrimidinic endonuclease. Structural and functional evidence for a disordered amino terminus and a tight globular carboxyl domain, J. Biol. Chem. 273 (1998) 14435–14441.
[101] C.D. Mol, T. Izumi, S. Mitra, J.A. Tainer, DNA-bound structures and mutants reveal abasic DNA binding by APE1 DNA repair and coordination, Nature 403 (2000) 451–456.
[102] P.T. Beernink, B.W. Segelke, M.Z. Hadi, J.P. Erzberger, D.M. Wilson, 3rd, B. Rupp, Two divalent metal ion in the active site of a new crystal form of human apurinic/apyrimidinic endonuclease, APE1: implications for the catalytic mechanism, J. Mol. Biol., in press (2001).
[103] C.D. Mol, C.F. Kuo, M.M. Thayer, R.P. Cunningham, J.A. Tainer, Structure and function of the multifunctional DNA-repair enzyme exonuclease III, Nature 374 (1995) 381–386.
[104] M. Dlakic, Functionally unrelated signalling proteins contain a fold similar to Mg^{2+}-dependent endonucleases, Trends Biochem. Sci. 25 (2000) 272–273.
[105] R.J. Roberts, On base flipping, Cell 82 (1995) 9–12.
[106] M. Takeuchi, R. Lillis, B. Demple, M. Takeshita, Interactions of *Escherichia coli* endonuclease IV and exonuclease III with abasic sites in DNA, J. Biol. Chem. 269 (1994) 21907–21914.
[107] D.M. Wilson III, M. Takeshita, A.P. Grollman, B. Demple, Incision activity of human apurinic endonuclease (Ape) at abasic site analogs in DNA, J. Biol. Chem. 270 (1995) 16002–16007.
[108] J.P. Erzberger, D. Barsky, O.D. Schärer, M.E. Colvin, D.M. Wilson III, Elements in abasic site recognition by the major human and *Escherichia coli* apurinic/apyrimidinic endonucleases, Nucleic Acids Res. 26 (1998) 2771–2778.
[109] B.J. Sanderson, C.N. Chang, A.P. Grollman, W.D. Henner, Mechanism of DNA cleavage and substrate recognition by a bovine apurinic endonuclease, Biochemistry 28 (1989) 3894–3901.
[110] J.P. Erzberger, D.M. Wilson III, The role of Mg^{2+} and specific amino acid residues in the catalytic reaction of the major human abasic endonuclease: new insights from EDTA-resistant incision of acyclic abasic site analogs and site-directed mutagenesis, J. Mol. Biol. 290 (1999) 447–457.
[111] Y. Masuda, R.A. Bennett, B. Demple, Dynamics of the interaction of human apurinic endonuclease (APE1) with its substrate and product, J. Biol. Chem. 273 (1998) 30352–30359.
[112] T. Shida, M. Noda, J. Sekiguchi, Cleavage of single- and double-stranded DNAs containing an abasic residue by *Escherichia coli* exonuclease III (AP endonuclease VI), Nucleic Acids Res. 24 (1996) 4572–4576.
[113] T. Behmoaras, J.J. Toulme, C. Helene, Specific recognition of apurinic sites in DNA by a tryptophan-containing peptide, Proc. Natl. Acad. Sci. U.S.A. 78 (1981) 926–930.
[114] T. Shida, K. Kaneda, T. Ogawa, J. Sekiguchi, Abasic site recognition mechanism by the *Escherichia coli* exonuclease III, Nucleic Acids Symp. Ser. 23 (1999) 195–196.

[115] C. Roll, C. Ketterlé, V. Faibis, G.V. Fazakerley, Y. Boulard, Conformations of nicked and gapped DNA structures by NMR and molecular dynamic simulations in water, Biochemistry 37 (1998) 4059–4070.
[116] P.R. Strauss, W.A. Beard, T.A. Patterson, S.H. Wilson, Substrate binding by human apurinic/apyrimidinic endonuclease indicates a Briggs–Haldane mechanism, J. Biol. Chem. 272 (1997) 1302–1307.
[117] D.M. Wilson III, M. Takeshita, B. Demple, Abasic site binding by the human apurinic endonuclease, Ape, and determination of the DNA contact sites, Nucleic Acids Res. 25 (1997) 933–939.
[118] A. Fersht, Structure and Mechanism in Protein Science: A Guide to Enzyme Catalysis and Protein Folding, W.H. Freeman and Company, New York, NY, 1999.
[119] D.C. Carey, P.R. Strauss, Human apurinic/apyrimidinic endonuclease is processive, Biochemistry 38 (1999) 16553–16560.
[120] C.D. Mol, D.J. Hosfield, J.A. Tainer, Abasic site recognition by two apurinic/apyrimidinic endonuclease families in DNA base excision repair: the 3′ ends justify the means, Mutat. Res. 460 (2000) 211–229.
[121] S. Cal, K.L. Tan, A. McGregor, B.A. Connolly, Conversion of bovine pancreatic DNase I to a repair endonuclease with a high selectivity for abasic sites, EMBO J. 17 (1998) 7128–7138.
[122] L.H. Nguyen, D. Barsky, J.P. Erzberger, D.M. Wilson III, Mapping the protein–DNA interface and the metal-binding site of the major human apurinic/apyrimidinic endonuclease, J. Mol. Biol. 298 (2000) 447–459.
[123] Q. Feng, J.V. Moran, H.H. Kazazian Jr., J.D. Boeke, Human L1 retrotransposon encodes a conserved endonuclease required for retrotransposition, Cell 87 (1996) 905–916.
[124] G.J. Cost, J.D. Boeke, Targeting of human retrotransposon integration is directed by the specificity of the L1 endonuclease for regions of unusual DNA structure, Biochemistry 37 (1998) 18081–18093.
[125] D. Suck, DNA recognition by DNase I, J. Mol. Recognit. 7 (1994) 65–70.
[126] M. Olivares, C. Alonso, M.C. López, The open reading frame 1 of the L1Tc retrotransposon of Trypanosoma cruzi codes for a protein with apurinic–apyrimidinic nuclease activity, J. Biol. Chem. 272 (1997) 25224–25228.
[127] F. Martín, C. Marañón, M. Olivares, C. Alonso, M.C. López, Characterization of a non-long terminal repeat retrotransposon cDNA (L1Tc) from Trypanosoma cruzi: homology of the first ORF with the ape family of DNA repair enzymes, J. Mol. Biol. 247 (1995) 49–59.
[128] B. Demple, A. Johnson, D. Fung, Exonuclease III and endonuclease IV remove 3′ blocks from DNA synthesis primers in H_2O_2-damaged *Escherichia coli*, Proc. Natl. Acad. Sci. U.S.A. 83 (1986) 7731–7735.
[129] G. Barzilay, L.J. Walker, C.N. Robson, I.D. Hickson, Site-directed mutagenesis of the human DNA repair enzyme HAP1: identification of residues important for AP endonuclease and RNase H activity, Nucleic Acids Res. 23 (1995) 1544–1550.
[130] B. Singer, B. Hang, Mammalian enzymatic repair of etheno and *para*-benzoquinone exocyclic adducts derived from the carcinogens vinyl chloride and benzene, IARC Sci. Publ. 17 (1999) 233–247.
[131] L. Aravind, D.R. Walker, E.V. Koonin, Conserved domains in DNA repair proteins and evolution of repair systems, Nucleic Acids Res. 27 (1999) 1223–1242.
[132] D.J. Hosfield, Y. Guan, B.J. Haas, R.P. Cunningham, J.A. Tainer, Structure of the DNA repair enzyme endonuclease IV and its DNA complex: double-nucleotide flipping at abasic sites and three-metal-ion catalysis, Cell 98 (1999) 397–408.
[133] L.F. Povirk, I.H. Goldberg, Endonuclease-resistant apyrimidinic sites formed by neocarzinostatin at cytosine residues in DNA: evidence for a possible role in mutagenesis, Proc. Natl. Acad. Sci. U.S.A. 82 (1985) 3182–3186.
[134] M.E. Hagensee, R.E. Moses, Bleomycin-treated DNA is specifically cleaved only by endonuclease IV in *E. coli*, Biochim. Biophys. Acta 1048 (1990) 19–23.
[135] M. Häring, H. Rüdiger, B. Demple, S. Boiteux, B. Epe, Recognition of oxidized abasic sites by repair endonucleases, Nucleic Acids Res. 22 (1994) 2010–2015.
[136] H. Ide, K. Tedzuka, H. Shimzu, Y. Kimura, A.A. Purmal, S.S. Wallace, Y.W. Kow, Alpha-deoxyadenosine, a major anoxic radiolysis product of adenine in DNA, is a substrate for *Escherichia coli* endonuclease IV, Biochemistry 33 (1994) 7842–7847.
[137] J.D. Levin, B. Demple, In vitro detection of endonuclease IV-specific DNA damage formed by bleomycin in vivo, Nucleic Acids Res. 24 (1996) 885–889.
[138] B. Hang, A. Chenna, J. Sági, B. Singer, Differential cleavage of oligonucleotides containing the benzene-derived adduct, $1,N_6$-benzetheno-dA, by the major human AP endonuclease HAP1 and *Escherichia coli* exonuclease III and endonuclease IV, Carcinogenesis 19 (1998) 1339–1343.
[139] B. Hang, D.G. Rothwell, J. Sagi, I.D. Hickson, B. Singer, Evidence for a common active site for cleavage of an AP site and the benzene-derived exocyclic adduct, $3,N_4$-benzetheno-dC, in the major human AP endonuclease, Biochemistry 36 (1997) 15411–15418.
[140] J.A. Gerlt, Mechanistic principles of enzyme-catalyzed cleavage of phosphodiester bonds, in: R.S.L. Stuart, M. Linn, R.J. Roberts (Eds.), Nucleases, Cold Spring Harbor Press, Plain view, NY, 1993, pp. 1–34.
[141] T. Izumi, J. Malecki, M.A. Chaudhry, M. Weinfeld, J.H. Hill, J.C. Lee, S. Mitra, Intragenic suppression of an active site mutation in the human apurinic/apyrimidinic endonuclease, J. Mol. Biol. 287 (1999) 47–57.
[142] G. Barzilay, C.D. Mol, C.N. Robson, L.J. Walker, R.P. Cunningham, J.A. Tainer, I.D. Hickson, Identification of critical active-site residues in the multifunctional human DNA repair enzyme HAP1, Nat. Struct. Biol. 2 (1995) 561–568.
[143] Y. Masuda, R.A. Bennett, B. Demple, Rapid dissociation of human apurinic endonuclease (APE1) from incised DNA induced by magnesium, J. Biol. Chem. 273 (1998) 30360–30365.
[144] J.A. Lucas, Y. Masuda, R.A. Bennett, N.S. Strauss, P.R. Strauss, Single-turnover analysis of mutant human apurinic/

apyrimidinic endonuclease, Biochemistry 38 (1999) 4958–4964.
[145] J.A. Cowen, Metal activation of enzymes in nucleic acid biochemistry, Chem. Rev. 98 (1998) 1067–1087.
[146] A. Lahm, D. Suck, DNase I-induced DNA conformation. 2 Å structure of a DNase I-octamer complex, J. Mol. Biol. 222 (1991) 645–667.
[147] S.A. Weston, A. Lahm, D. Suck, X-ray structure of the DNase I-d(GGTATACC)2 complex at 2.3 Å resolution, J. Mol. Biol. 226 (1992) 1237–1256.
[148] D.G. Rothwell, B. Hang, M.A. Gorman, P.S. Freemont, B. Singer, I.D. Hickson, Substitution of asp-210 in HAP1 (APE/REF-1) eliminates endonuclease activity but stabilizes substrate binding, Nucleic Acids Res. 28 (2000) 2207–2213.
[149] S.J. Jones, A.F. Worrall, B.A. Connolly, Site-directed mutagenesis of the catalytic residues of bovine pancreatic deoxyribonuclease I, J. Mol. Biol. 264 (1996) 1154–1163.
[150] L.S. Beese, T.A. Steitz, Structural basis for the 3′–5′ exonuclease activity of *Escherichia coli* DNA polymerase. I. A two metal ion mechanism, EMBO J. 10 (1991) 25–33.
[151] R.A. Bennett, D.M. Wilson III, D. Wong, B. Demple, Interaction of human apurinic endonuclease and DNA polymerase beta in the base excision repair pathway, Proc. Natl. Acad. Sci. U.S.A. 94 (1997) 7166–7169.
[152] S.S. Parikh, C.D. Mol, G. Slupphaug, S. Bharati, H.E. Krokan, J.A. Tainer, Base excision repair initiation revealed by crystal structures and binding kinetics of human uracil–DNA glycosylase with DNA, EMBO J. 17 (1998) 5214–5226.
[153] T.R. Waters, P. Gallinari, J. Jiricny, P.F. Swann, Human thymine DNA glycosylase binds to apurinic sites in DNA but is displaced by human apurinic endonuclease 1, J. Biol. Chem. 274 (1999) 67–74.
[154] E.K. Dimitriadis, R. Prasad, M.K. Vaske, L. Chen, A.E. Tomkinson, M.S. Lewis, S.H. Wilson, Thermodynamics of human DNA ligase I trimerization and association with DNA polymerase beta, J. Biol. Chem. 273 (1998) 20540–20550.
[155] S.H. Wilson, T.A. Kunkel, Passing the baton in base excision repair [news], Nat. Struct. Biol. 7 (2000) 176–178.
[156] S. Xanthoudakis, G. Miao, F. Wang, Y.C. Pan, T. Curran, Redox activation of Fos–Jun DNA binding activity is mediated by a DNA repair enzyme, EMBO J. 11 (1992) 3323–3335.
[157] C. Abate, L. Patel, F.J.d. Rauscher, T. Curran, Redox regulation of Fos and Jun DNA-binding activity in vitro, Science 249 (1990) 1157–1161.
[158] S. Xanthoudakis, T. Curran, Identification and characterization of REF-1, a nuclear protein that facilitates AP-1 DNA-binding activity, EMBO J. 11 (1992) 653–665.
[159] R.P. Huang, E.D. Adamson, Characterization of the DNA-binding properties of the early growth response-1 (Egr-1) transcription factor: evidence for modulation by a redox mechanism, DNA Cell Biol. 12 (1993) 265–273.
[160] L. Jayaraman, K.G. Murthy, C. Zhu, T. Curran, S. Xanthoudakis, C. Prives, Identification of redox/repair protein REF-1 as a potent activator of p53, Genes Dev. 11 (1997) 558–570.
[161] M. Ema, K. Hirota, J. Mimura, H. Abe, J. Yodoi, K. Sogawa, L. Poellinger, Y. Fujii-Kuriyama, Molecular mechanisms of transcription activation by HLF and HIF1alpha in response to hypoxia: their stabilization and redox signal-induced interaction with CBP/p300, EMBO J. 18 (1999) 1905–1914.
[162] D. Lando, I. Pongratz, L. Poellinger, M.L. Whitelaw, A redox mechanism controls differential DNA binding activities of hypoxia-inducible factor (HIF) 1alpha and the HIF-like factor, J. Biol. Chem. 275 (2000) 4618–4627.
[163] G. Tell, A. Zecca, L. Pellizzari, P. Spessotto, A. Colombatti, M.R. Kelley, G. Damante, C. Pucillo, An 'environment to nucleus' signaling system operates in B lymphocytes: redox status modulates BSAP/Pax-5 activation through REF-1 nuclear translocation, Nucleic Acids Res. 28 (2000) 1099–1105.
[164] J. Qin, G.M. Clore, W.P. Kennedy, J. Kuszewski, A.M. Gronenborn, The solution structure of human thioredoxin complexed with its target from REF-1 reveals peptide chain reversal, Structure 4 (1996) 613–620.
[165] K. Hirota, M. Matsui, S. Iwata, A. Nishiyama, K. Mori, J. Yodoi, AP-1 transcriptional activity is regulated by a direct association between thioredoxin and REF-1, Proc. Natl. Acad. Sci. U.S.A. 94 (1997) 3633–3638.
[166] S. Xanthoudakis, G.G. Miao, T. Curran, The redox and DNA-repair activities of REF-1 are encoded by nonoverlapping domains, Proc. Natl. Acad. Sci. U.S.A. 91 (1994) 23–27.
[167] T. Izumi, S. Mitra, Deletion analysis of human AP-endonuclease: minimum sequence required for the endonuclease activity, Carcinogenesis 19 (1998) 525–527.
[168] J.R. Duguid, J.N. Eble, T.M. Wilson, M.R. Kelley, Differential cellular and subcellular expression of the human multifunctional apurinic/apyrimidinic endonuclease (APE/REF-1) DNA repair enzyme, Cancer Res. 55 (1995) 6097–6102.
[169] A. Yacoub, M.R. Kelley, W.A. Deutsch, The DNA repair activity of human redox/repair protein APE/REF-1 is inactivated by phosphorylation, Cancer Res. 57 (1997) 5457–5459.
[170] S. Kakolyris, L. Kaklamanis, A. Giatromanolaki, M. Koukourakis, I.D. Hickson, G. Barzilay, H. Turley, R.D. Leek, P. Kanavaros, V. Georgoulias, K.C. Gatter, A.L. Harris, Expression and subcellular localization of human AP endonuclease 1 (HAP1/REF-1) protein: a basis for its role in human disease, Histopathology 33 (1998) 561–569.
[171] G. Fritz, B. Kaina, Phosphorylation of the DNA repair protein APE/REF-1 by CKII affects redox regulation of AP-1, Oncogene 18 (1999) 1033–1040.
[172] L.J. Walker, C.N. Robson, E. Black, D. Gillespie, I.D. Hickson, Identification of residues in the human DNA repair enzyme HAP1 (REF-1) that are essential for redox regulation of Jun DNA binding, Mol. Cell Biol. 13 (1993) 5370–5376.
[173] T. Okazaki, U. Chung, T. Nishishita, S. Ebisu, S. Usuda, S. Mishiro, S. Xanthoudakis, T. Igarashi, E. Ogata, A redox factor protein, Ref1, is involved in negative gene regulation by extracellular calcium, J. Biol. Chem. 269 (1994) 27855–27862.

[174] U. Chung, T. Igarashi, T. Nishishita, H. Iwanari, A. Iwamatsu, A. Suwa, T. Mimori, K. Hata, S. Ebisu, E. Ogata, T. Fujita, T. Okazaki, The interaction between Ku antigen and REF1 protein mediates negative gene regulation by extracellular calcium, J. Biol. Chem. 271 (1996) 8593–8598.
[175] T. Izumi, W.D. Henner, S. Mitra, Negative regulation of the major human AP-endonuclease, a multifunctional protein, Biochemistry 35 (1996) 14679–14683.
[176] Y.J. Suzuki, H.J. Forman, A. Sevanian, Oxidants as stimulators of signal transduction, Free Radic. Biol. Med. 22 (1997) 269–285.
[177] A.R. Evans, M. Limp-Foster, M.R. Kelley, Going APE over REF-1, Mutat. Res. 461 (2000) 83–108.
[178] S. Xanthoudakis, R.J. Smeyne, J.D. Wallace, T. Curran, The redox/DNA repair protein, REF-1, is essential for early embryonic development in mice, Proc. Natl. Acad. Sci. U.S.A. 93 (1996) 8919–8923.
[179] D.L. Ludwig, M.A. MacInnes, Y. Takiguchi, P.E. Purtymun, M. Henrie, M. Flannery, J. Meneses, R.A. Pedersen, D.J. Chen, A murine AP-endonuclease gene-targeted deficiency with post-implantation embryonic progression and ionizing radiation sensitivity, Mutat. Res. 409 (1998) 17–29.
[180] L.J. Walker, R.B. Craig, A.L. Harris, I.D. Hickson, A role for the human DNA repair enzyme HAP1 in cellular protection against DNA damaging agents and hypoxic stress, Nucleic Acids Res. 22 (1994) 4884–4889.
[181] D.S. Chen, Z.L. Olkowski, Biological responses of human apurinic endonuclease to radiation-induced DNA damage, Ann. N. Y. Acad. Sci. 726 (1994) 306–308.
[182] Y. Ono, T. Furuta, T. Ohmoto, K. Akiyama, S. Seki, Stable expression in rat glioma cells of sense and antisense nucleic acids to a human multifunctional DNA repair enzyme, APEX nuclease, Mutat. Res. 315 (1994) 55–63.
[183] B. Demple, J. Halbrook, S. Linn, *Escherichia coli* xth mutants are hypersensitive to hydrogen peroxide, J. Bacteriol. 153 (1983) 1079–1082.
[184] R.P. Cunningham, S.M. Saporito, S.G. Spitzer, B. Weiss, Endonuclease IV (nfo) mutant of *Escherichia coli*, J. Bacteriol. 168 (1986) 1120–1127.
[185] D. Ramotar, S.C. Popoff, E.B. Gralla, B. Demple, Cellular role of yeast Apn1 apurinic endonuclease/3'-diesterase: repair of oxidative and alkylation DNA damage and control of spontaneous mutation, Mol. Cell Biol. 11 (1991) 4537–4544.
[186] A. Redaelli, R. Magrassi, S. Bonassi, A. Abbondandolo, G. Frosina, AP endonuclease activity in humans: development of a simple assay and analysis of ten normal individuals, Teratog. Carcinog. Mutagen. 18 (1998) 17–26.
[187] L.B. Meira, D.L. Cheo, R.E. Hammer, D.K. Burns, A. Reis, E.C. Friedberg, Genetic interaction between HAP1/REF-1 and p53, Nat. Genet. 17 (1997) 145.
[188] Z.L. Olkowski, Mutant AP endonuclease in patients with amyotrophic lateral sclerosis, Neuroreport 9 (1998) 239–242.
[189] G.E. Kisby, J. Milne, C. Sweatt, Evidence of reduced DNA repair in amyotrophic lateral sclerosis brain tissue, Neuroreport 8 (1997) 1337–1340.
[190] C. Hayward, S. Colville, R.J. Swingler, D.J. Brock, Molecular genetic analysis of the APEX nuclease gene in amyotrophic lateral sclerosis, Neurology 52 (1999) 1899–1901.
[191] J. Tomkins, S. Dempster, S.J. Banner, M.R. Cookson, P.J. Shaw, Screening of AP endonuclease as a candidate gene for amyotrophic lateral sclerosis, Neuroreport 11 (2000) 1695–1697.
[192] M.Z. Hadi, M.A. Coleman, K. Fidelis, H.W. Mohrenweiser, D.M. Wilson III, Functional characterization of APE1 variants identified in the human population, Nucleic Acids. Res. 28 (2000) 3871–3879.
[193] Y. Xu, D.H. Moore, J. Broshears, L. Liu, T.M. Wilson, M.R. Kelley, The apurinic/apyrimidinic endonuclease (APE/REF-1) DNA repair enzyme is elevated in premalignant and malignant cervical cancer, Anticancer Res. 17 (1997) 3713–3719.
[194] S. Kakolyris, L. Kaklamanis, K. Engels, S.B. Fox, M. Taylor, I.D. Hickson, K.C. Gatter, A.L. Harris, Human AP endonuclease 1 (HAP1) protein expression in breast cancer correlates with lymph node status and angiogenesis, Br. J. Cancer 77 (1998) 1169–1173.
[195] S. Kakolyris, A. Giatromanolaki, M. Koukourakis, L. Kaklamanis, P. Kanavaros, I.D. Hickson, G. Barzilay, V. Georgoulias, K.C. Gatter, A.L. Harris, Nuclear localization of human AP endonuclease 1 (HAP1/REF-1) associates with prognosis in early operable non-small cell lung cancer (NSCLC), J. Pathol. 189 (1999) 351–357.
[196] D.H. Moore, H. Michael, R. Tritt, S.H. Parsons, M.R. Kelley, Alterations in the expression of the DNA repair/redox enzyme APE/REF-1 in epithelial ovarian cancers, Clin. Cancer Res. 6 (2000) 602–609.
[197] R.L. Swanson, N.J. Morey, P.W. Doetsch, S. Jinks-Robertson, Overlapping specificities of base excision repair, nucleotide excision repair, recombination, and translesion synthesis pathways for DNA base damage in Saccharomyces cerevisiae, Mol. Cell Biol. 19 (1999) 2929–2935.
[198] A. Snowden, Y.W. Kow, B. Van Houten, Damage repertoire of the *Escherichia coli* UvrABC nuclease complex includes abasic sites, base-damage analogues, and lesions containing adjacent 5′ or 3′ nicks, Biochemistry 29 (1990) 7251–7259.
[199] J.T. Reardon, T. Bessho, H.C. Kung, P.H. Bolton, A. Sancar, In vitro repair of oxidative DNA damage by human nucleotide excision repair system: possible explanation for neurodegeneration in xeroderma pigmentosum patients, Proc. Natl. Acad Sci. U.S.A. 94 (1997) 9463–9468.
[200] C.A. Torres-Ramos, R.E. Johnson, L. Prakash, S. Prakash, Evidence for the involvement of nucleotide excision repair in the removal of abasic sites in yeast, Mol. Cell Biol. 20 (2000) 3522–3528.
[201] M. Manoharan, A. Mazumder, S.C. Ransom, J.A. Gerlt, P.H. Bolton, Mechanism of UV endonuclease V cleavage of abasic sites in DNA determined by ^{13}C labeling, J. Am. Chem. Soc. 110 (1988) 2690–2691.
[202] M. Takeshita, C.N. Chang, F. Johnson, S. Will, A.P. Grollman, Oligodeoxynucleotides containing synthetic abasic sites. Model substrates for DNA polymerases and apurinic/apyrimidinic endonucleases, J. Biol. Chem. 262 (1987) 10171–10179.

[203] D.M. Wilson III, L.H. Thompson, Life without DNA repair, Proc. Natl. Acad. Sci. U.S.A. 94 (1997) 12754–12757.
[204] S.H. Wilson, Mammalian base excision repair and DNA polymerase beta, Mutat. Res. 407 (1998) 203–215.
[205] A. Memisoglu, L. Samson, Base excision repair in yeast and mammals, Mutat. Res. 451 (2000) 39–51.
[206] T. Lindahl, Suppression of spontaneous mutagenesis in human cells by DNA base excision-repair, Mutat. Res. 462 (2000) 129–135.
[207] L.H. Thompson, M.G. West, XRCC1 keeps DNA from getting stranded, Mutat. Res. 459 (2000) 1–18.
[208] S. Shall, G. de Murcia, Poly(ADP-ribose) polymerase-1: what have we learned from the deficient mouse model? Mutat. Res. 460 (2000) 1–15.
[209] C. Oefner, D. Suck, Crystallographic refinement and structure of DNase I at 2 Å resolution, J. Mol. Biol. 192 (1986) 605–632.
[210] A. Varshney, F.P. Brooks, W.V. Wright, Linearly scalable computation of smooth molecular surfaces, IEEE Comp. Graph. Applic. 14 (1994) 19–25.
[211] W. Humphrey, A. Dalke, K. Schulten, VMD: visual molecular dynamics, J. Mol. Graph. 14 (1996) 27–38.
[212] E.A. Merritt, D.J. Bacon, Raster3D: photorealistic molecular graphics, Meth. Enzymol. 277 (1997) 505–524.
[213] A. Zemla, C. Venclovas, J. Moult, K. Fidelis, Processing and analysis of CASP3 protein structure predictions, Proteins 3 (Suppl.) (1999) 22–29.
[214] D. Ramotar, J. Vadnais, J.Y. Masson, S. Tremblay, Schizosaccharomyces pombe apn1 encodes a homologue of the *Escherichia coli* endonuclease IV family of DNA repair proteins, Biochim. Biophys. Acta 1396 (1998) 15–20.
[215] The Arabidopsis Genome Initiative. Analysis of the genome sequence of the flowing plant *Arabidopsis thaliana*, Nature 408 (2000) 796–815.

Ape1 as a Rate-Limiting Factor in Cellular Resistance to DNA-damaging and Anti-cancer Agents

Laura J. Schild, Kerry W. Brookman[1],

Larry H. Thompson, and David M. Wilson III*

Molecular and Structural Biology Division, Biology and Biotechnology Research Program, Lawrence Livermore National Laboratory, Livermore CA 94551. [1]Current address: Odyssey Pharmaceuticals, Inc. 4550 Norris Canyon Road Suite 140, San Ramon, CA 94583 USA

*Correspondence to: David M. Wilson III, Lawrence Livermore National Laboratory, Molecular and Structural Biology Division, Biology and Biotechnology Research Program, L-441, 7000 East Avenue, Livermore CA, 94551. Email: wilson61@llnl.gov.

Abstract

In vitro biochemical studies indicate that Ape1 is the major mammalian enzyme responsible for repairing abasic lesions in DNA and a significant factor in the processing of specific 3'-replication-blocking termini. However, the current picture of the biological role of Ape1 in resistance to specific DNA-damaging and anti-cancer/viral agents is less clear. Towards addressing this issue, we constructed a Chinese Hamster Ovary (CHO) cell line, AA8-Ape1, that exhibits a 7-fold higher Ape1-dependent repair activity. The sensitivity of AA8-Ape1 to a number of agents was compared to the AA8 parental control. Our data indicates that Ape1 activity is not rate-limiting for the repair of cytotoxic damages induced by the alkylating agent methyl methanesulfonate (MMS), the oxidizing agent hydrogen peroxide (H_2O_2) or ionizing radiation (IR). In contrast, AA8-Ape1 cells did exhibit increased resistance to bleomycin following a chronic 3 day exposure, but not to more acute challenges (1 hr). In combination with previous findings, these data indicate that Ape1 activity is not a good prognostic indicator for sensitivity to MMS and H_2O_2, but may in some circumstances be for IR or bleomycin. Moreover, the AA8-Ape1 line displayed ~1.7 fold elevated resistance to the replication-blocking nucleoside analog dioxolane cytidine (L-OddC), a slightly increased resistance to azidothymidine (AZT), but normal sensitivity to arabinosylcytosine (AraC) and 2',3'-dideoxy-2',3'-dihydrothymidine (d4T). This is the first cell-based study demonstrating a role for Ape1 in influencing cellular resistance to anti-cancer/viral antimetabolites.

Introduction

Alkylating and oxidizing agents, from both exogenous and endogenous sources, can introduce chemical modifications in DNA (1). Several of these modifications are potentially mutagenic or cytotoxic. For instance, a prototypical alkylating agent, methylmethanesulfonate (MMS), forms alkylated bases, which can promote error-prone DNA synthesis or block the replication machinery leading to cell death (2). Such base lesions can also lead to the production of non-instructional abasic sites by increasing the hydrolysis rate of the N-glycosylic bond (1) or through the repair activity of DNA glycosylases, which excise substrate bases from DNA (3-4). Hydrogen peroxide (H_2O_2), a model oxidizing agent, can introduce a disperse distribution of oxidized bases, abasic lesions, and DNA strand breaks that harbor 3'-termini (e.g. 3'-phosphate groups) that are inhibitory to DNA synthesis and ligation (5-6). Many of these "environmentally-induced" DNA products are also generated spontaneously, due to the inherent chemical instability of DNA or reactions with naturally-formed endogenous oxidizing and alkylating chemicals (1).

Notably, many anti-cancer agents elicit their cell killing effect through the introduction of cytotoxic DNA damage. Ionizing radiation (IR), one of the most commonly used anti-cancer therapies, introduces many of the same damages formed by chemical oxidizing agents, yet generates a more complex, clustered array of lesions (i.e. multiply damaged sites) leading to an increased number of double-strand breaks (7-8). The antibiotic bleomycin is a radiomimetic anti-cancer drug that produces a highly specific set of DNA strand breaks harboring 5'-phosphate and 3'-phosphoglycolate termini, oxidized abasic sites and a small amount of bistranded damage (e.g. an abasic site with an opposed strand break or strand breaks in opposite strands) (9). Another commonly used class of anti-cancer agents (also used in anti-viral therapies) is

nucleoside analogs (also called antimetabolites). Such analogs, which include dioxolane cytidine (L-OddC) and azidothymidine (AZT), typically lack the 3'-hydroxyl group necessary for primer elongation during DNA replication, and thus, upon incorporation into DNA, cause premature chain termination, resulting in cell death (10). L-OddC was the first L-configuration nucleoside analog shown to have anti-cancer activity, in addition to its anti-viral properties (11-12). AZT was one of the first nucleoside reverse transcriptase inhibitors to receive FDA approval for the treatment of HIV and AIDS.

Biochemical studies indicate that Ape1 (also called APEX or HAP1) is likely the major mammalian enzyme responsible for repairing abasic lesions in DNA (reviewed in 13). However, unlike the major yeast or bacterial AP endonuclease/3' diesterase proteins, human Ape1 possesses relatively weak 3' to 5' exonuclease and 3'-repair phosphodiesterase activities (reviewed in 14, 15-17). Despite this apparently weak in vitro function, recent studies have found that Ape1 is the predominant (and perhaps only) enzyme in crude cell extracts that can excise L-configuration nucleoside analogs from the 3'-termini of DNA (18). Detailed biochemical analysis revealed that Ape1 has a 3' to 5' excision specificity of L-OddC > L-2',3'-dideoxy-2',3'-didehydro-5-fluorocytidine > L-2',3'-dideoxycytidine > L-2',3'-dideoxy-3'-thiocytidine >> D-2',3'-dideoxycytidine > D-2'-difluorodeoxycytidine > D-2'-deoxycytidine > β-D-arabinofuranosylcytosine (AraC) (18). More recent studies have found that Ape1 can also excise AZT and 2',3'-dideoxy-2',3'-dihydrothymidine (d4T) from DNA in vitro (19).

Despite this wealth of biochemical information, a clear picture of Ape1's cellular functions in mammals has been hampered by the fact that null mice are inviable. Embryos die at day E5.5-7.5 during development, indicating that Ape1 is essential for normal embryogenesis (20-21). In addition, *APE1* conditional null or site-specifically modified cells have not yet been

reported. We sought to assess the cellular contribution(s) of Ape1 in resistance to specific DNA modifications, with a particular interest in anti-cancer and anti-viral nucleoside analogs. Towards this goal, we generated an Ape1 overexpressing CHO AA8 cell line (AA8-Ape1), and evaluated the sensitivity of this line to MMS, H_2O_2, bleomycin, IR and the nucleoside analogs, L-OddC, AZT, d4T and AraC, relative to the parental cell line. As will be discussed, based on the observations within and in conjunction with the studies of others, Ape1 does not appear to be a good prognostic marker for resistance to MMS and H_2O_2, but may be a potential rate-limiting marker for specific antimetabolites and in some instances IR and bleomycin.

Materials and Methods

Reagents

All reagents were molecular biology grade and purchased from Sigma (St. Louis, MO) unless otherwise indicated. Restriction enzymes were purchased from New England Biolabs (Beverly, MA). Radionuclides and ECL solutions were from Amersham (Arlington Heights, IL). Tet System Approved fetal bovine serum (Tc-App FBS) was obtained from Clontech (Palo Alto, CA). Nitrocellulose membranes were obtained from Schleicher and Schuell (Keene, NH). Anti-rabbit IgG-HRP was from Santa Cruz Biotechnology (Santa Cruz, CA). α-Minimum Essential Medium (α-MEM), penicillin, streptomycin, and trypsin were purchased from Gibco-BRL (Rockville, MD). The tetracycline (Tc)-responsive plasmid pBI-EGFP was purchased from Clontech (Palo Alto, CA). The laboratory of Dr. S. Takeda (Kyoto University Medical School, Japan) graciously provided pTA-Hyg.

Cell Culture

CHO AA8 cells (22) were grown in α-MEM media supplemented with 100 IU/ml penicillin, 100 μg/ml streptomycin and 10 % Tc-App FBS and were maintained in 6 % CO_2 atmosphere at 37°C. Cell line doubling times and particle size were monitored by a Coulter Particle Counter (Coulter Multisizer II, Coulter Corporation, Miami, FL).

Generation of Tc-Regulated Human Ape1 Overexpressing CHO AA8 Cells

Hygromycin B (Life Technology, Rockville, MD) was solubilized at 50 mg/ml in PBS. Tc (Sigma) was diluted to 1 mg/ml in 70% ethanol. pET11d containing the human APE1 cDNA (23) was digested with MluI and NheI, and the Ape1 fragment was purified by gel electrophoresis and ligated into pBI-EGFP. The pTA-Hyg and pBI-EGFP-Ape1 plasmids were linearized by PvuI and HindIII, respectively, and transfected into AA8 cells by calcium

phosphate precipitation. Transfected cells were selected in media containing hygromycin B (700 μg /ml) for 12 days.

Identification of Human Ape1 Overexpressing CHO AA8 Cells

To identify candidate Ape1 expressing cells, hygromycin resistant clones were examined for enhanced green fluorescent protein (EGFP) expression by fluorescence microscopy. Individual colonies were removed using Pipetman tips and plated into a separate petri dish containing a 22x22 mm sterile glass coverslip. When the cells approached confluency, the coverslips were removed from the petri dishes, washed in phosphate buffered saline (PBS; 137 mM NaCl, 2.7 mM KCl, 4.3 mM $Na_2HPO_4 \cdot 7H_2O$, 1.4 mM KH_2PO_4) containing 0.49 mM magnesium and 1.19 mM calcium, and stained with 0.1 mg/ml DAPI (4',6-Diamidino-2-phenylindole) in SlowFade Light (Molecular Probes, Eugene, OR). The cells were then examined under a 492 nm excitation filter for EGFP expression using a Zeiss Axioskop fluorescence microscope. EGFP expressing clones were subsequently tested for human Ape1 expression by Western blot analysis. Ten μg of cellular protein extract was separated on a 12% SDS-polyacrylamide gel and electroblotted onto a nitrocellulose membrane. Immunoblotting was performed using human Ape1-specific antibody (1:1000) (24) and anti-Rabbit IgG-HRP secondary antibody (1:1000). After extensive washing, the antibody-antigen complexes were visualized by chemiluminescence using ECL.

Tc-Regulation of Human Ape1 Expression

To examine Ape1 transgene Tc responsiveness, cells were grown in the presence or absence of 0.3 μg/ml Tc (determined to be the optimal concentration that inhibited human Ape1 expression in a dose response curve using 0.3, 1, 3, and 10 μg/ml Tc) for up to 96 hr. Cells were harvested during this period at 24, 48, 72 and 96 hr, washed, pelleted and stored at –80°C. The

cell pellet was resuspended in lysis buffer (50 mM Tris, pH 8, 1 mM EDTA, 1 mM DTT, 10% glycerol, 0.5 mM PMSF) and disrupted by sonication (Ultrasonic processor XL, Misonix Inc., Farmingdale, NY) at 4°C. Cell debris was removed by centrifugation (14,000 rpm, 4°C, 20 minutes). Protein levels of the supernatant were quantitated by Bradford assay (25).

AP Endonuclease Activity

AP endonuclease assays were performed essentially as described (26). In brief, an 18-mer (sequence 5'-GTC ACC GTC FTA CGA CTC-3', where F indicates the site of the tetrahydrofuran abasic site analog) was 5' radiolabeled. One tenth μg of CHO whole cell protein extract was incubated with duplex radiolabeled abasic DNA substrate for 5 min at 37°C in 50 mM Hepes-KOH pH 7.5, 50 mM KCl, 100 μg/ml BSA, 10 mM $MgCl_2$, 10% glycerol and 0.01% Triton X-100. The products were separated from substrate by electrophoresis on a 16% denaturing polyacrylamide gel, and the percent conversion determined by visualization and quantitation using a Storm 860 phosphorimager and ImageQuant v2.10 software (Molecular Dynamics, Sunnyvale, CA) as described (23).

Cell Sensitivity Assays

Sensitivity was measured by treating exponentially growing cells in suspension with a specific mutagen and then measuring survival. H_2O_2 (30%, EM Science, Gibbstown, NJ), AZT and bleomycin (Sigma, St. Louis, MO) were diluted in sterile water, MMS (Aldrich, Milwaukee, WI) and AraC (Sigma, St. Louis, MO) in PBS, and L-OddC and d4T (Drug Synthesis & Chemistry Branch, Developmental Therapeutics Program, Division of Cancer Treatment and Diagnosis, National Cancer Institute) in saline (0.9% NaCl) and sterile water, respectively. 1×10^6 cells in 10 ml αMEM supplemented with 10% Tc-App FBS were incubated with increasing doses of MMS, H_2O_2 and bleomycin for 1 hr at 37°C. For treatment with L-OddC (and

bleomycin again), 1×10^6 cells were incubated for 24 hr at 37°C at the doses indicated. Following all chemical treatments, cells were pelleted and rinsed prior to survival analysis. For the IR studies, 1×10^6 cells were exposed to the indicated doses, and were kept on ice before and after γ-irradiation by a Cesium-137 source (Mark I Irradiator, J.L. Shepherd and Associates, Glendale, CA). Treated and untreated cells were plated (1000-5000 cells/dish) and incubated under standard conditions at 37°C for 7-12 days. Cells were then fixed with 95% ethanol and stained with crystal violet (0.5% crystal violet, 6% ethanol, and 0.25% ammonium oxalate), which allows visual detection of cell colonies. Colonies were counted, and cell survival was calculated as the ratio of the number of colonies per dish to the original number of cells plated, divided by the plating efficiency. Cytotoxicity of the chemical compounds was also determined by a differential cytotoxicity (DC) assay as described in Hoy et al. (27). 3×10^4 cells in 1 ml of αMEM supplemented with 10% Tc-App FBS were seeded into each well of a 24 well tray and then incubated for 2 hr at 37°C to permit cell attachment. Increasing doses of the compounds were subsequently added in 1 ml of αMEM supplemented with 10% Tc-App FBS and the cells incubated for 72 hr at 37°C. Cells were fixed and stained as above.

Results

Generation of a Tc-Regulated Ape1 Overexpressing CHO AA8 Cell Line

To explore the role of Ape1 in regulating cellular resistance to a number of DNA-damaging and anti-cancer/viral agents, we generated an Ape1 overexpressing CHO AA8 cell line (Figure 1). Linearized pBI-EGFP-Ape1, containing a Tc-regulated bi-directional promoter for simultaneous (regulatable) expression of EGFP and Ape1, and linearized pTA-Hyg, which contains the Tc transactivator element and a hygromycin B selection marker, were co-transfected into CHO AA8 cells (see Materials and Methods). Thirty of 34 (88%) hygromycin-resistant colonies exhibited green fluorescence, and of the 30 $EGFP^+$ lines examined, 16 (53%) expressed human Ape1 protein as determined by Western blot analysis. The doubling times and particle size of each overexpressing line was identical to the parental line (data not shown).

Three of the 16 human Ape1-expressing clones were examined for Tc responsiveness. The isolates and the parental line were exposed to 0 or 0.3 μg/ml Tc for 0, 24, 48, 72 and 96 hr; this dose of Tc did not alter the doubling times or particle size of any cell line examined (data not shown). At the indicated time points, cell extracts were prepared, and 10 μg of protein was examined by Western blot analysis for relative human Ape1 protein expression. The results of one isolate (AA8-Ape1) are shown (Figure 2A). Absence of a signal in the parental AA8 extracts (Figure 2A, upper panel) indicates that the endogenous Chinese hamster Ape1 does not cross react with the human Ape1-specific antibody. Over the 96 hr Tc exposure period, the expression of human Ape1 in AA8-Ape1 (Figure 2A, lower panel) decreased to an undetectable level by 72 hr, indicating that Tc abolishes production of the human protein.

For accurate quantitation, protein extracts were analyzed for AP endonuclease activity using an abasic site analog (F)-containing duplex DNA substrate. The parental CHO AA8 cell

extracts demonstrated a relatively stable level of incision activity (Figure 2B, upper panel), independent of Tc. In the absence of Tc, AA8-Ape1 cells demonstrated a ~7-fold higher activity (Figure 2B, lower panel). Consistent with the Western blot analysis, exposure to 0.3 μg/ml Tc reduced the AP endonuclease activity of the overexpressing clone to control levels by 72 - 96 hr. The quantitated results from the incision assays are reported in Table I.

Role of Ape1 in Mediating Resistance to MMS, H_2O_2, bleomycin and IR

To determine the contribution of Ape1 to the repair of alkylation-induced DNA damage, and presumably "natural" AP site repair, we assessed the sensitivity of the Ape1 overexpressing cell line to MMS, relative to the parental control. We also examined the sensitivity of AA8-Ape1 to the free radical-generating agents, H_2O_2, IR and bleomycin, which each introduce a unique spectrum of DNA damage. Under the conditions employed, Ape1 overexpression did not significantly alter cellular sensitivity to MMS, H_2O_2 or IR (Figure 3), suggesting that Ape1 activity is not rate-limiting for the repair of associated DNA lesions. Similarly, the Ape1 overexpressing line exhibited no increased resistance following a 1 hr bleomycin exposure; however, following a 24 hr exposure, the AA8-Ape1 cells displayed a slight increase in resistance to bleomycin relative to the parental control cells (Figure 3D).

To explore the effects of a more chronic exposure (3 days) to these chemical genotoxins, as opposed to the acute exposures ($\leq$ 24 hr) used in the survival curves above, we performed differential cytotoxicity (DC) assays (27). These assays also permitted analysis of the effects of Tc on the observed resistance, since Tc is stable at 37°C for only 4 days (Sigma). As shown in Figure 4, the higher cell density (visualized as an increase in cell staining) observed with the AA8-Ape1 cell line relative to the parental control indicates a dramatically increased resistance to chronic bleomycin exposure. Moreover, the addition of Tc to the overexpressing cell line

reduced this increased resistance to bleomycin, suggesting that the observed protection is due to elevated Ape1 activity. Similar DC experiments were performed with MMS and H_2O_2, and as observed with the survival curve assays, no increased resistance was found with AA8-Ape1 cells (data not shown).

Role of Ape1 in Mediating Resistance to Nucleoside Analogs

Ape1 has recently been shown to be the major enzyme responsible for excising the anticancer nucleoside analog L-OddC (Figure 5A) from DNA (18). These authors hypothesized that the level of Ape1 activity might therefore affect the pharmacological outcome of this and other L-configuration nucleoside analogs. We found that the AA8-Ape1 cells are indeed more resistant than the parental control at doses of L-OddC $\geq$0.75 mM, with the most dramatic resistance (~1.7 fold) being observed at the higher doses, presumably where higher nucleotide incorporation occurs (Figure 5B).

To assess more generally the role of Ape1 in regulating cellular resistance to the cytotoxic effects of nucleoside analogs, a series of anti-cancer/viral compounds (Figure 5A) were tested in DC assays. Perhaps more impressive than the survival assays above (Figure 5B), AA8-Ape1 cells exposed to L-OddC (Figure 6) showed a marked increase in growth (i.e. staining intensity or cell density) relative to the parental cells. A consistent, but only slight increase in staining was observed with AZT, indicating a less dramatic role for Ape1 in regulating the cytotoxic potential of this agent. AA8-Ape1 cells exposed to the nucleoside analogs AraC (Figure 6) or d4T (data not shown) exhibited little or no more resistance than the control cells. AA8-Ape1 cells exposed simultaneously to Tc and either AZT or L-OddC displayed essentially control level resistance (data not shown).

Discussion

It is evident that Ape1 exhibits a powerful AP endonuclease activity, and a comparatively weak, although substrate-dependent, 3' to 5' exonuclease activity in vitro. However, the in vivo contributions of Ape1 remain less clear, primarily due to the lack of a defined mutant. Towards clarifying the cellular contributions of Ape1 to DNA-damaging agent and nucleoside analog resistance, we established an Ape1 overexpressing cell line that exhibits ~7-fold higher AP endonuclease activity than its parental line.

Increased Ape1-dependent activity did not affect cellular sensitivity to MMS and H_2O_2, suggesting that the level of Ape1 activity in AA8 is not rate-limiting for the repair of the cytotoxic DNA damages associated with these genotoxins. These observations are consistent with the findings of Herring et al. (28) and Prieto-Alamo et al. (29), who found that overexpression of Ape1 in mammalian cells did not modify sensitivity to these agents. Similarly, in vitro studies by Podlutsky et al. (30) and Nakamura et al. (31) have shown that the deoxyribose-5'-phosphate lyase function of Polβ, and not the activity of Ape1, is rate-limiting for the repair of natural AP sites (and thus for base excision repair), damages or repair intermediates typically associated with MMS. The recent in vitro finding of Izumi et al. (32) indicating that Ape1 may be rate-limiting for the repair of 3'-blocking damage in ROS-induced single-strand breaks is in apparent discord with the in vivo H_2O_2 results. However, this potential discrepancy could be explained by specific cellular complexities, e.g. more efficient reconstitution of a fully-functional repair complex in vivo, the nature of the cytotoxic damage induced in cells, or simply the defined character of the in vitro biochemical assays. Regardless, the general consensus, across multiple cell types, is that Ape1 is not rate-limiting in the repair of natural AP sites, e.g.

those formed by MMS, or "simple" (i.e. non-clustered) oxidation products, e.g. those induced by H_2O_2.

Ape1 overexpression did not affect cellular sensitivity to bleomycin exposures of <24 hr, as assessed by survival assays. However, AA8-Ape1 cells exposed to bleomycin for 72 hr did exhibit increased resistance. This latter finding is consistent with the report of Robertson et al. (34), who found that increased Ape1 levels in a human germ cell tumor line correlated with elevated resistance to chronic bleomycin exposures (5-7 days). In addition, our studies are in agreement with the results of Prieto-Alamo et al. (29), who found that an Ape1-overexpressing CHO-9 line showed control-level resistance following a 1 hr exposure to bleomycin. Thus, sensitivity to bleomycin, at least as a function of Ape1 activity, appears to be influenced by the treatment strategy, and may indicate that the longer exposures result in the accumulation of a greater proportion of Ape1-repairable DNA damage (e.g. single-strand breaks harboring 3'-damage).

Our finding that AA8-Ape1 does not exhibit altered resistance to IR is in potential conflict with the reports of Herring et al. (33) and Robertson et al. (34), who both found increased resistance to IR in human cells expressing elevated levels of Ape1. However, Herring and colleagues found that Ape1 overexpression in rat glioma cells did not alter cellular sensitivity to IR (28). Thus, the current picture regarding Ape1's role in determining IR resistance is more complex. These discrepancies may stem from species-specific or cell-specific differences, where factors such as the relative efficiency of alternative repair pathways determine whether Ape1 activity is rate-limiting. Nonetheless, until the precise reason(s) for the discrepancies is known, Ape1 nuclease activity should not be considered a good prognostic indicator for responsiveness to IR.

The results presented here are the first to suggest that Ape1 nuclease activity correlates with cellular resistance to the cytotoxic effects of the replication-terminating nucleoside analog L-OddC, presumably through the enzyme's excision activity. Notably, prior biochemical studies (18), which found Ape1 to be more efficient at removing L-OddC, but relatively ineffective at excising AraC, agree with our cellular observations. That is, AA8-Ape1 is markedly more resistant to L-OddC and little or no more resistant to AraC in comparison to the matched controls. While Ape1 has been reported to excise AZT and d4T, there are presently no published quantitative excision rates for these analogs, and thus the cellular response to these compounds observed here can not be evaluated in comparison to the other antimetabolites.

In summary, the available data indicates that, in some circumstances, Ape1 levels can influence cellular sensitivity to certain anti-cancer agents, most notably IR, bleomycin and specific nucleoside analogs. Since Ape1 activity has been shown to vary up to 3-fold in a small set of human lymphocyte samples (35), and genetic variation that imparts reduced activity to Ape1 has been observed in the human population (36), prior knowledge of Ape1 activity may help prioritize which agents and dosing regimes will be most effective at eradicating the disease. However, before this can be successfully achieved, further studies at defining the precise reasons (e.g. differences in the efficiencies of alternative repair pathways) for the discrepancies in the association of Ape1 activity with cellular resistance to IR and bleomycin are necessary. Moreover, a more thorough investigation of the relationship of Ape1 activity and the effectiveness of IR, bleomycin and nucleoside analogs in a clinical setting is needed. Future studies aimed at abolishing Ape1 activity are required to address whether this enzyme is a potential target for sensitization to specific anti-cancer/viral agents.

Acknowledgements

The authors would like to thank Dr. S. Takeda (Kyoto University Medical School, Japan) for sharing plasmids and Dr. Allen Christian (Lawrence Livermore National Laboratory) for assistance with the fluorescence microscopy, as well as the members of the Wilson Laboratory (M. Fernandez, L. Nguyen, and M. Hadi) and the Thompson Laboratory (R. Tebbs, E. Salazar, N. Liu, C. Salmon, J. Lamerdin) for helpful comments and suggestions during the course of these studies. We also thank Dr. Irene Jones (Lawrence Livermore National Laboratory) for critical reading of the manuscript. This work was performed under the auspices of the U.S. Department of Energy by the University of California, Lawrence Livermore National Laboratory under Contract No. W-7405-Eng-48 and supported by ARMY (BC980514) and NIH (CA79056) grants to DMWIII.

References

1. Lindahl,T. (1993) Instability and decay of the primary structure of DNA. Nature **362**, 709-715.

2. Friedberg,E.C., Walker,G.C. and Siede,W. (1995) DNA Repair and Mutagenesis. ASM Press, Washington, D.C.

3. Krokan,H.E., Nilsen,H., Skorpen,F., Otterlei,M. and Slupphaug,G. (2000) Base excision repair of DNA in mammalian cells. FEBS Lett. **476**, 73-77.

4. McCullough,A.K., Dodson,M.L. and Lloyd,R.S. (1999) Initiation of base excision repair: Glycosylase mechanisms and structures. Annu. Rev. Biochem. **68**, 255-285.

5. Williams,G.M. and Jeffrey,A.M. (2000) Oxidative DNA damage: Endogenous and chemically induced. Regulatory Toxicology and Pharmacology **32**, 283-292.

6. Termini,J. (2000) Hydroperoxide-induced DNA damage and mutations. Mutat. Res. **450**, 107-124.

7. Goodhead,D.T. (1994) Initial events in the cellular effects of ionizing radiations: Clustered damage in DNA. Int. J. Radiat. Biol. **65**, 7-17.

8. Ward,J.F. (1995) Radiation mutagenesis: The initial DNA lesions responsible. Radiat. Res. **142**, 362-368.

9. Povirk,L.F. (1996) DNA damage and mutagenesis by radiomimetic DNA-cleaving agents: Bleomycin, neocarzinostatin and other enediynes. Mutat. Res. **355**, 71-89.

10. Tan,X., Chu,C.K., and Boudinot,F.D. (1999) Development and optimization of anti-HIV nucleoside analogs and prodrugs: A review of their cellular pharmacology, structure-activity relationships and pharmacokinetics. Advanced Drug Delivery Reviews **39**, 117-151.

11. Grove,K.L., and Cheng,Y.-C. (1996) Uptake and metabolism of the new anticancer compound β-L-(-)-dioxolane-cytidine in human prostate carcinoma DU-145 cells. Cancer Res. **56**, 4187-4191.

12. Grove,K.L., Guo,X., Liu,S.-H., Gao,Z., Chu,C.K. and Cheng,Y.-C. (1995) Anticancer activity of β-L-dioxolane-cytidine, a novel nucleoside analogue with the unnatural L configuration. Cancer Res. **55**, 3008-3011.

13. Wilson III,D.M. and Barsky,D. (2001) The major human abasic endonuclease Ape1: Formation, consequences and repair of abasic lesions in DNA. Mutat. Res. **484**, 283-307.

14. Demple,B. and Harrison,L. (1994) Repair of oxidative damage to DNA: Enzymology and biology. Annu. Rev. Biochem. **63**, 915-948.

15. Winters,T.A., Henner,W.D., Russell,P.S., McCullough,A. and Jorgensen,T.J. (1994) Removal of 3'-phosphoglycolate from DNA strand-break damage in an oligonucleotide substrate by recombinant human apurinic/apyrimidinic endonuclease 1. Nucleic Acids Res. **22**, 1866-1873.

16. Wilson III,D.M., Bennett,R.A.O., Marquis,J.C., Ansari,P. and Demple,B. (1995) Trans-complementation by human apurinic endonuclease (Ape) of hypersensitivity to DNA damage and spontaneous mutator phenotype in apn1⁻ yeast. Nucleic Acids Res. **23**, 5027-5033.

17. Suh,D., Wilson III,D.M., and Povirk,L.F. (1997) 3'-phosphodiesterase activity of human apurinic/apyrimidinic endonuclease at DNA double-strand break ends. Nucleic Acids Res. 25, 2495-2500.

18. Chou,K.-M., Kukhanova,M. and Cheng,Y.-C. (2000) A novel action of human apurinic/apyrimidinic endonuclease: Excision of L-configuration deoxyribonucleoside analogs from the 3' termini of DNA. J. Biol. Chem. **275**, 31009-31015.

19. Chou,K.-M., Lam,W. and Cheng,Y.-C. (2001) A novel DNA exonuclease activity of human apurinic/apyrimidinic endonuclease (APE1): Implication in DNA mismatch repair. Proceed. of the AACR **42**, 556.

20. Xanthousdakis,S., Smeyne,R.J., Wallace,J.D. and Curran,T. (1996) The redox/DNA repair protein, Ref-1, is essential for early embryonic development in mice. Proc. Natl. Acad. Sci. USA **93**, 8919-8923.

21. Ludwig,D.L., MacInnes,M.A., Takiguchi,Y., Purtymun,P.E., Henrie,M., Flannery,M., Meneses,J., Pedersen,R.A. and Chen,D.J. (1998) A murine AP-endonuclease gene-targeted deficiency with post-implantation embryonic progression and ionizing radiation sensitivity. Mutat. Res. **409**, 17-29.

22. Thompson,L.H., Fong,S., and Brookman,K. (1980) Validation of conditions for efficient detection of HPRT and APRT mutations in suspension-cultured Chinese hamster ovary cells. Mutat. Res. **74**, 21-36.

23. Erzberger,J.P., Barsky,D., Schärer,O.D., Colvin,M.E., and Wilson III,D.M. (1998) Elements in abasic site recognition by the major human and *Escherichia coli* apurinic/apyrimidinic endonucleases. Nucleic Acids Res. **26**, 2771-2778.

24. Demple,B., Herman,T., and Chen,D.S. (1991) Cloning and expression of APE, the cDNA encoding the major human apurinic endonuclease: Definition of a family of DNA repair enzymes. Proc. Natl. Acad. Sci. USA **88**, 11450-11454.

25. Bradford,M.M. (1976) A rapid and sensitive method for the quantitation of microgram quantities of protein utilizing the principle of protein-dye binding. Anal. Biochem. **72**, 248-254.

26. Wilson III,D.M., Takesita,M., Grollman,A.P., and Demple,B. (1995) Incision activity of human apurinic endonuclease (Ape) at abasic site analogs in DNA. J. Biol. Chem. **270**, 16002-16007.

27. Hoy,C.A., Salazar,E.P. and Thompson,L.H. (1984) Rapid detection of DNA-damaging agents using repair-deficient CHO cells. Mutat. Res. **130**, 321-332.

28. Herring,C.J., Deans,B., Elder,R.H., Rafferty,J.A., MacKinnon,J., Barzilay,G., Hickson,I.D., Hendry,J.H., and Margison,G.P. (1999) Expression levels of the DNA repair enzyme HAP1 do not correlate with the radiosensitivities of human or HAP1-transfected rat cell lines. Br. J. Cancer **80**, 940-945.

29. Prieto-Alamo,M.J., and Laval,F. (1999) Overexpression of the human HAP1 protein sensitizes cells to the lethal effect of bioreductive drugs. Carcinogenesis **20**, 415-419.

30. Podlutsky,A.J., Dianova,I.I., Wilson,S.H., Bohr,V.A., and Dianov,G.L. (2001) DNA synthesis and dRPase activities of polymerase beta are both essential for single-nucleotide patch base excision repair in mammalian cell extracts. Biochemistry **40**, 809-813.

31. Nakamura,J., La,D.K., and Swenberg,J.A. (2000) 5'-nicked apurinic/apyrimidinic sites are resistant to beta-elimination by beta-polymerase and are persistent in human cultured cells after oxidative stress. J. Biol. Chem. **275**, 5323-5328.

32. Izumi,T., Hazra,T.K., Boldogh,I., Tomkinson,A.E., Park,M.S., Ikeda,S., and Mitra,S. (2000) Requirement for human AP endonuclease 1 for repair of 3'-blocking damage at

DNA single-strand breaks induced by reactive oxygen species. Carcinogenesis **21**, 1329-1334.

33. Herring,C.J., West,C.M.L., Wilks,D.P., Davidson,S.E., Hunter,R.D., Berry,P., Forster,G., MacKinnon,J., Rafferty,J.A., Elder,R.H., Hendry,J.H., and Margison,G.P. (1998) Levels of the DNA repair enzyme human apurinic/apyrimidinic endonuclease (APE1, APEX, Ref-1) are associated with the intrinsic radiosensitivity of cervical cancers. Br. J. Cancer. **78**, 1128-1133.

34. Robertson,K.A., Bullock,H.A., Xu,Y., Tritt,R., Zimmerman,E., Ulbright,T.M., Foster,R.S., Einhorn,L.E. and Kelley,M.R. (2001) Altered expression of Ape1/ref-1 in germ cell tumors and overexpression in NT2 cells confers resistance to bleomycin and radiation. Cancer Res. **61**, 2220-2225.

35. Redaelli,A., Magrassi,R., Bonassi,S., Abbondandolo,A. and Frosina,G. (1998) AP endonuclease activity in humans: Development of a simple assay and analysis of ten normal individuals. Teratogenesis, Carcinogenesis, and Mutagenesis **18**, 17-26.

36. Hadi,M.Z., Coleman,M.A., Fidelis,K., Mohrenweiser,H.W. and Wilson III,D.M. (2000) Functional characterization of Ape1 variants identified in the human population. Nucleic Acids Res. **28**, 3871-3879.

Figure Legends

Table 1. Specific AP endonuclease activity of AA8 and AA8-Ape1 cells. Cells were exposed to 0 or 0.3 μg Tc/ml for 0 to 96 hr as described in the Materials and Methods, and were then harvested, pelleted and stored at –80°C. One tenth μg CHO cell extract was assayed for AP endonuclease activity using 1 pmol of 18F duplex DNA. Specific activity is defined as pmol of 18-mer F containing DNA substrate converted to 9-mer product at 37°C per min per mg of total cellular protein. Tc-response experiments were performed twice, and two incision assays were used for each Tc response experiment for these analyses (i.e. the values shown represent the average and standard deviation of 4 specific activity values). Fold increase of the AP endonuclease activity of AA8-Ape1 over the average specific activity of the parental line is indicated in parenthesis. For comparison, the average HeLa cell extract (± Tc) specific activity was determined to be ~880 pmol/mg/min.

Fig. 1. Schematic of the plasmids used to generate the Tc-regulated Ape1 expressing CHO AA8 cells. pTA-hyg contains the transcriptional activator (tTA) as well as the hygromycin B resistance gene. pBI-EGFP-Ape1 contains a Tc-regulated bi-directional promoter (Pbi-1) for the expression of EGFP and Ape1. The Tc-controlled tTA is a fusion of the wild type Tc-repressor to the Herpes Simplex Virus VP16 activation domain. In the absence of Tc, the tTA binds to the Pbi-1, which contains the Tc response element, and activates transcription. In the presence of Tc, the tTA-Tc complex is unable to bind to the Pbi-1 and therefore transcription of neither EGFP or Ape1 is activated.

Fig. 2. Tc regulation of Ape1 protein expression and activity. (A). Western blot analysis of protein extracts from a typical Tc response experiment. CHO AA8 (upper panel) and AA8-Ape1 (lower panel) cells were exposed to 0 (-) or 0.3 (+) μg Tc/ml for 0, 24, 48, 72 and 96 hr and processed as described in Materials and Methods. Ten μg of protein extract was electrophoresed on a 12% SDS-PAG, transferred to nitrocellulose, and immunostained using anti-human Ape1 serum. One tenth μg of purified recombinant human Ape1 protein (left) was included as a positive control. (B). Representative AP endonuclease incision gel from a Tc response experiment. One tenth μg cell extract from either AA8 (upper panel) or AA8-Ape1 (lower panel) ± Tc was assayed for incision activity for 5 min at 37°C with 1 pmol of 18F DNA substrate (see Materials and Methods). Arrows denote the location of the 18-mer starting (intact) DNA substrate and the 9-mer incised product.

Fig. 3. Survival of AA8 and AA8-Ape1 after mutagen treatment. Cells were exposed to MMS (A), H_2O_2 (B), IR (C) or Bleomycin (D) as described in Materials and Methods. Each data point represents the mean ± SD of 6 independent data points from 2-3 independent treatments.

Fig. 4. DC assays comparing parental AA8 and AA8-Ape1 cells for sensitivity to bleomycin. Increasing doses (as indicated) of bleomycin were added to each well, and cells were then incubated for 72 hr at 37°C, stained and visualized with crystal violet (see Materials and Methods). Cell density (i.e. staining) differences between the parental AA8 cells (upper row), AA8-Ape1 cells (middle row) and AA8-Ape1 cells + Tc (lower row) allow the comparison of the relative cytotoxicity of the compounds.

Fig. 5. Nucleoside analog structures and sensitivity of Ape1 overexpressing cells to these anti-cancer/viral agents. (A). The chemical structures of L-OddC, AZT, d4T and AraC. (B). Cell survival following L-OddC treatment. Cells were exposed to a range of doses of L-OddC for 24 hr at 37°C and processed as described in the Figure 3 legend. Each data point represents the mean $\pm$ SD of at least 6 independent data points from 2-3 independent treatments.

Fig. 6. DC assays comparing parental AA8 and AA8-Ape1 cells for sensitivity to several nucleoside analogs. Increasing doses (as indicated) of L-OddC, AZT or AraC were added to each well, and cells were then incubated for 72 hr at 37°C, stained and visualized with crystal violet. Cell density differences between the parental cells (upper row of wells) and AA8-Ape1 cells (lower row of wells) allow comparison of the relative cytotoxicity of the various compounds.

Table 1.

AP Endonuclease Specific Activity

	AA8 Specific Activity		AA8-Ape1 Specific Activity	
Time (hr)	- Tc	+ Tc	- Tc	+ Tc
0	200 ± 92		1800 ± 16 (7.2)	
24	260 ± 26	140 ± 21	1800 ± 20 (7.4)	1800 ± 30 (10.3)
48	240 ± 43	230 ± 60	1800 ± 22 (7.3)	1000 ± 340 (5.7)
72	340 ± 160	140 ± 37	1800 ± 21 (7.3)	370 ± 18 (2.1)
96	200 ± 34	170 ± 29	1800 ± 27 (7.3)	260 ± 44 (1.5)

Figure 1.

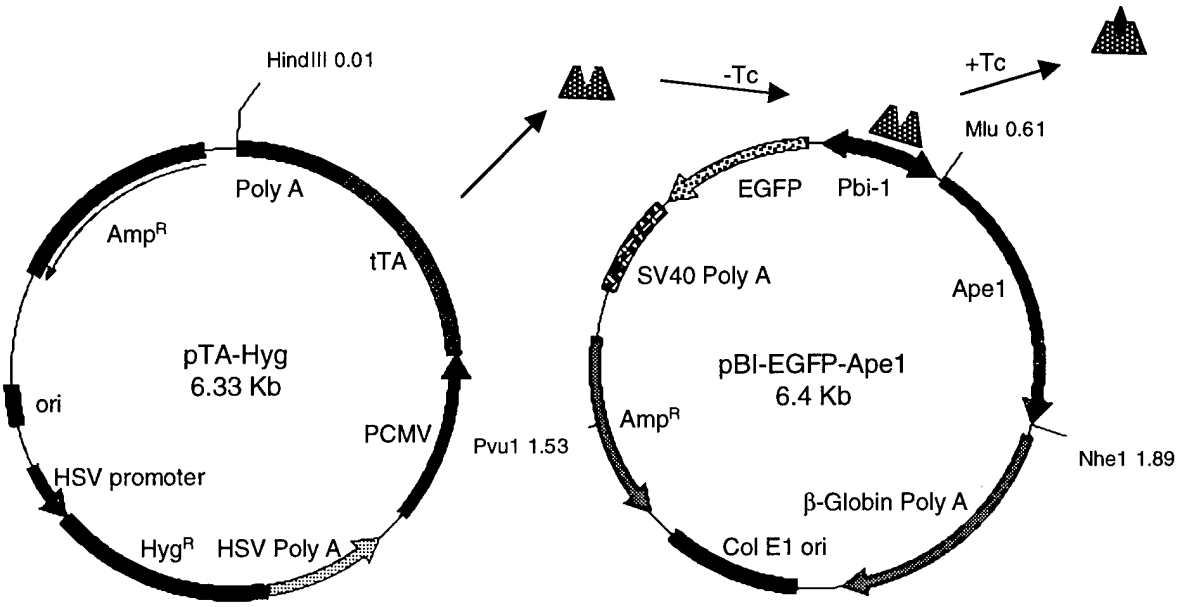
HindIII 0.01
Poly A
Amp^R
tTA
pTA-Hyg
6.33 Kb
ori
PCMV
HSV promoter
Hyg^R
HSV Poly A
Pvu1 1.53
-Tc
+Tc
Mlu 0.61
EGFP
Pbi-1
SV40 Poly A
Ape1
pBI-EGFP-Ape1
6.4 Kb
Amp^R
Nhe1 1.89
β-Globin Poly A
Col E1 ori

Figure 2.

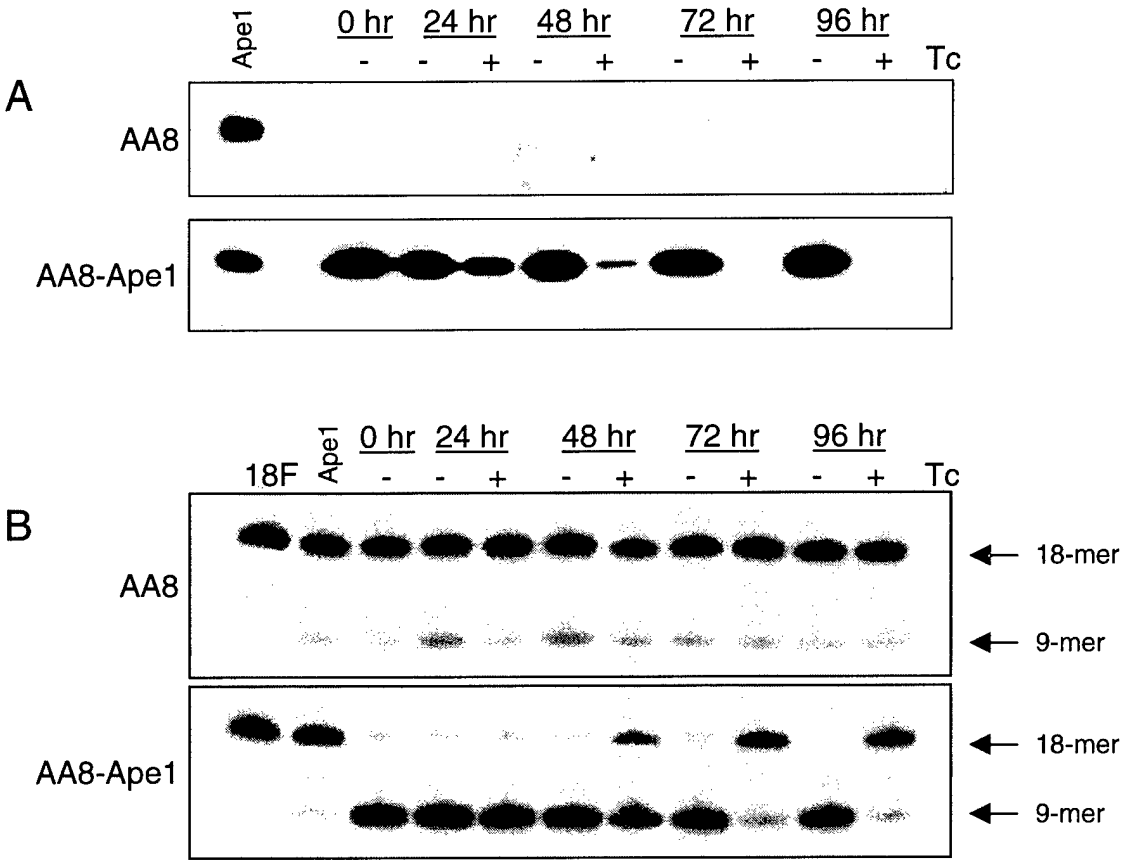
A
Ape1
0 hr
24 hr
48 hr
72 hr
96 hr
- - + - + - + - + Tc
AA8
AA8-Ape1
B
18F
Ape1
0 hr
24 hr
48 hr
72 hr
96 hr
- - + - + - + - + Tc
AA8
AA8-Ape1
18-mer
9-mer
18-mer
9-mer

Figure 3.

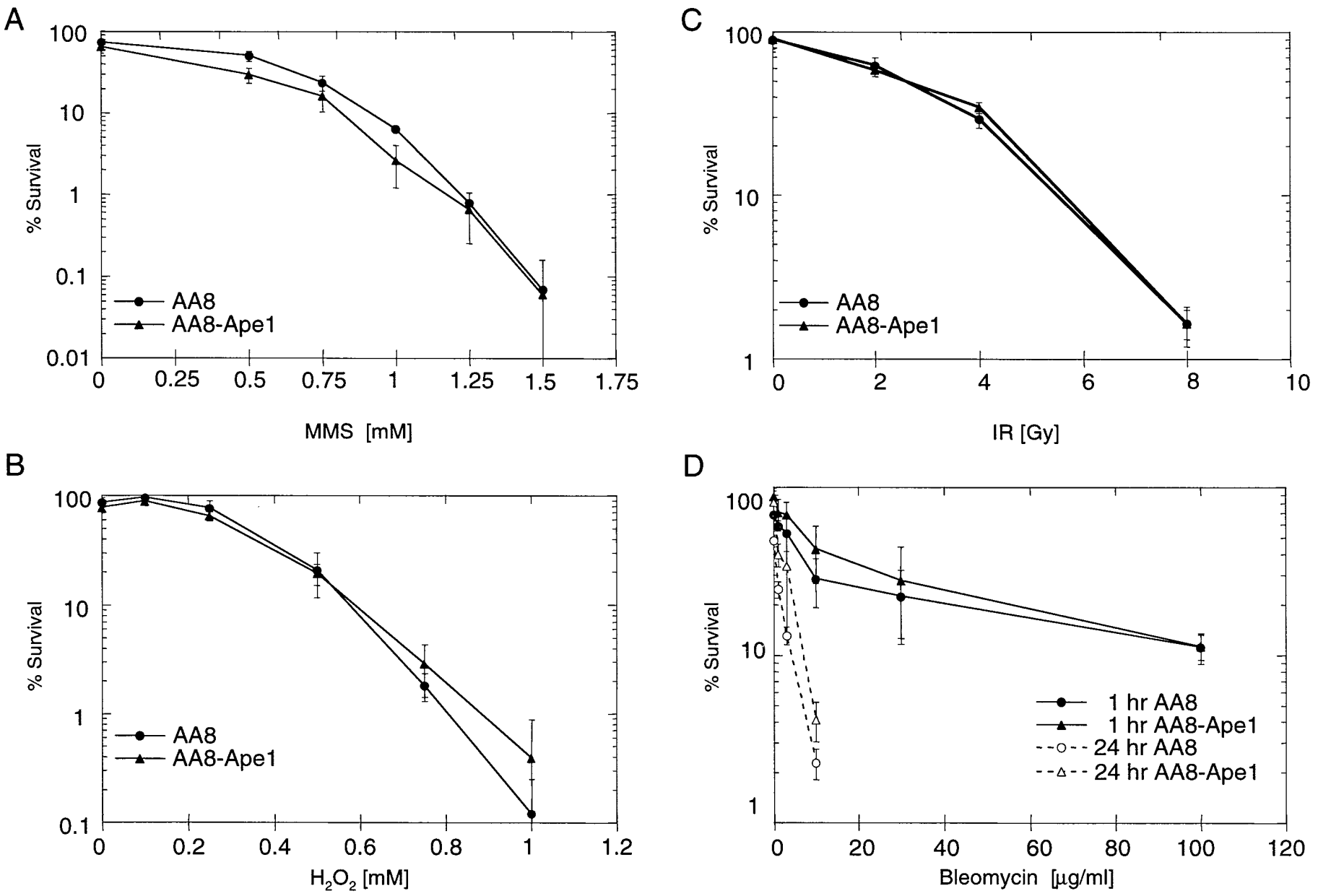
A
100
10
1
0.1
0.01
% Survival
AA8
AA8-Ape1
0
0.25
0.5
0.75
1
1.25
1.5
1.75
MMS [mM]
C
100
10
1
% Survival
AA8
AA8-Ape1
0
2
4
6
8
10
IR [Gy]
B
100
10
1
0.1
% Survival
AA8
AA8-Ape1
0
0.2
0.4
0.6
0.8
1
1.2
H2O2 [mM]
D
100
10
1
% Survival
1 hr AA8
1 hr AA8-Ape1
24 hr AA8
24 hr AA8-Ape1
0
20
40
60
80
100
120
Bleomycin [µg/ml]

Figure 4.

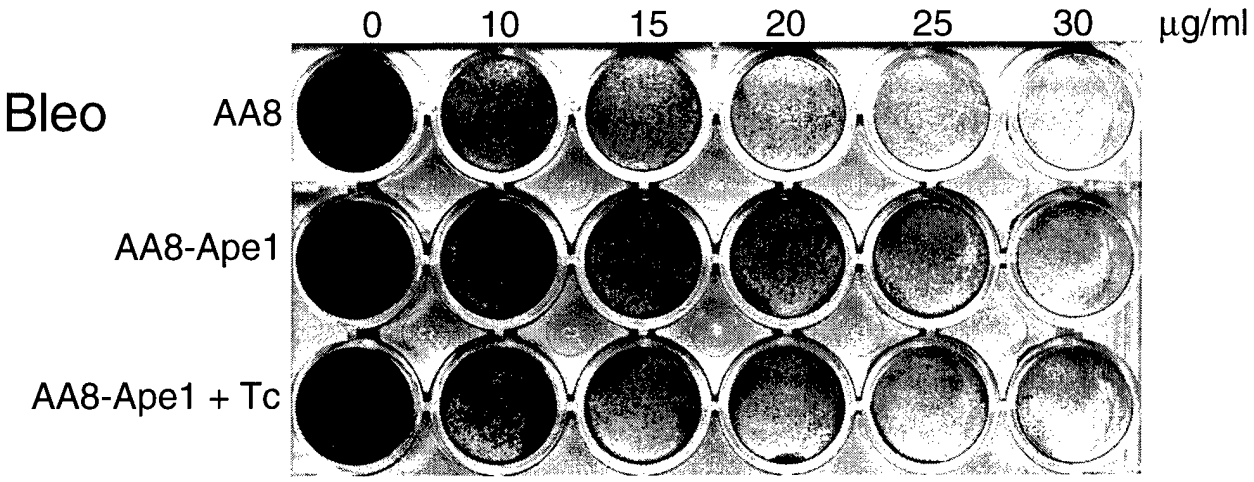

Figure 5.

A

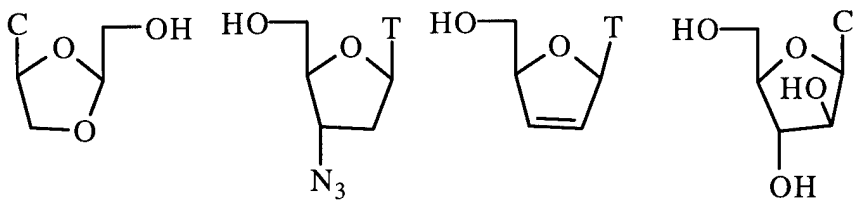

L-OddC AZT d4T AraC

B

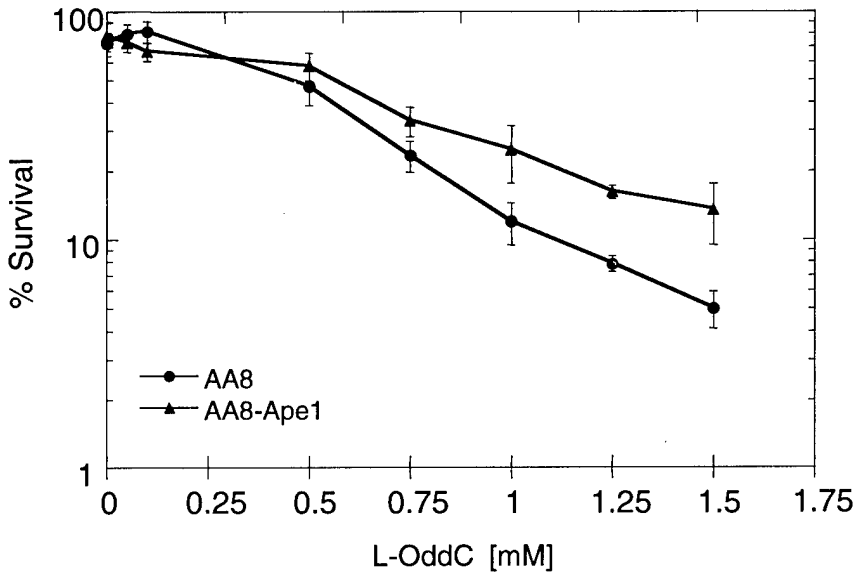

Figure 6.

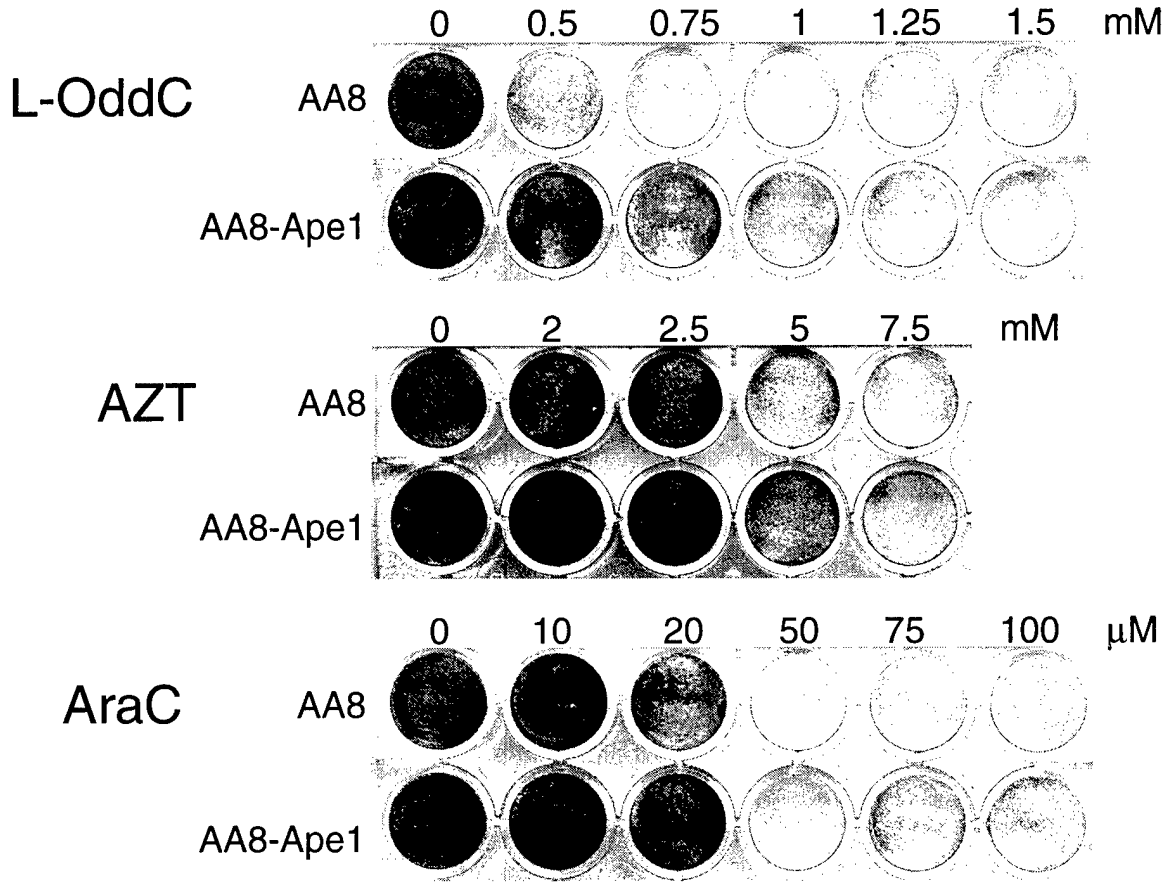
0 0.5 0.75 1 1.25 1.5 mM
L-OddC
AA8
AA8-Ape1
0 2 2.5 5 7.5 mM
AZT
AA8
AA8-Ape1
0 10 20 50 75 100 μM
AraC
AA8
AA8-Ape1